NATURAL DISSOLVED ORGANIC MATTER DYNAMICS IN A KARSTIC SURFACE-GROUNDWATER EXCHANGE SYSTEM

By

JIN JIN

A DISSERTATION PRESENTED TO THE GRADUATE SCHOOL
OF THE UNIVERSITY OF FLORIDA IN PARTIAL FULFILLMENT
OF THE REQUIREMENTS FOR THE DEGREE OF
DOCTOR OF PHILOSOPHY

UNIVERSITY OF FLORIDA

2012

To my parents

ACKNOWLEDGMENTS

First and foremost, I would like to thank my beloved parents for their endless love and support during each and every stage of my life. You raise me up to more than I can be. I owe you so much.

I would like to sincerely thank my advisor, Dr. Andrew Zimmerman, for his advice and guidance throughout my graduate study in the Department of Geological Sciences. His patience and encouragement helped me overcome lots of difficulties and eventually make this dissertation possible. I am also grateful to my supervisory committee members, Drs. Jonathan Martin, Elizabeth Screaton, Michael Annable, and Jean-Claude Bonzongo, for all the help and advice they provided during my research and dissertation development.

I thank Dr. Jason Curtis for his assistance with the C isotope and DIC measurement. I thank Dr. Stuart Norton and Cindy Fischler for coordinating the incubation experiments in the FGS lab. I thank Dr. Willie Harris for performing the mineralogical investigation on the aquifer core materials. I thank Dr. PJ Moore, Amy Brown, and Kelly Deuerling for measuring major ion concentrations. I thank Dr. PJ Moore, Mitra Khadka, and Chad Foster for their assistance with the field water sample collection. I also would like to thank Kathleen McKee and Megan Wetherington for their help with the hydrologic data. The funding provided by UF Geology Department, NSF, UF Water Institute, SWFWMD, and FGS is gratefully acknowledged. Special thanks go to my former lab mates, Dr. Gabriel Kasozi and Dr. Atanu Mukherjee, for their music, laughter, and friendship. I am also grateful to all my friends at University of Florida – you made the Gainesville Chapter of my life enjoyable and precious.

TABLE OF CONTENTS

page

LIST OF TABLES

LIST OF FIGURES

Abstract of Dissertation Presented to the Graduate School
of the University of Florida in Partial Fulfillment of the
Requirements for the Degree of Doctor of Philosophy

NATURAL DISSOLVED ORGANIC MATTER DYNAMICS IN A KARSTIC SURFACE-GROUNDWATER EXCHANGE SYSTEM

By

Jin Jin

August 2012

Chair: Andrew Zimmerman
Major: Geology

Spatiotemporal variation in natural dissolved organic matter (NDOM) and associated biogeochemical processes were studied in three independent but related surface-groundwater exchange systems in North Florida: the Santa Fe River Watershed (SFRW), the O'Leno Sink-Rise system, and a laboratory simulation of an aquifer storage and recovery (ASR) operation. In the surface waters of the SFRW, both NDOM mineralization and carbonate rock dissolution occurred to the greatest extent during low flow conditions and in the upper watershed. Evidence for carbonate precipitation was found during high flow as well as in the lower watershed during low flow conditions. NDOM-mineral sorption and desorption were often spatiotemporally associated with carbonate precipitation and dissolution, respectively. In the O'Leno Sink-Rise system, surface waters could be characterized as net autotrophic while the groundwater was net heterotrophic except for portions of the deep aquifer where chemoautotrophy was identified. NDOM mineralization occurred in both shallow and deep portions of the aquifers and to a greater extent during low flow periods. The NDOM mineralization in deep portion of the aquifer may be fueled by deep-sourced autochthonous NDOM, rather than NDOM imported from the surface. Carbonate mineral dissolution occurred

throughout the system and during all flow conditions, which contradicts prevailing thought that dissolution occurs primarily during high flow conditions. During a laboratory simulation of an ASR operation, As mobilization from the aquifer materials was found to occur via microbially-mediated reactions fueled by labile NDOM. Abiotic processes such as oxidative dissolution and reductive dissolution also caused As mobilization. Thus, the greatest amount of As mobilization in the Floridan Aquifer may be linked to the oscillation of redox conditions whereby reduced iron-sulfides are converted to iron oxides which then release As when microbially-reduced. This study demonstrates the important influence of hydrology and biogeochemical processes on water quality and aquifer evolution in a karstic surface-groundwater exchange system and has important implications for microbial ecology, contaminant remediation, and global carbon cycling.

CHAPTER 1
INTRODUCTION

Karstic aquifers are important as they cover 25% of the land surface globally and provide 25% of the drinking water supplies to all humans (Ford and Williams, 2007). The high permeability of karstic aquifers (Worthington, 1994) allows extensive exchange of surface water and groundwater, leading to the high potential for contamination of groundwater, a critical water resource, and a reintroduction of this contamination to surficial springs, often important ecological and recreation resources. Thus, it is important to understand the extent of this exchange and the biogeochemical reactions which occur at this critical interface.

The exchange of surface water and groundwater also allows introduction of large fluxes of natural dissolved organic matter (NDOM, Lau and Mink, 1987), which is known to interact with aquifer components (e.g., rocks, metals, and microbes) and affect groundwater geochemistry. For example, NDOM can act as a proton donor/acceptor and as a pH buffer (Frimmel, 1998), influence mineral precipitation and dissolution, and affect the transport and degradation of pollutants (Findlay et al., 2003; Schlautman and Morgan, 1994). NDOM may even encourage the growth of potentially harmful microbial populations (Boyes and Elliott, 2006; Fisher et al., 2006). The presence of NDOM also considerably influences the mobilization and fixation of heavy metals (e.g., As, Lee et al., 2005).

Despite its importance to karstic aquifers, scientific study of NDOM in these systems is rare in the literature, mainly due to methodological difficulties related to the heterogeneity and remoteness of the karstic aquifer. In addition, the system is extremely complex with NDOM continuously being consumed, produced, and transformed during

various biogeochemical processes in the subsurface (Lovley and Chapelle, 1995; Lovley and Chapelle, 1996). Thus, the spatiotemporal occurrence of these biogeochemical processes, their relative magnitudes and their effects remain poorly understood.

This study is designed to attain a better understanding of NDOM dynamics in surface-groundwater exchange systems. It focuses on the North Florida karstic system, including the upper Floridan aquifer and surficial waters with which it exchanges. The overarching questions addressed in the dissertation are: *what biogeochemical processes alter the quantity and quality of NDOM in karstic systems, what are their spatiotemporal variability, and what effects do they have on environmental concerns such as As release?* This study uses a combined field and laboratory approach to address these questions in three related projects. Two of the three projects examine NDOM in the Santa Fe River system, a major tributary of the Suwannee River in north Florida. The first (Chapter 2) examines watershed-scale spatiotemporal geochemical information on NDOM dynamics in surface waters of the Santa Fe River Watershed. The second (Chapter 3) focuses on NDOM dynamics in a geologically unique location on the Santa Fe River, the O'Leno Sink-Rise system. There, the Santa Fe River traverses the Cody Escarpment that divides the watershed into confined and unconfined portions, making it an ideal setting to explore the NDOM dynamics and mixing of surface water and groundwater. The third project (Chapter 4) utilizes a laboratory incubation approach to explore the influence of NDOM and microbial processes on arsenic (As) mobilization during karstic groundwater-surface water exchange such as might occur in an aquifer storage and recovery (ASR) operation.

In providing insights into the spatiotemporal transformation of NDOM in a karstic aquifer and the hydrologic controls on those transformations, this study increases our overall understanding of biogeochemical cycling in aquifers and more generally, the global carbon cycling. The results of this study will also contribute to the understanding of possible environmental consequences and improvement of hydrogeologic projects such as ASR and aquifer recharge (AR). These will be important for preservation and management of water supplies in Florida and many parts of the world that rely on groundwater resources. The results of this study also have implications in such diverse fields as microbial ecology, karst and petroleum reservoir evolution and contaminant remediation.

CHAPTER 2
SPATIOTEMPORAL VARIATION IN CARBON DYNAMICS IN A KARSTIC RIVER COURSE: SANTA FE RIVER, FLORIDA, USA

Background

Karstic aquifers are important as they cover 25% of the land surface globally and provide 25% of the drinking water supplies to all humans (Ford and Williams, 2007). Due to their typically high permeability (Worthington, 1994) and thus, close connectivity to the surface, they receive relatively large fluxes of natural dissolved organic matter (NDOM, Lau and Mink, 1987) and associated nutrients. Likewise, karstic aquifers are susceptible to contaminates from the surface, whose fate and transport is largely controlled by the water-rock-microbe interactions in the subsurface. Karstic areas may also be an important but overlooked part of global carbon (C) cycling. As the largest C reservoir on the Earth, carbonate rocks contain about 6.1×10^{7} billion tons of C, which is a few thousand times greater than the amount in the ocean, the next larger reservoir (Falkowski et al., 2000; Houghton and Woodwell, 1989). The annual C uptake by karstic aquifers has been estimated to be up to 0.6 billion tons of C, which is about one ninth of the amount annually released during combustion of fossil fuels globally (Quay et al., 1992).

Natural dissolved organic matter (NDOM) is derived mainly from microbes and plants and their degradation products. Its structure is complex and heterogeneous and may have a wide range of molecular masses in any particular water source (Findlay and Sinsabaugh, 2003; Frimmel, 1998). Through its interaction with other aquifer components including rocks, metals, and microbes, NDOM could play an important role in controlling the biogeochemistry and the chemical composition of groundwater. For example, NDOM can act as both a proton donor and acceptor, thereby buffering pH

(Frimmel, 1998; Jiang and Kappler, 2008; Ratasuk and Nanny, 2007), influencing mineral precipitation and dissolution, and fueling microbial biogeochemical reactions (Findlay and Sinsabaugh, 2003; Schlautman and Morgan, 1994). The presence of NDOM can mobilize or fix heavy metals such as As (Lee et al., 2005; Petrovic et al., 1999) and thus, may be a controlling factor in groundwater quality.

Among the abiotic NDOM transformations that may take place in karstic aquifers are sorption to mineral surfaces and dissolution/precipitation reactions of carbonate minerals. Sorption of NDOM by inorganic solid surfaces significantly alters the physiochemical properties of the underlying solid whose chemical behavior may become dominated by the adsorbed NDOM (Davis, 1982). Jin and Zimmerman (2010) found sorption of soil NDOM, as well as desorption of indigenous NDOM from carbonate rocks of the Floridan aquifer system. Organic compounds were found to enhance carbonate mineral dissolution or at least inhibit their precipitation by some studies (Inskeep and Bloom, 1986; Wu and Grant, 2002), while to inhibit carbonate dissolution as well as enhance precipitation by others (Hoch et al., 2000; Jin and Zimmerman, 2010; Lin and Singer, 2005) possibly by surface protection. Enhanced carbonate dissolution may lead to geological hazards such as land surface subsidence (Wu, 2003). Dissolution leads to enhanced permeability, exchange of surface water and groundwater, and thus, increased NDOM concentrations, which may act as a positive feedback to increase dissolution.

Transformations of NDOM in the subsurface usually involve consumption, production and alteration by subsurface microbes, which mediate biogeochemical redox reactions that can also alter dissolved inorganic species (Lovley and Chapelle, 1995;

Lovley and Chapelle, 1996). The NDOM used for these processes is largely supplied from the surface (Hancock et al., 2005). Consequently, concentrations of NDOM (measured by concentration of dissolved organic carbon, or DOC) and terminal electron acceptors such as O_2 and NO_3^- decrease away from recharge areas along flow paths due to microbial decomposition of NDOM (Alberic and Lepiller, 1998; Aravena et al., 2004; Lindroos et al., 2002; McCarthy et al., 1996; Pabich et al., 2001; Rauch and Drewes, 2004), while the products of NDOM mineralization, such as dissolved inorganic carbon (DIC) should display concomitant increases. Changes in DOC concentrations along flow paths may identify sources and movement of groundwater (Batiot et al., 2003; Lee and Krothe, 2001), although mineral dissolution/precipitation and other abiotic reactions may also affect its concentration. The number of processes that may change NDOM concentrations implies a multiple tracer approach, including DOC, DIC and major ion concentrations, stable isotopes, and OM composition, may be useful in discriminating among the various possible processes.

In this study, a multiple tracer approach was used to explore the abiotic/biotic processes that alter the quantity and quality of NDOM in a karstic system. Specifically, the relative magnitudes of physical mixing of various source waters, and abiotic and biotic chemical processes that control the quantity and quality of NDOM are assessed over a period of about 1 year in the surface waters of the Santa Fe River Watershed (SFRW), in north-central Florida, USA.

Study area

The SFRW is an ideal location for this type of study for a number of reasons. The watershed is variably confined and unconfined resulting in differences among regions in interactions of surface water and groundwater and its effect on NDOM transport and

transformation. Seasonal variations in precipitation, and associated NDOM input, generates a range of hydrologic conditions and allows for an assessment of flow controls on NDOM transformations.

The SFRW (Figure 2-1) drains water to the Suwannee River from 3585 km^2 of forests, agricultural land, and small towns in north-central Florida (Hunn and Slack, 1983). The watershed is entirely underlain by the upper Floridan aquifer, which is composed of Oligocene and Eocene carbonate rocks. The aquifer is confined by siliciclastic rocks of the Miocene Hawthorn Group in the eastern portion of the watershed and unconfined in the western portion (Figure 2-1). Average precipitation in the SFRW is 140 cm/year, which recharges the aquifer at different rates depending on seasonal changes in temperature, wind speeds, solar radiation, canopy cover, and the spatial variability of the confining Hawthorn Group (Grubbs, 1998; Ritorto et al., 2009). The recharge rates to the confined upper Floridan aquifer were determined to be less than 30 cm/year while recharge to the unconfined portion was between 40-80 cm/year (Grubbs, 1998).

The boundary between confined and semi-confined/unconfined portions of the upper Floridan aquifer is marked by the Cody Scarp, a marine terrace that is the erosional edge of the Hawthorn Group rocks (Scott et al., 1998). Where the Santa Fe River crosses the Cody Scarp, it descends into the ‘River Sink’ and flows approximately 7 km underground, re-emerging at the ‘River Rise’ (Martin and Dean, 2001). The Cody Scarp also marks the boundary between distinctly different river water compositions with high levels of DOC, low specific conductivity (SpC), comparatively high levels of P and low levels of N in the confined upper SFRW and, low DOC, high SpC, high N and

low P concentrations because of extensive mixing of surface water and groundwater in the unconfined lower SFRW (Katz, 1992). The SFRW is determined as oligotrophic based on the low chlorophyll-a data (< 0.1 mg/L at most sites, data obtained from STORET Data Warehouse http://www.epa.gov/storet).

Most surface water-groundwater exchange occurs near the Cody Scarp (Martin and Dean, 2001; Upchurch and Lawrence, 1984), but the extent of exchange depends on flow. Following large rainfall events, flows are dominated by overland runoff creating a blackwater phase (DOC-rich) along the entire course of the river. In contrast, during low flow periods, flows are dominated by groundwater discharging to the river through numerous springs and seeps in the lower watershed. Although these broad patterns of mixing between surface water and groundwater are known, less is known of how NDOM character varies with hydrologic condition, and how this influences other chemical processes.

Methods

Field sampling

During eight sampling trips between June 2010 and May 2011, surface water samples were collected at six USGS gauging stations, and River Sink and River Rise along the Santa Fe River and two of its major tributaries (Figure 2-1). The gauging stations, from upstream to downstream, are #23220700, #23221000 (on the New River), #23221500, #23222500, #23222700 (on the Ichetucknee River), and #23222800. Each station is referred to by the final number designation (e.g., 700, 1000, 1500, 2500, 2700, and 2800). No sample was collected at 2500 in June 2010 due to hard rain. New River and the lower reach of the Santa Fe River beyond 1500 were deemed to be the main

trunk of the river, for the purposes of this study because of its greater length and higher flow compared to the upper reach of the Santa Fe River.

Surface water samples were collected from the shore using a peristaltic pump (Geotech Geopump 2) attached to tubing that was extended close to center/main flow of the river and lowered to ~1 m below the surface where the channel was sufficiently deep and approximately half way between the water surface and the channel bed where the depth was less than 1 m. Before recording values of field parameters and collecting surface water samples, all tubing was flushed with at least four times the tubing volume of ambient water. Following flushing, field parameters including SpC, pH, dissolved oxygen (DO) and temperature were monitored with a calibrated YSI multiprobe model 556 placed in a free-flow cell until all field parameters stabilized (±5.0 % for SpC, ±0.2 for pH, ±20% for DO, and ±0.2 °C for temperature).

Samples for DIC and C stable isotope analyses were collected unfiltered, in glass vials leaving no airspace, and immediately preserved with $HgCl_2$ to prevent biological activity. All other samples were filtered in the field with 0.45 µm pore size in-line, trace-metal grade, canister filters. Samples for DOC analysis were collected in 40 mL amber glass vials that had been pre-combusted (450 °C, 4 h), and immediately preserved with 1M HCl to a pH ~3. Samples for spectrometric analysis were also collected in the same amber glass vials but with no addition of preservative. Anions and alkalinity (Alk) samples were collected filtered in high density polyethylene bottles with no preservatives added. Cations samples were collected filtered in 20 mL acid-washed bottles and preserved with trace-metal grade nitric acid to a pH < 2. All the samples were stored on ice and in the dark until they were delivered to the laboratory. In the

laboratory, the nutrient samples were frozen, and all other samples were refrigerated (4 ºC) prior to analysis.

Laboratory analyses

Analyses of DOC were performed on a Shimadzu TOC-5000A total organic carbon analyzer. After sparging for 2 minutes with carbon-free air to remove inorganic C, CO_2 was measured by IR detection after high temperature catalyzed combustion. Three to five injections of a 60 µL sample were measured and the mean of the injections was reported. Replicates of each samples had <5% coefficient of variance. The DIC concentrations were measured on CO_2 extracted by acidifying samples using an AutoMate Prep Device coupled with a UIC (Coulometrics) 5011 carbon coulometer. Results were standardized by measurement of dissolved $KHCO_3$ and had an accuracy of ±0.15 mg/L (n = 6). Stable isotopes of the DIC ($\delta^{13}C_{DIC}$) were measured using a ThermoFinnigan MAT 252 mass spectrometer. Isotopic results are expressed in standard delta notation relative to Vienna Peedee Belemnite (VPDB). Analytical precision was calculated to be ± 0.1‰.

Spectrophotometric characteristics, or 3-D excitation-emission matrices (EEMs), of the NDOM were examined using a fluorescence spectrometer (Hitachi F-7000). Spectrometric samples were kept in the dark before measurement and analyzed at room temperature. Excitation wavelengths range was set at 200 to 400 nm incremented at 10 nm intervals and emission wavelengths range from 200 to 600 nm at 3 nm intervals. Inner-filter corrections were carried out for each EEM using their absorbance spectrum (McKnight et al., 2001).

Major ions (F^-, Cl^-, Na^+, K^+, Ca^{2+}, Mg^{2+}, and SO_4^{2-}) were measured using an automated Dionex DX500 ion chromatograph. Charge balance errors for 48 out of 63

samples were less than ±5%. Saturation indices with respect to calcite and dolomite ($SI_{calcite}$ and $SI_{dolomite}$) were calculated using the geochemical code, PHREEQCI, Version 2.18.3-5570 and are given as:

$$SI = \log(\frac{IAP}{K}) \quad (2\text{-}1)$$

where IAP is the ion activity product and K is the equilibrium constant for a given mineral. Thermodynamic data for calculations were from the *phreeqc.dat* database. Partial pressure of CO_2 (P_{CO2}) for each sample collected was calculated using the same geochemical code and database. Alkalinity samples were titrated and measured at room temperature within 24 hours of sample collection. All sample analyses were conducted at the Department of Geological Sciences, University of Florida.

Collection of hydrologic data

Rainfall data were obtained from Suwannee River Water Management District data website (SRWMD, http://www.srwmd.state.fl.us/index.aspx?nid=345). Rainfall for each sampling site was obtained from the nearest SRWMD rainfall stations, which for sites 700, 2500, 2700 and 2800 were rain stations #02320601, #02322703, #241 and #02322800, respectively. Rainfall at 1000 and 1500 was obtained from station #235, while rainfall at the River Sink and Rise was obtained from station #240. Discharges at the six USGS gauge stations were obtained from the USGS website (http://waterdata.usgs.gov/fl/nwis/rt). Discharges were calculated from stage data (obtained from http://www.srwmd.state.fl.us/index.aspx?nid=345) using a rating curves developed (Screaton et al., 2004) for the River Rise, and the SRWMD for the River Sink (Rating No.9 for Station Number 02321898, Santa Fe River at O'Leno State Park).

Results

Hydrologic conditions

Although no major flooding occurred on the river during the sampling period, the river flow varied between about the 20th and 50th percentile of its 10-year average of flow, with the highest flow about 45% greater than base flow. For this study, eight sampling events were binned into periods of 'high flow' (Jun-10, Jul-10 and Sep-10), 'intermediate flow' (Feb-11 and Mar-11), and 'low flow' (Oct-10, Dec-10 and May-11), considering the discharge and rainfall in the study area on the sample days (Figure 2-2). Specifically, the binning was based on relative discharge at 1000 and 2800, which compose the upstream and downstream stations, compared to the historic discharge for that sampling day; discharges at these sites were close to historic values during 'high flow', but were far below historic values during 'low flow'. During the study period (June 2010 to May 2011), the discharge of Santa Fe River at 1000 and 2800 ranged from 0.0 to 4.2 m^3/s (average of 0.4 ± 0.7 m^3/s) and 25.7 to 42.5 m^3/s (average of 32.8 ± 5.1 m^3/s), respectively. The river discharges increased following precipitation with an approximate 3 day lag.

Organic carbon concentration variations

Concentrations of DOC were generally greatest near the Santa Fe headwaters and decreased downstream (Figure 2-3). The DOC concentrations in the upper SFRW ranged from 2.5 mg/L on Dec-10 to 63.4 mg/L on Jul-10 (average of 21.8 ± 16.6 mg/L, n = 32). These values are significantly different ($p < 0.001$) from those in the lower watershed, which ranged from 0.0 mg/L on Dec-10 to 44.0 mg/L on Sep-10 (average of 6.0 ± 9.0 mg/L, n = 31). At all stations, DOC concentrations varied with stage of the river, with highest concentrations occurring at times of elevated flow (Figure 2-3). For the

upper confined SFRW, DOC concentrations ranged from 12.4 to 63.4 mg/L (33.5 ± 18.3 mg/L, n = 12) during high flow, from 17.6 to 32.7 mg/L (26.4 ± 4.9 mg/L, n = 8) during intermediate flow, and from 2.5 to 15.3 mg/L (6.9 ± 4.0 mg/L, n = 12) during low flow. The DOC concentrations in the lower unconfined SFRW varied less relative to changes in discharge than in the upper confined region. For the lower watershed, DOC levels averaged 10.5 ± 12.9 mg/L (n = 11) during high flow, while they averaged 6.7 ± 6.3 mg/L (n = 8) and 1.5 ± 1.3 mg/L (n = 12) during intermediate and low flow, respectively. Differences in DOC concentrations in the upper watershed were significantly different ($p < 0.001$) during different flow conditions, but were not significantly different in the lower watershed.

Inorganic carbon concentration variations

Concentrations of DIC generally increased from the upper to lower portions of the watershed (Figure 2-3). The DIC concentrations in the confined upper SFRW ranged from 1.5 to 40.9 mg/L (16.5 ± 12.3 mg/L, n = 32), and were significantly ($p < 0.001$) lower than in the unconfined lower SFRW, where concentrations ranged from 9.0 to 40.8 mg/L (32.4 ± 7.2 mg/L, n = 31). Unlike DOC, the DIC concentrations were usually lower during high flow condition, and were higher during the low flow. For the upper watershed, DIC concentrations averaged 9.1 ± 8.0 mg/L (n = 12) during high flow, 10.7 ± 6.1 mg/L (n = 8) during intermediate flow, and 27.9 ± 10.5 mg/L (n = 12) during low flow. For the lower watershed, DIC concentrations averaged 28.4 ± 7.6 mg/L (n = 11) during high flow, 31.0 ± 7.9 mg/L (n = 8) during intermediate flow, and 37.1 ± 2.6 mg/L (n = 12) during low flow.

The DIC and DOC concentrations were found to be linearly and inversely correlated (significantly correlated during low flow, $p < 0.0001$), with slopes that became

more negative as river flow decreased (Figure 2-3).The slopes were -0.6 ± 0.0 (n = 3) at high flow, -1.0 (n=2) at intermediate flows, and -2.2 ± 0.3 (n = 3) at low flow. These changes in slope reflect a large decrease in DOC concentrations and a small increase in DIC concentrations with decreasing river discharge.

Stable carbon isotopic variations

Similar to DOC and DIC concentrations, $\delta^{13}C_{DIC}$ values varied spatiotemporally in the SFRW (Figure 2-4). In the upper watershed, the $\delta^{13}C_{DIC}$ values ranged from -18.5 to -10.2‰ (average of -13.2 ± 2.2‰, n = 32), and were significantly ($p < 0.001$) lighter and less constant than in the lower watershed, which ranged from -13.1 to -8.9‰ (average of -10.6 ± 0.9‰, n = 31). The $\delta^{13}C_{DIC}$ values also varied through time, with the lightest $\delta^{13}C_{DIC}$ values occurring during high flow and the heaviest during low flow. For the upper SFRW, $\delta^{13}C_{DIC}$ ranged from -18.5 to -10.4‰ (-14.2 ± 2.7‰, n = 12) during high flow, while they ranged from -15.8 to -12.0‰ (-13.8 ± 1.3‰, n = 8) during intermediate flow, and -13.7 to -10.2‰ (-11.7 ± 1.2‰, n = 12) during low flow. In the lower watershed, the $\delta^{13}C_{DIC}$ values varied little through time, without any significant differences between values for the different flows. The $\delta^{13}C_{DIC}$ values correlate positively with the DIC concentrations and have the largest slopes during high flow conditions.

NDOM spectophotometric characteristics

Changes in the quality of NDOM through the SFRW were examined by measuring excitation-emission matrices (EEMs) on a range of water samples. Representative EEMs from 700, 1500, River Sink, 2500 and 2800 during each flow conditions are shown in Figure 2-5 and all EEMs are presented in Appendix A. Fluorescence intensity is represented in arbitrary unit (a.u.). Most water samples had similar EEMs that contained both humic-like (A, excitation/emission wavelengths: 210-260 nm/410-450 nm)

and fulvic-like (C, 310-340/410-420 nm) fluorophores. In addition, most samples exhibited two relatively weak protein-like fluorophores (T1, 275-280/340-360 nm and T2, 215-220/310-340 nm). The protein-like fluorophores may be too weak to appear in Figure 5, but are clearly visible at higher resolution scales. These four main fluorophores detected were identical to those identified by others previously working in groundwater systems (Baker and Lamont-Black, 2001; Hudson et al., 2007).

Two fluorescence-derived indices, the fluorescence index (FI) and the humification index (HIX), have been used to identify the quality and origin of NDOM (Birdwell and Engel, 2010; Chen et al., 2010; Inamdar et al., 2012). The FI parameter provides a metric for estimating the degree of aromaticity, thus distinguishes between NDOM of terrestrial/soil origin (indicated by a low FI, < 1.4) and NDOM of microbial origin (indicated by a large FI, > 1.9, McKnight et al., 2001). The HIX provides an indicator of material's age and recalcitrance within a natural system. A HIX smaller than 5 suggests fresh NDOM, derived perhaps from aquatic production, while an HIX > 10 suggests humified NDOM(Ohno, 2002; Zsolnay et al., 1999).

The relationships between FI and HIX for the SFRW samples show consistent trends (Figure 2-7). Water collected at site 700 during high flow conditions displayed the most refractory NDOM composition in the SFRW, possessing the highest HIX and the lowest FI, and a fluorescence signature closest to a humic acid standard (Sigma-Aldrich, CAS#: 1415-93-6). Samples collected from 2700 on the Ichetucknee River, on the other hand, generally exhibited the most labile NDOM in the watershed, as they displayed the lowest HIX and the highest FI.

Discussion

These data reflect two endmember water types, a refractory DOC-rich/DIC-poor/$^{13}C_{DIC}$-depleted water in the upper watershed, and a more labile DOC-poor/DIC-rich/$^{13}C_{DIC}$-enrich water in the lower watershed. Water in the upper watershed is likely sourced from wetlands or soil water and join the rivers from overland flow, or, more likely, through the vadose zone. Water in the lower watershed is likely from groundwater discharged from springs discharging from the upper Floridan aquifer. Much of the spatiotemporal variations in DOC and DIC concentrations in the SFRW can be simply attributed to mixing of these two water sources, with a greater volume of DOC-rich during elevated flow and more DIC-rich water during low flow. The exports of DOC and DIC at different locations in the watershed and at different times are examined below to further understand variations in their relative contributions.

Riverine export of DOC and DIC at each sampling site were calculated by multiplying daily water discharge rates by their concentrations. During most flow conditions, DOC export generally increased downstream (Figure 2-6), suggesting that decreases in DOC concentrations are more likely due to dilution by DOC-poor groundwater than to consumptive processes. Greater export of DOC were recorded during high flow conditions, which typically occur during summer months, suggesting that inputs of DOC to the Santa Fe River are carried by surface runoff or rain water which infiltrates through the vadose zone, picking up various solutes such as NDOM.

Locations at which increased DOC export is found speak more to the distribution of stream capture points than to actual sources of NDOM. The greater increases in DOC export in the upper watershed, then, speak to the greater degree of soil infiltration and travel through the vadose zone in this confined portion of the watershed compared

to the lower watershed. As mentioned before, no major flooding occurred on the Santa Fe River during the 1-year sampling period. According to previous findings, the river should be gaining water as well as NDOM (if there was any in the matrix water) from the aquifer matrix between the Sink and the Rise during the study period (Martin and Dean, 2001; Moore et al., 2009). However, the prominent drop in NDOM export between the Sink and the Rise during intermediate flow contradicted with the pervious findings, indicating the inconsistence between the discharge data for the Sink/Rise (estimated by rating curves) and other sites (measured by USGS). Therefore, caution was used when dealing with the export at the Sink and the Rise.

The DIC export did not vary greatly with flow condition (Figure 2-6), suggesting that inputs of DIC-rich groundwater derived from the upper Floridan aquifer have a greater impact on DIC concentrations than biogeochemical processes in the watershed, and there was little temporal variation in the quantity of flow paths of these inputs. Regardless of flow condition, DIC export remained low in the confined portion of the SFRW and increased with distance below the Rise in the lower watershed. The greatest increase in DIC occurs between the Rise and site 2500, a portion of the river with an abundance of high magnitude springs. These springs contribute water with DIC concentrations similar to that found at site 2700.

These trends in DOC and DIC concentrations and exportations suggest qualitatively their sources and mixing proportions, these data may provide quantitative information on mixing proportions, as well as identify any DOC or DIC consumption or production within the watershed. Consequently, a model is developed below which

accounts for mixing in order to identify times and locations of biogeochemical reaction within the watershed that produce and consume DOC and DIC.

Biogeochemical processes affecting C dynamics in the SFRW

While it is recognized that numerous biogeochemical processes could influence DIC and NDOM quantity and quality in a riverine system, three pair of processes were deemed most important at the time and space scales examined: microbial mineralization/autotrophic production of NDOM, dissolution/precipitation of carbonate minerals, sorption/desorption of NDOM onto/from carbonate (Drever, 2002; Findlay and Sinsabaugh, 2003; Findlay et al., 2003; Frimmel, 1998).

Mineralization and autotrophic production of NDOM - Both microbial mineralization and algal production of NDOM is known to vary at the examined spatiotemporal scales in rivers (e.g., Birdwell and Engel, 2010). These processes can be generalized by the following reaction (Schwarzenbach et al., 2003), which proceeds to the right for mineralization, and to the left for production assuming eventual transformation of algal biomass to NDOM via exudation, lysis, etc.:

$$NDOM + Oxidant \longleftrightarrow DIC + H^+ + H_2O \quad (2\text{-}2)$$

During mineralization, NDOM is decomposed to DIC by heterotrophic microbes or during nighttime respiration of subaquatic plants (e.g., de Montety et al., 2011) using an oxidant such as free oxygen and releasing protons in the process. The increased acidity could drive dissolution of carbonate minerals. Mineralization of NDOM is also likely to add isotopically light biogenic C to the water, shifting $\delta^{13}C_{DIC}$ toward values ranging -30 to -25‰ (Clark and Fritz, 1997).

The reverse reaction of NDOM mineralization, autotrophy or the production of OM from an inorganic C source, might increase concentrations of DOC and oxygen, while decreasing DIC and raising water pH and $\delta^{13}C_{DIC}$ due to preferential uptake of isotopically light C. Thus, autotrophic production of NDOM may enhance precipitation of carbonate.

Dissolution and precipitation of carbonate minerals - Dissolution and precipitation of carbonate minerals (e.g., calcite and dolomite) are common in natural aquatic systems (Drever, 2002). Extensive surface water-groundwater exchange, such as in the SFRW, can affect river water composition. Calcite and dolomite dissolution, respectively, can be represented by the following equations (Drever, 2002):

$$CaCO_3 + H^+ \longleftrightarrow Ca^{2+} + HCO_3^- \quad (2\text{-}3)$$

$$CaMg(CO_3)_2 + 2H^+ \longleftrightarrow Ca^{2+} + Mg^{2+} + 2HCO_3^- \quad (2\text{-}4)$$

During carbonate mineral dissolution, concentrations of Ca^{2+} and Mg^{2+} are likely to increase, as is the total alkalinity and SpC of the water. The $\delta^{13}C_{DIC}$ value of the water will also increase, shifting toward the C isotopic signature of marine limestone (about 0‰, Clark and Fritz, 1997). In addition, pH should increase due to H^+ consumption, as should $SI_{calcite}$ and $SI_{dolomite}$. Lastly, carbonate dissolution may release OM that is incorporated in the structure of the carbonate minerals, as has been observed experimentally for these rocks (Jin and Zimmerman, 2010).

NDOM Sorption/desorption - Sorption/desorption of NDOM by carbonate minerals might affect both the quantity and quality of NDOM without altering DIC concentration or $\delta^{13}C_{DIC}$ values (Findlay and Sinsabaugh, 2003; Frimmel, 1998; Schwarzenbach et al., 2003). Floridan aquifer materials were reported to contain OM in concentrations ranging

0.38 to 1.29 wt. % with up to 6.6% of it subject to desorption (Jin and Zimmerman, 2010). Sorption/desorption of NDOM may also influence NDOM composition as higher molecular weight, and thus more refractory, NDOM will be preferentially sorbed by carbonate minerals (Jin and Zimmerman, 2010). Sorption of NDOM has also been shown, in various studies, to either enhance precipitation or inhibit dissolution of carbonate (Frye and Thomas, 1993; Jin and Zimmerman, 2010; Thomas et al., 1993).

Water source mixing model

Effects of mixing different water sources on DOC and DIC of river water must be assessed before it is possible to identify the times and locations of the occurrence of various biogeochemical processes and their relative magnitudes. To do this, a quantitative mixing model was developed based on assumed concentrations of Na^+, Cl^- and SO_4^{2-}in endmember waters. Expected DOC and DIC concentrations were calculated based on mixing ratios derived from the ion concentrations. Difference between the modeled and observed concentrations in a given water sample were assumed to represent a local biogeochemical production or consumption of DOC or DIC.

Construction of the mixing model: Mixing of three SFRW endmember water sources were identified, based upon the above observations and previous work (Moore et al., 2009; Moore et al., 2010): a soil water, a groundwater and a deep water. Water collected from site 700 during high flow on Jul-10 is assumed to represent the soil water endmember because this sample showed the lowest DIC and highest DOC levels and the lightest $\delta^{13}C_{DIC}$ values among all samples collected during the one-year sampling period. The groundwater endmember is assumed to be represented by water from site 2700 on the Ichetucknee River on Jul-10 since it displayed the heaviest $\delta^{13}C_{DIC}$ values among all samples. The deep water endmember is assumed to have elevated SO_4^{2-},

Ca^{2+} and Mg^{2+} concentrations (Moore et al., 2009; Moore et al., 2010) but similar DOC and DIC concentrations and $\delta^{13}C_{DIC}$ signature as the upper Floridan aquifer groundwater. Moore et al. (2009) identified this water as upwelling from several hundred meters depth in the aquifer and estimated it may represent up to 24% of the River Rise discharge at low flow conditions. The composition of the deep water source was represented by water collected at Well 2, a groundwater monitoring well located ~2 km southwest of the River Sink on 1/17/2007, as this sample had the highest overall inorganic ion concentrations during the monitoring period 2003-2007 (Moore et al., 2009). The water chemistry of each endmember is provided in Appendix D.

The concentrations of Na^+, Cl^- and SO_4^{2-} were used to define the mixing model endmembers and to estimate the proportions of water from each source at each site because all three were assumed to be conservative in this system. Na^+ and Cl^- show a good linear correlation ($R^2 = 0.81$, $p < 0.0001$, Appendix B) with an average molar Na/Cl ratio of 0.87 ± 0.18 (n = 63), similar to that of seawater (0.86). This ratio suggests Na^+ and Cl^- are sourced from sea spray entrained into precipitation and are not modified by reactions. SO_4^{2-} is enriched in the deep water endmember to an even greater extent (about 15 times) than Ca^{2+} and Mg^{2+} (Appendix D, Moore et al., 2009). Because DO and NO_3^- concentrations are elevated in Santa Fe River water, SO_4^{2-} should not be reduced and thus is less reactive than Ca^{2+} or Mg^{2+}, which could be modified by carbonate mineral dissolution and precipitation (de Montety et al., 2011), and thus, was not likely to be involved in biogeochemical reactions.

The mixing model was based on a mass-balance approach, assuming the following four equations:

$$f_{soil} + f_{gw} + f_{deep} = 1 \quad (2\text{-}5)$$

$$SO4_n = f_{soil} SO4_{soil} + f_{gw} SO4_{gw} + f_{deep} SO4_{deep} \quad (2\text{-}6)$$

$$Na_n = f_{soil} Na_{soil} + f_{gw} Na_{gw} + f_{deep} Na_{deep} \quad (2\text{-}7)$$

$$Cl_n = f_{soil} Cl_{soil} + f_{gw} Cl_{gw} + f_{deep} Cl_{deep} \quad (2\text{-}8)$$

where *f* is the volumetric fraction of each endmember: 'soil', 'gw' and 'deep' representing soil water, groundwater, and deep water, respectively. $SO4_n$, Na_n and Cl_n are the concentrations of SO_4^{2-}, Na^+ and Cl^- in any given water sample *n*. The equations were solved simultaneously using the concentrations of each sample to estimate the fraction of each endmember.

Source water mixing patterns: Soil and groundwater endmember sources account for most of spatial and temporal variations in mixing (Figure 2-8). In general, the fraction of soil endmember source decreased and groundwater endmember source increased downstream. The largest spatial change occurs across the Cody Scarp (between 1500 and the Sink), with the soil water endmember contribution ranging from ~43% to 100% in the upper watershed (sites 700, 1000 and 1500) and 0% to ~27% in the lower watershed (sites 2500, 2700 and 2800). The groundwater endmember contribution ranged 0% to ~55% in the upper watershed and ~67% to 100% in the lower watershed. The soil water and groundwater endmembers contributed to the river flow without temporal difference, all ranging from ~0% to ~100%. The largest contribution of deep water to the river was lower than the largest contribution found by Moore et al. (2009), ranging from 0 to ~19%. Similar to Moore et al., (2009), the largest proportions occurred at the Rise site. The fraction of deep water was not correlated with the fraction of soil water or groundwater sources.

In order to evaluate the stability and quality of our mixing model, a series of sensitivity analyses were performed (details in Appendix E), in which the chemistry of each endmember was altered by one standard deviation and examining the resulting change in source contributions calculated. The sensitivity analysis showed that the proportion of soil water and groundwater endmember could change up to 29% by altering the Cl^- or Na^+ concentration, whether during high or low flow periods, particularly in the upper watershed. Other than that, the model is generally insensitive to the small changes in endmember chemistry.

Biogeochemical processes: The compositions of all solutes that are not included in the mixing calculations (DOC, DIC, Ca^{2+}, DO, pH etc.) are predicted by assuming the compositions are controlled solely by mixing of the different endmembers. The difference between the predicted and actual measured value (Δ) result from biogeochemical process which causes a gain (for a positive Δ value) or a loss (for a negative Δ value) of the component (Figure 2-9). In Figure 2-9, samples that plot within Quadrants I and IV, have gained DOC, while samples that plot in Quadrants I and II have gained DIC over the value that would occur simply from mixing. Similarly, samples that plot in quadrants II and III have lost DOC, while samples that plot in Quadrants III and IV have lost DIC.

DIC production (Quadrants I and II) may occur through either NDOM mineralization or carbonate dissolution. Dissolution of atmosphere CO_2 as a source of DIC is unlikely because the SFRW was supersaturated with respect to atmospheric CO_2 ($\log P_{CO2} = -2.4 \pm 0.5$ atm). Loss of DIC (Quadrants III and IV) may occur through either microbial autotrophic activities or carbonate precipitation. DIC may be lost through

degassing to the atmosphere (Hoffer-French and Herman, 1989; Li et al., 2010; Telmer and Veizer, 1999) and uptake by subaquatic vegetation (de Montety et al., 2011), but both were considered to be a smaller magnitude than carbonate precipitation because of the nature of the karstic hydrological system (de Montety et al., 2011; Li et al., 2010). These trends and the association of specific samples with biogeochemical processes are discussed further in the following.

Quadrant II: More samples plot in Quadrant II than any other quadrants and all hydrologic conditions and sample locations are represented (Figure 2-9). Twenty five of the 40 samples in Quadrant II (Figure 2-9), have $\Delta DO < 0$ indicating oxygen is being consumed. Oxygen consumption, along with the positive ΔDIC and negative ΔDOC values, suggests microbial mineralization of NDOM although other geochemical parameters (e.g., ΔCa, ΔSpC, SI) suggest carbonate mineral reactions may also affect the DIC and DOC concentrations.

The samples in Quadrant II can be divided into two groups, with Group 1 samples generally showing more positive ΔDIC and more negative ΔDOC than Group 2 samples. The 20 samples in Group 1 have significantly greater ΔSpC values ($p < 0.001$, 111.5 ± 48.2 µS/cm) than those in Group 2 (63.8 ± 34.6 µS/cm) and higher ΔCa ($p = 0.11$, 0.3 ± 0.2 mg/L) and ΔMg ($p < 0.001$, 0.3 ± 0.2 mg/L) values than group 2 samples (ΔCa = 0.2 ± 0.2 mg/L, ΔMg = 0.1 ± 0.1 mg/L). In addition, $\delta^{13}C_{DIC}$ values of samples in Group 1 are isotopically heavier than expected from mixing ($\Delta\delta^{13}C_{DIC}$ = 3.7 ± 2.3‰), suggesting they may derive some DIC from carbonate mineral dissolution. In contrast the $\Delta\delta^{13}C_{DIC}$ values in Group 2 exhibited little difference from its endmember sources ($\Delta\delta^{13}C_{DIC}$ = -0.2 ± 0.8‰). Lastly, $SI_{calcite}$ and $SI_{dolomite}$ for Group 1 samples are negative indicating

undersaturation with respect to these minerals (-0.4 ± 0.7 and -1.2 ± 1.4, respectively) and significantly lower ($p < 0.0001$) than those in Group 2 (0.4 ± 0.4 and 0.3 ± 0.9, respectively), which are supersaturated. Group 1 samples also have positive ΔHIX (31.8 ± 12.9) and negative ΔFI (-0.1 ± 0.2) values.

These observations suggest that Group 1 samples were modified by dissolution of carbonate minerals, while Group 2 samples might have lost DIC via carbonate precipitation. Dissolution would be expected from the increase in acidity as a result of NDOM mineralization (Alberic and Lepiller, 1998; Li et al., 2010). Group 1 samples may also have gained DOC via desorption of NDOM from carbonate rocks (Jin and Zimmerman, 2010). The positive ΔHIX and negative ΔFI suggest the occurrence of both NDOM mineralization and carbonate mineral dissolution, which would cause the NDOM pool to become more refractory. Because the ΔDOC is negative, DOC loss by NDOM mineralization must have occurred at a greater rate than DOC gain by carbonate dissolution.

Group 2 samples may experience NDOM-mineral sorption, which is often linked with carbonate precipitation (Frye and Thomas, 1993; Jin and Zimmerman, 2010; Thomas et al., 1993) and could be responsible for the observed shift toward a more labile NDOM pool as evidenced by its smaller ΔHIX (6.1 ± 3.5) compared to Group 1 samples (31.8 ± 12.9). The significantly lower ΔpH values of Group 2 versus Group 1 samples ($p < 0.0001$, 0.2 ± 0.4 versus 1.7 ± 1.3, respectively) may reflect preferential sorption of acidic moieties in NDOM by carbonate from Group 2 water samples (Jin and Zimmerman, 2010) as well as carbonate precipitation. However, based on the positive

ΔDIC of Group 2 samples, DIC loss by NDOM mineralization must have occurred at a greater rate than DIC loss by carbonate precipitation.

The samples with the greatest NDOM mineralization were collected during low or intermediate flow conditions and most are from Sites 700, 1000, and 1500. Slow flow in the upper watershed may allow more time for heterotrophic microbes to respire NDOM and for biogeochemical products such as DIC and H^+ to accumulate, the latter leading to carbonate dissolution. The lower watershed receives more groundwater, which is often supersaturated with carbonate minerals and likely to degas CO_2 after leaving the subsurface environment, which may result in carbonate precipitation (Hoffer-French and Herman, 1989; Li et al., 2010). Extensive NDOM mineralization in the upper watershed would preferentially consume labile NDOM, resulting in the observed more refractory NDOM pool in the upper than lower watershed.

Quadrant III: The second most common ΔDIC and ΔDOC values occur in Quadrant III, with 12 samples (Figure 2-9). Most of these samples (≥ 8) also have negative ΔCa, ΔDIC, ΔAlk, and ΔSpC values as well as positive ΔpH, suggesting carbonate minerals may have precipitated. However, all samples were undersaturated with respect to carbonate minerals. It may be that SI calculations are not reliable in that concentrations of PO_4^{3-} were not taken into consideration. Most samples in this quadrant were collected from the upper SFRW where high levels of phosphorus are often measured (Katz, 1992). The precipitation of carbonate may affect the NDOM concentrations through sorption (Frye and Thomas, 1993; Jin and Zimmerman, 2010; Thomas et al., 1993), which is supported by positive ΔpH values in most samples resulting from sorption of acidic NDOM groups. On the other hand, observations that

imply the occurrence of NDOM mineralization include the negative ΔDO values found in 8 out of 12 samples and lighter $\delta^{13}C_{DIC}$ values (-14.0 ± 2.3‰) than those in other quadrants. In any case, the net loss of DIC indicates that carbonate precipitation likely occurs at a greater rate than NDOM mineralization.

Most samples that plot in Quadrant III were collected during high and intermediate flow conditions. Carbonate precipitation is more likely during these warmer periods, because higher water temperature often induces more CO_2 outgassing (Hoffer-French and Herman, 1989; Li et al., 2010; Telmer and Veizer, 1999). Carbonate precipitation should be more common in the upper than the lower watershed, perhaps because the water in the upper SFRW during high and intermediate flow conditions is higher in temperature (26.0 ± 0.9 °C versus 19.9 ± 5.4 °C for the lower watershed) resulting from its darker color or lack of groundwater input.

Quadrant IV: Though plotting in a quadrant indicative of net autotrophic production, most of the five samples in Quadrant IV show evidence of NDOM mineralization: negative $\Delta\delta^{13}C_{DIC}$ and ΔDO values (Figure 2-9). Mineralization of NDOM increases water acidity (ΔAlk < 0 in all samples; ΔpH < 0 in 3 of 5 samples) and may induce carbonate dissolution (Alberic and Lepiller, 1998; Li et al., 2010). Evidence of carbonate dissolution is found in the positive ΔSpC in 2 of 5 samples and negative $SI_{calcite}$ and $SI_{dolomite}$ in 4 of the 5. Dissolution of Floridan aquifer materials may result in NDOM-mineral desorption and produce the positive ΔDOC values of these samples (Jin and Zimmerman, 2010). Positive ΔDOC values show that DOC gain via desorption and carbonate dissolution outpaced the DOC loss via mineralization. The interplay and

relative reaction magnitudes of these two processes are also reflected in the lower ΔHIX in this quadrant (i.e. less lability decrease, 0.4 ± 5.7) than those in others.

Negative ΔDIC values suggest DIC is lost by CO_2 outgassing. All the samples were collected during high flow when higher water temperature makes CO_2 outgassing more likely (Hoffer-French and Herman, 1989). Further, the increase in acidity in water may also cause more CO_2 degassing by limiting the hydrolysis of H_2CO_3 (Drever, 2002).

Samples in Quadrant I and others close to the origin: Ten samples including, all those within Quadrant I, display small deviations in DIC or DOC from those values expected by mixing and are within 4 mg/L of the origin. Most of them were collected from the Rise or site 2700 during low or intermediate flow conditions where most of the river water originates from the aquifer. When conduit water is largely comprised of aquifer matrix water with long aquifer residence time in the aquifer and so is expected to be ion-rich due to carbonate dissolution (Martin and Dean, 2001; Moore et al., 2009; Screaton et al., 2004). Yet, only small positive ΔSpC, ΔCa, ΔMg and ΔpH are found in most samples. This model suggests, therefore, that carbonate dissolution may be common when the matrix water emerges into conduits or springs.

Spatiotemporal variations in biogeochemical processes

Mineralization of NDOM has been noted in several studies of karstic subsurface (Hancock et al., 2005; Kortelainen and Karhu, 2006; McMahon, 2001; Pronk et al., 2006). For example, about 20 - 24% of the injected NDOM was reported mineralized during an aquifer storage and recovery (ASR) operation in a karstic aquifer in South Australia (Vanderzalm et al., 2006). Similar to these other studies, NDOM is lost throughout the SFRW, as the model indicates that almost all samples collected experienced some degrees of NDOM mineralization. This finding is consistent with the

fact that most inland aquatic ecosystems are net heterotrophic (Wetzel, 2001). The greatest net NDOM mineralization was found to occur during low flow condition and mainly in the upper watershed (Quadrant II-Group 1 samples; Figure 2-8). This mineralization is unlikely to result from input of soil NDOM in the upper watershed, which would occur during high rather than low flow, and this type of NDOM is refractory (Figure 2-7). Instead, this pattern may be attributed to the higher water temperatures enhancing microbial heterotrophic activity, and lower primary productivity due to lower nutrient and more colored (i.e. UV light absorbing, Laurion et al., 1997; Morris et al., 1995) waters in the upper relative to the lower watershed. Furthermore, larger fractions of soil-derived water in the upper watershed may contain more heterotrophic microorganisms and terminal electron acceptors, and therefore, allow greater microbial respiration rates.

The occurrence of net autotrophy (NDOM production) is not apparent from the model results, possibly due to its smaller magnitude than NDOM mineralization. Despite this, one might still expect greater rates of autotrophic production during the summer, stimulated by greater solar radiation. Indeed, greater riverine autotrophic production might have rendered the river water more oxygenated during summer (ORP = 215.1 ± 64.6 mV versus 160.4 ± 123.6 mV during winter, $p = 0.11$). Autotrophic production in the lower watershed is suggested by the observation of positive correlations between DOC and intensity of protein-like fluorophores (Appendix C, T1: $R^2 = 0.8$, T2: $R^2 = 0.3$, both $p < 0.001$), representing fresh microbially derived components (Baker and Spencer, 2004; Coble, 1996; Parlanti et al., 2000). In contrast, samples from the upper watershed exhibited inverse correlations (T1: $R^2 = 0.3$, T2: $R^2 = 0.8$, both $p < 0.001$), implying that

autotrophic activity did not contribute to DOC, perhaps related to light limitation as DOC concentrations increased. Autotrophic production may not be primarily from algal photosynthesis, because the algal biomass (i.e. chlorophyll-a concentrations) is low in the entire watershed (data obtained from STORET Data Warehouse http://www.epa.gov/storet). Instead, subaquatic vegetation photosynthesis is of greater importance, as dense native submerged C3-macrophytes, including tapegrass (*Vallisneria Americana*) and eelgrass (*Sagittaria kurziana*) cover up to 78% of the surface of the river bed in some Florida springs (Canfield and Hoyer, 1988; Kurz et al., 2004). Previous studies assessed the Ichetucknee River in the lower watershed to be high in benthic production (Heffernan et al., 2010), which also support autotrophic production mainly occur via subaquatic vegetation photosynthesis.

Based on where samples plot on Figure 9, carbonate dissolution occurred mostly commonly in the upper watershed during low flow periods, while carbonate precipitation occurred in the lower watershed during all flow conditions. Calcite and dolomite saturation indices support this observation, with most negative SI values occurred in upper watershed samples during low flow, while most positive values occurred in the lower watershed samples during low flow. In contrast, carbonate precipitation was also indicated during high flow, as most samples fall in Quadrant III were collected during high flow periods. The lower ions concentrations detected in the water during high flow (Ca/Cl ratio = 3.0 ± 2.4, Mg/Cl ratio = 0.7 ± 0.3, SpC = 245.9 ± 116.0 µS/cm) versus low flow (Ca/Cl ratio = 4.3 ± 2.3, Mg/Cl ratio = 1.5 ± 1.0, SpC = 358.5 ± 98.4 µS/cm) may be further evidence of carbonate precipitation. Net carbonate dissolution in the upper watershed during low flow may be an outcome of extensive NDOM mineralization as

suggested by previous studies that found this relationship in other karstic systems (Alberic and Lepiller, 1998; Li et al., 2010). On the other hand, net carbonate precipitation in the lower watershed is likely as CO_2 charged water degases as it discharges from the aquifer (Martin and Dean, 2001; Moore et al., 2010).

NDOM-mineral desorption was commonly indicated in the upper SFRW during low flow, while NDOM-mineral sorption was more commonly indicated in high flow as well as in the lower SFRW during low flow. Previous laboratory sorption experiments showed that refractory NDOM is preferentially sorbed by aquifer materials (Jin and Zimmerman, 2010). Thus, NDOM-mineral sorption may be more common during high flow because of its greater abundance at this time. However, one study of an artificial recharge (AR) operation in southern Finland, found 23% of the decrease in DOC in the injection water was attributed to mineral adsorption (Kortelainen and Karhu, 2006).

The above biogeochemical processes, mineralization/production of NDOM, dissolution/precipitation of carbonate, and sorption/desorption of NDOM, had less influence on C variations in the SFRW than hydrologic mixing. Biogeochemical processes were more important to the water chemistry in the upper watershed and during low flow periods than in the lower watershed. For example, the biogeochemical processes at site 2800 on Sep-10 altered DOC and DIC by 0.9 mg/L and 2.3 mg/L, respectively, while hydrologic mixing changed DOC and DIC by 9.4 mg/L and 27.8 mg/L, respectively. On the same day at site 1000, biogeochemical processes had a greater influence on C concentrations, producing changes in DOC and DIC that were roughly half to a third those of hydrological mixing. However, the prominent variations in C

dynamics resulting from biogeochemical processes were clearly related to or driven by hydrologic mixing, and seasonal variations of the watershed hydrology.

Riverine carbon export

Spatiotemporal variation in DOC and DIC transport through the SFRW results from the net effect of water source mixing and biogeochemical processes (Figure 2-10). The amounts of DOC and DIC originating in the lower watershed, estimated as the difference in C export between these two sites, exceed those produced in the upper watershed. On a daily average basis, the DIC that is exported from the lower watershed is estimated to be 104 ton during high flow and 94 ton during low flow (about 20 and 134 times that of the upper watershed). Most of this DIC originates from inflow of carbonate-equilibrated groundwater in the lower watershed.

However, the greater amount of DOC originating in the lower versus upper watershed, despite its smaller area, is surprising. The lower watershed produced 10.9 ton/day DOC during high flow and 2.5 ton/day during low flow, 1.5 and 25 times greater than the upper watershed, respectively. While a small part or this lower watershed-derived DOC is from soil NDOM, the majority of it (10.2 ton/day or 93.6% during high flow periods) is associated with groundwater influx. A small portion of this DOC may also be produced by lower watershed autotrophy.

During the year of this study, and making the assumption, supported by hydrographic data (Figure 2-2), that there were about 6-months of high flow and 6-months of low flow, the SFRW was calculated to export ~8500 ton of dissolved C. This is a very small portion of the estimated 0.8×10^9 - 1.6×10^9 ton of dissolved C delivered by rivers each year to the global ocean (Ludwig et al., 1996; Suchet et al., 2003). On an area-normalized basis, however, the dissolved C exported from the SFRW was about

7.6 ton/km^2/year, including 3.2 ton/km^2/year DOC and 4.4 ton/km^2/year DIC. This area-normalized DOC export is similar to that of other temperate watersheds in the U.S., such as the Suwannee River, FL (4.3), Russian River, CA (2.6), Pearl River, LA (3.2), and Satilla River, GA (4.6) (Mulholland and Watts, 1982), and only somewhat lower than that of tropical or peat-dominated watersheds, which are on the order of 5-10 ton/km^2/year (Aitkenhead and McDowell, 2000). On the other hand, the SFRW exported more DIC than many high-latitude watersheds (e.g., Ottawa River Basin: 3.5 ton/km^2/year, Telmer and Veizer, 1999) and tropical watershed (e.g., Nyong watershed: 0.9 ton/km^2/year, Brunet et al., 2009). Also, it should be recognized that the 8500 ton C/year figure for SFRW is likely a low estimate given that the year studied was a relatively dry year. Thus, generalizing further, karstic watersheds may export a globally significant amount of C considering their vast coverage on earth surface. For instance, given that karst areas occupy 20% of land surface in the U.S. (Ford and Williams, 2007) and assuming the measured SFRW C exports are typical, karst watershed may contribute ~15.2×10^6 ton of C per year, an amount of C similar to half the amount of CO_2 emitted by cement production in U.S. in 2010 (30.5×10^6 ton, USEPA, 2012).

Conclusions

Much of the spatiotemporal variations of organic and inorganic C observed in the SFRW during the 1-year sampling period could be ascribed to mixing of three water sources in the SFRW (groundwater, soil water and deep water). By taking into account the effects of mixing, C dynamics were found also include biogeochemical processes such as NDOM mineralization/production, carbonate dissolution/precipitation and NDOM sorption/desorption. Therefore, the source water mixing model used here has

shown itself to be a powerful tool to evaluate watershed-scale investigations of C dynamic processes in this complex system.

The results of this study indicate that karstic watersheds export a significant amount of C given their vast coverage on earth surface. Thus, the study of C dynamics in karstic watershed could contribute to a more comprehensive understanding of regional and global C cycling. This study also has implications for the management of hydrogeologic projects such as ASR and aquifer recharge. For instance, it is clear from this study that groundwater chemistry, and NDOM in particular, can alter riverine biogeochemical processes in karstic areas. In addition, biogeochemical processes in a watershed have significant effects on riverine ecology and water quality. For example, subaquatic vegetation growth was found to be closely linked with the riverine nutrient and oxygen dynamics (Heffernan et al., 2010; Schulz and Kohler, 2006) both of which are tied to riparian zone C dynamics. Also, carbonate precipitation/dissolution can influence concentrations of phosphorus (House, 1990; Neal et al., 2002) and metals (Nimick et al., 2003; Zachara et al., 1991) in natural fresh water systems.

Future work is needed that will simultaneously examine spatiotemporal variation in additional chemical proxies such as nutrients, stable isotope of organic C, and metals (e.g., iron) to better identify the occurrence of and quantify rates of biogeochemical processes. High resolution sampling during larger flood events and over diurnal cycles are also recommended in order to scrutinize the evolution of watershed-scale biogeochemical processes. Direct sampling of groundwater in both shallow and deep aquifer would also be helpful in expanding our understanding of karstic biogeochemistry and surface-subsurface interactions.

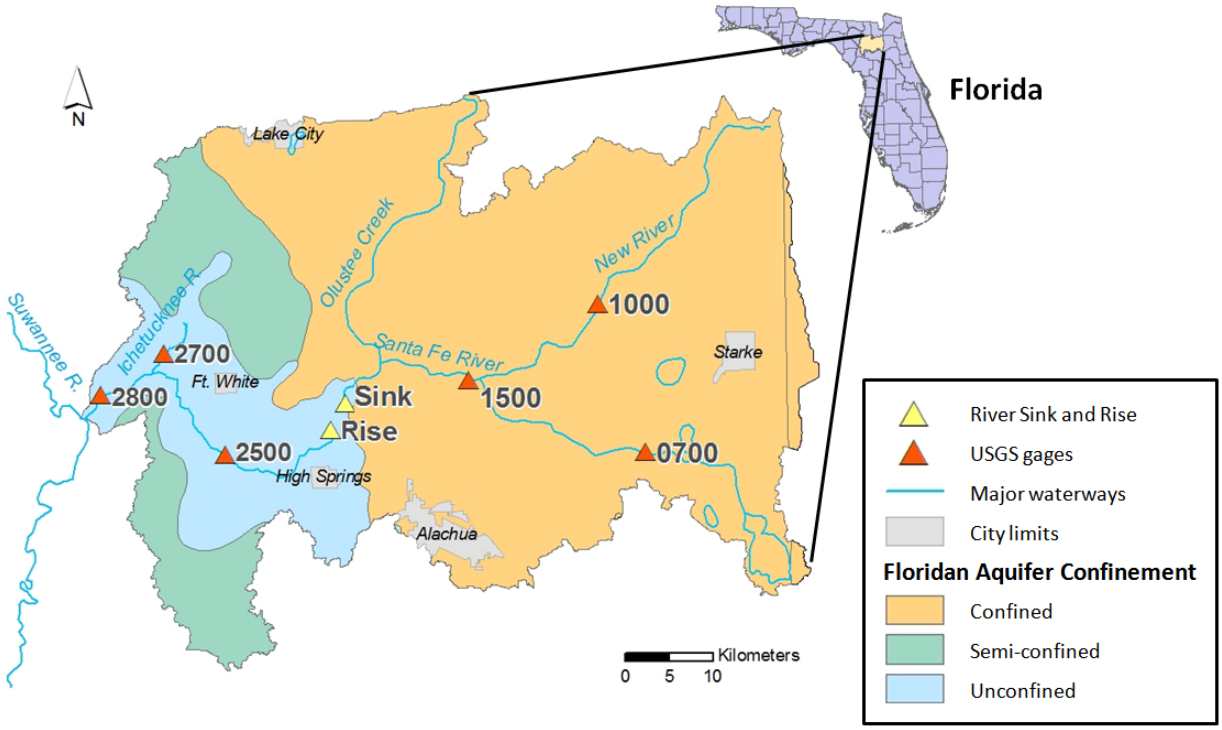

Figure 2-1. Study area in north Florida showing hydrogeologic regimes, and sampling sites: six USGS gage stations and River Sink and River Rise in the O'Leno State Park.

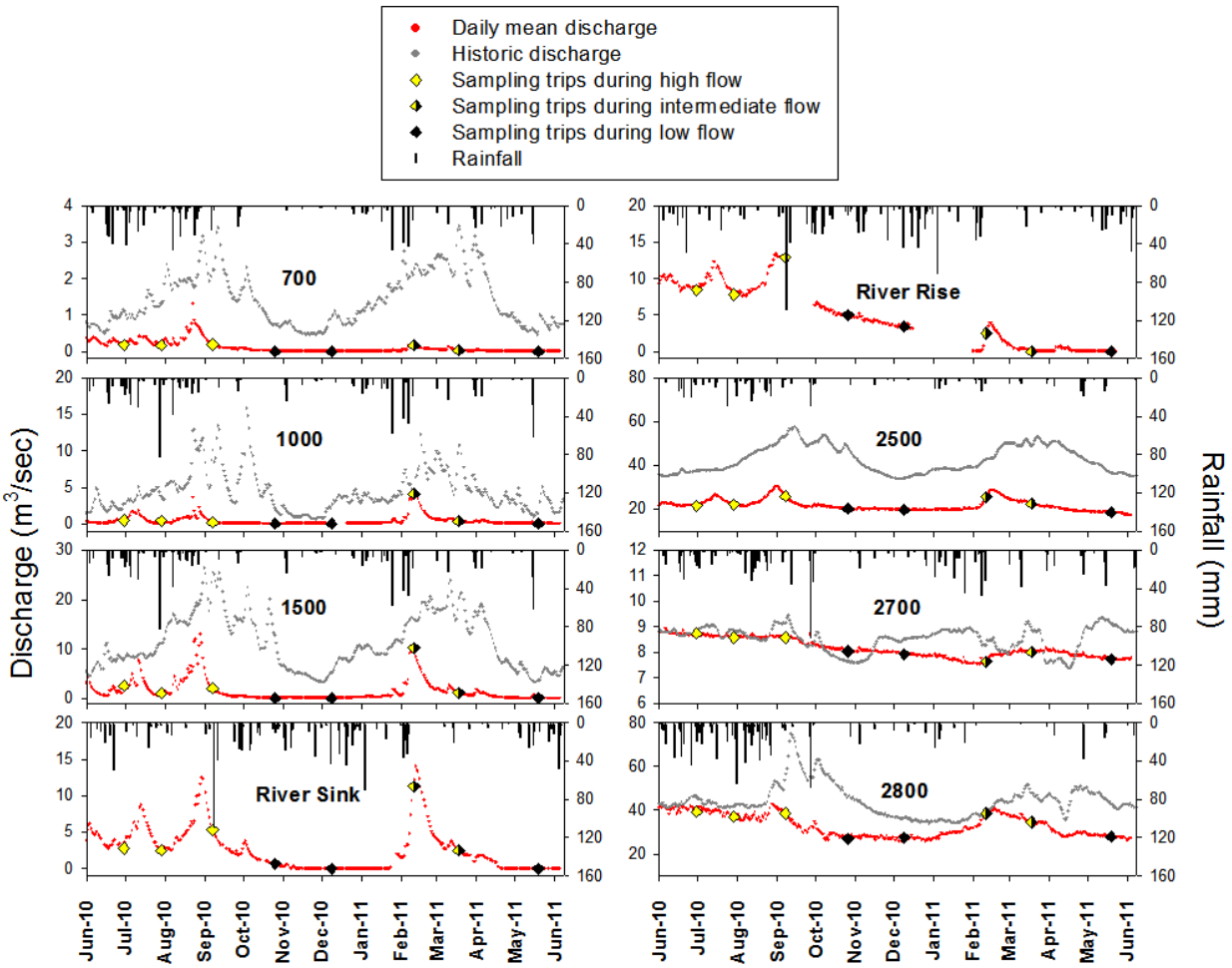

Figure 2-2. Hydrologic condition of the SFRW. Daily mean (red points) and historic mean (grey points) discharge (in m^3/sec; calculated for about 50 y of data) of the Santa Fe River at eight sampling sites as well as rainfall data recorded at nearby SRWMD rainfall stations. The River Rise and River Sink do not have long term records of flow. Eight sampling times are designated as either high, intermediate or low flow (yellow, half-yellow or black diamonds, respectively).

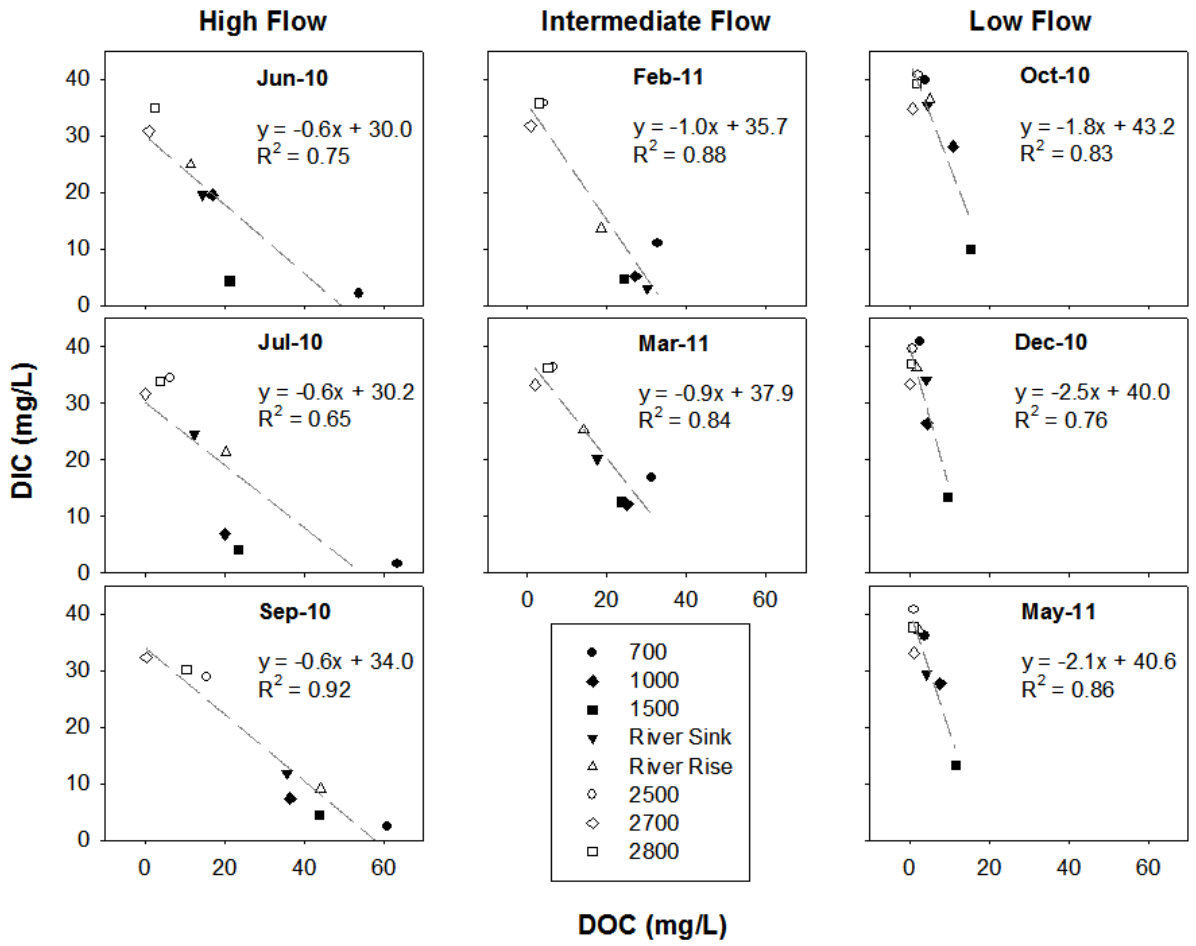

Figure 2-3. Relationship between DIC and DOC concentrations in water samples collected from both confined (closed symbols) and unconfined (open symbols) portions of SFRW during high, intermediate and low flow conditions (in columns left to right). Dashed lines and the equations indicate the linear regression of the DIC-DOC relationship.

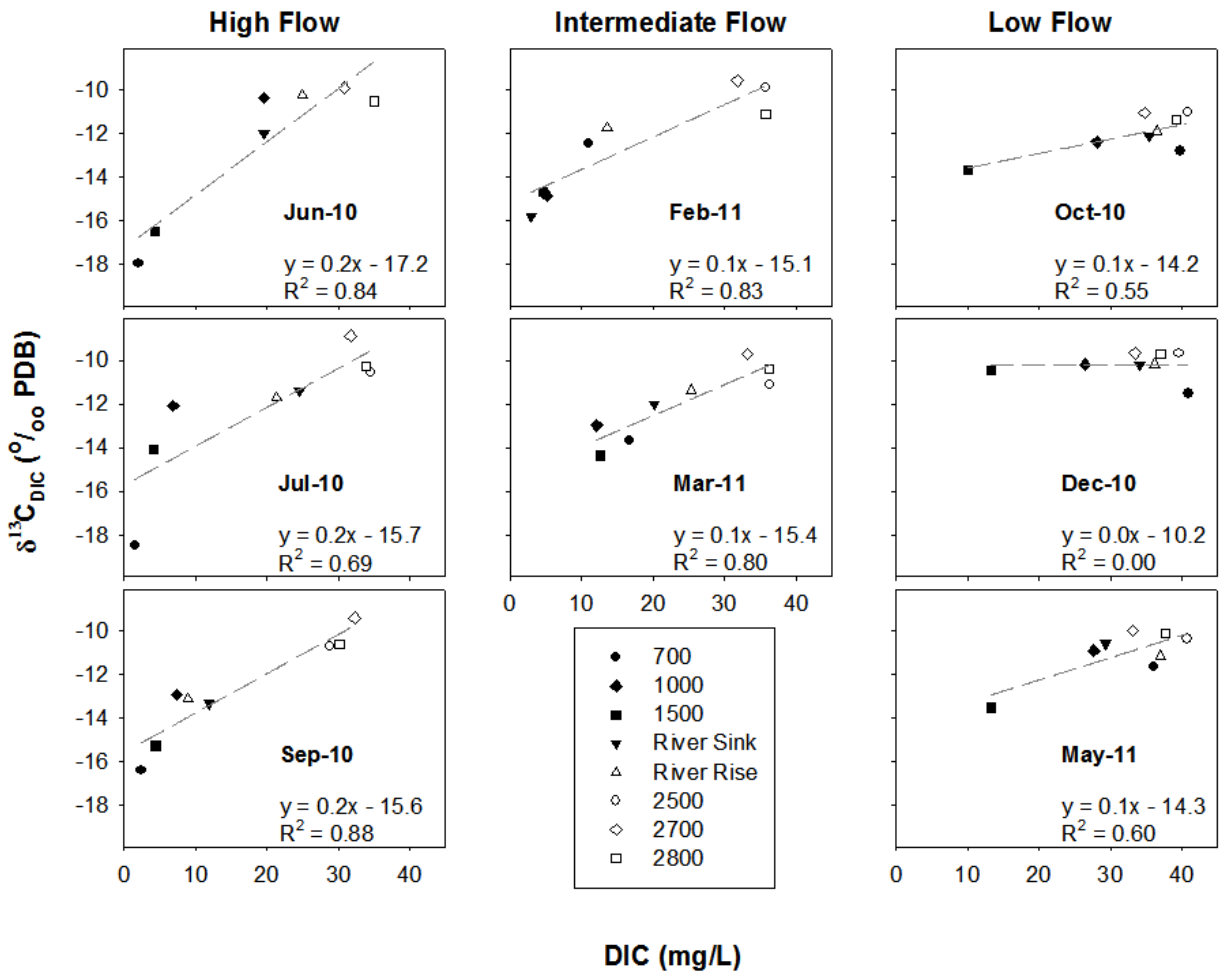

Figure 2-4. Relationship between $\delta^{13}C_{DIC}$ and DIC concentrations for water samples collected from both confined (closed symbols) and unconfined (open symbols) portions of SFRW, during high, intermediate and low flow conditions (in columns left to right). Dashed lines and the equation indicate the linear regression of the DIC-$\delta^{13}C_{DIC}$ relationship.

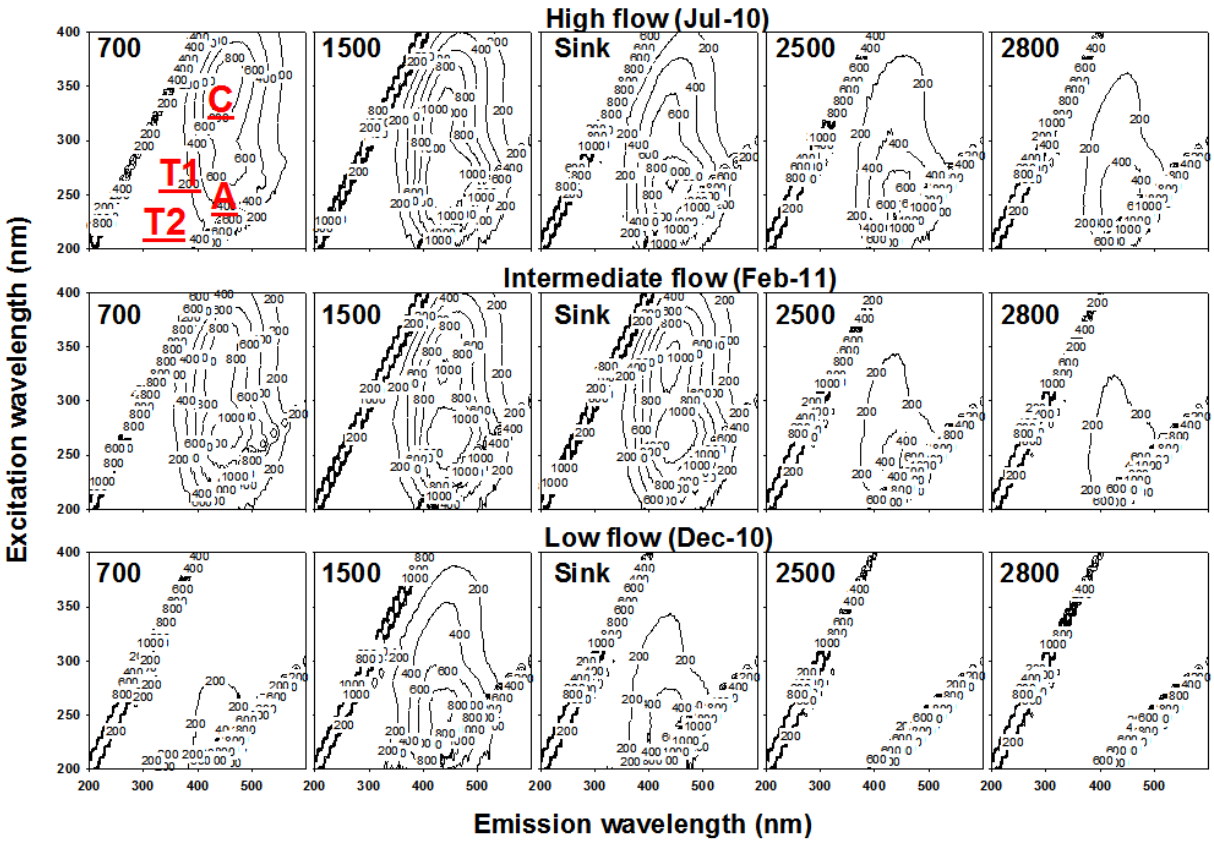

Figure 2-5. Representative excitation-emission matrices (EEMs) for water samples of the SFRW with position of fulvic-like (Peak C), humic-like (Peak A), and tryptophan-like (Peaks T1 and T2) fluorophores indicated in upper left panel only. Shown are EEMs from sites 700, 1500, River Sink, 2500 and 2800 during high flow (Jul-10), intermediate flow (Feb-11), and low flow conditions (Dec-10). The diagonal lines in each EEM are caused by the Rayleigh-Tyndall effect. Fluorescence intensity is represented in arbitrary unit.

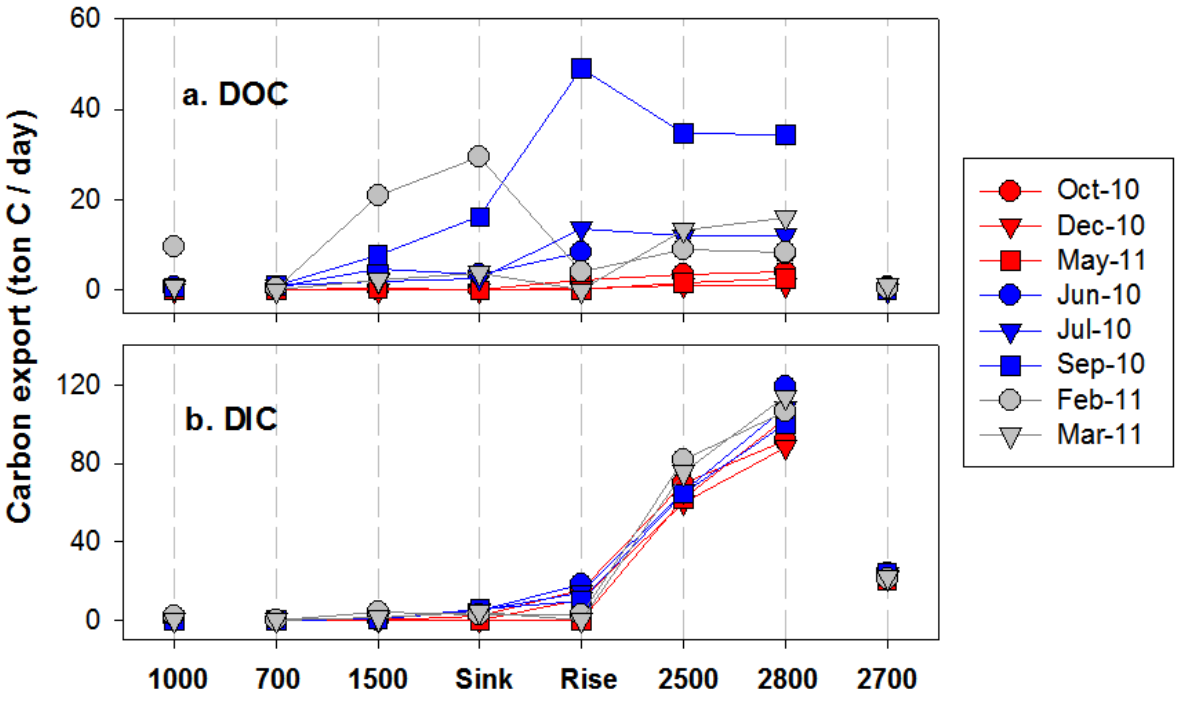

Figure 2-6. Riverine carbon exports at sampling sites in the SFRW, during high (blue), intermediate (grey) and low flow (red) conditions.

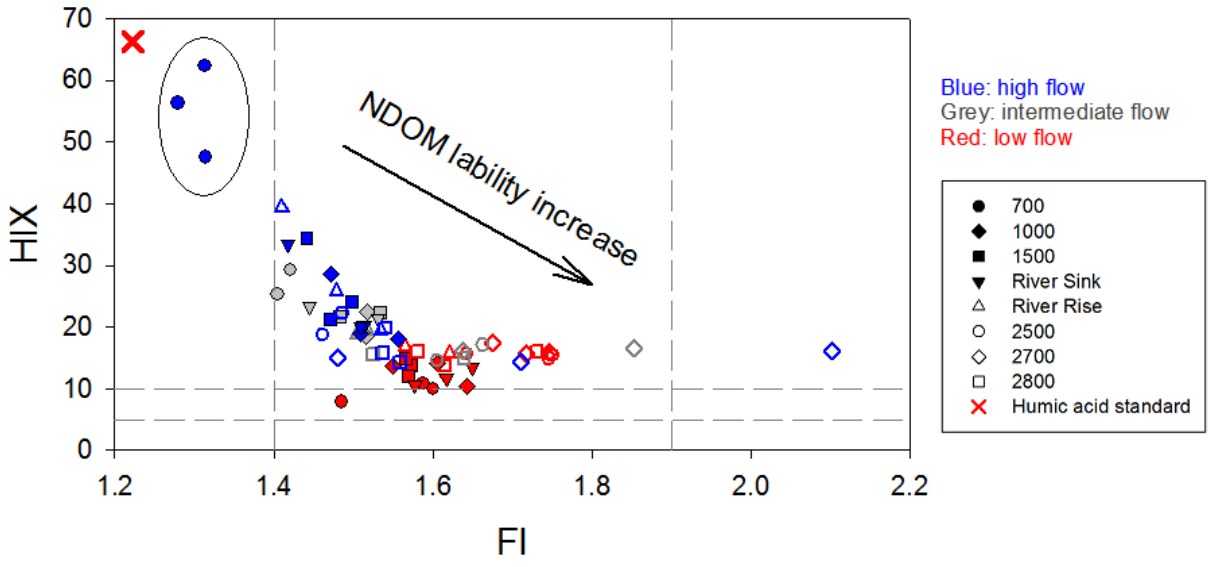

Figure 2-7. Relationship between two fluorescence indices, FI and HIX for water samples collected from both confined (closed symbols) and unconfined (open symbols) portions of SFRW, during high (blue), intermediate (grey) and low flow (red) conditions. Data in circles are those collected from site 700 during high flow conditions.

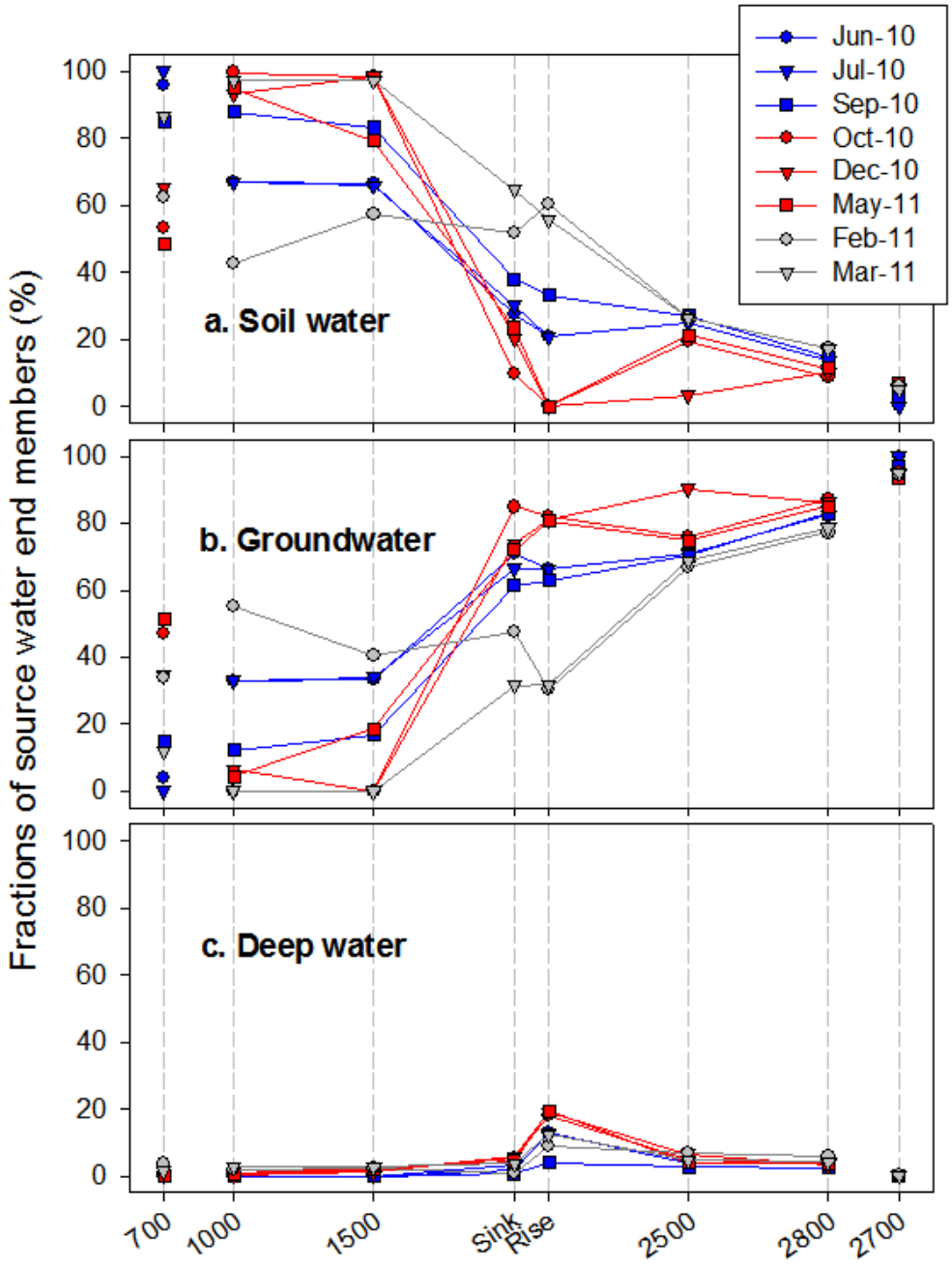

Figure 2-8. Results of the water source mixing model shown as the fractions (in %) of a) soil water, b) groundwater, and c) deep water theoretical endmembers in each sample collected at each of eight sites during high (blue), intermediate (grey), and low (red) flow conditions. Scales on X-axis represent the approximate distance downstream between sampling sites following the main channel down the New River at Site 1000 to Site 2800 on the Santa Fe River(Fig. 1). Sites 700 and 2700 are included to demonstrate their compositions.

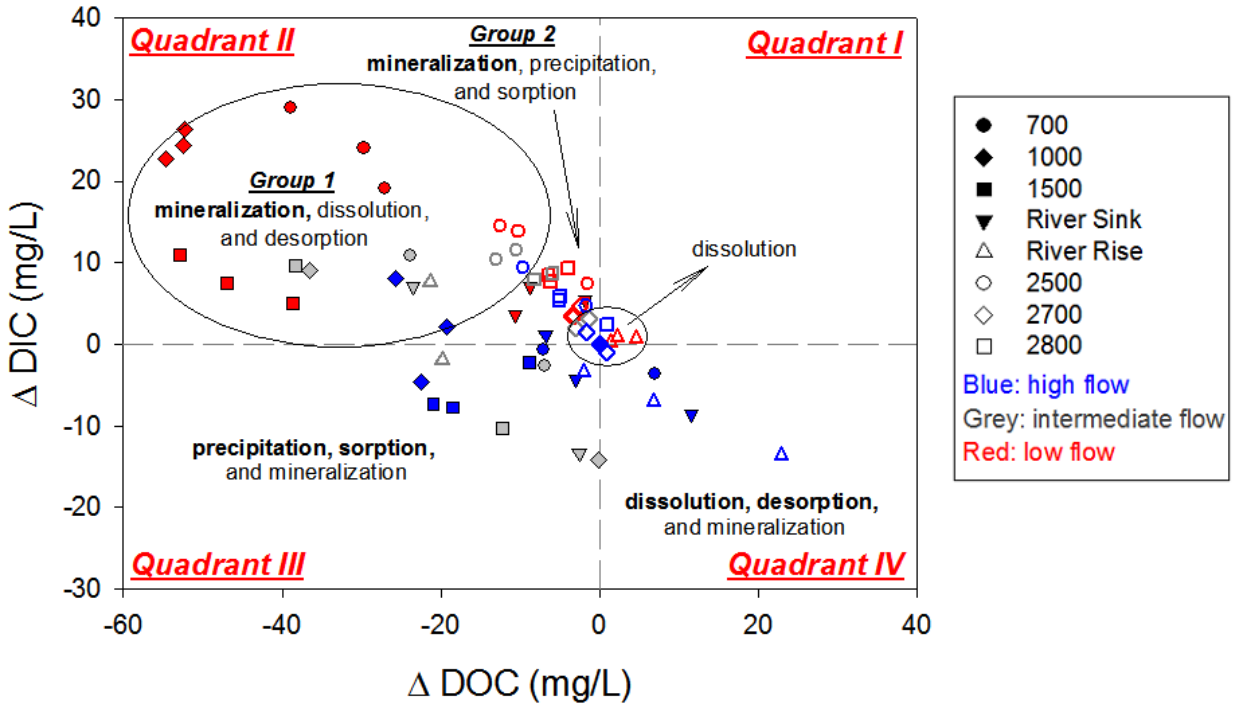

Figure 2-9. Differences between the model-predicted and actual measured dissolved aqueous inorganic carbon and organic carbon concentrations (ΔDIC and ΔDOC, respectively) in samples from confined and unconfined (open and closed symbols, respectively) portions of the SFRW during high, intermediate and low (blue, grey, and red, respectively) flow conditions. Possible biogeochemical processes responsible for differences are listed in each quadrant, with the dominant ones, as proposed in text, in bold font.

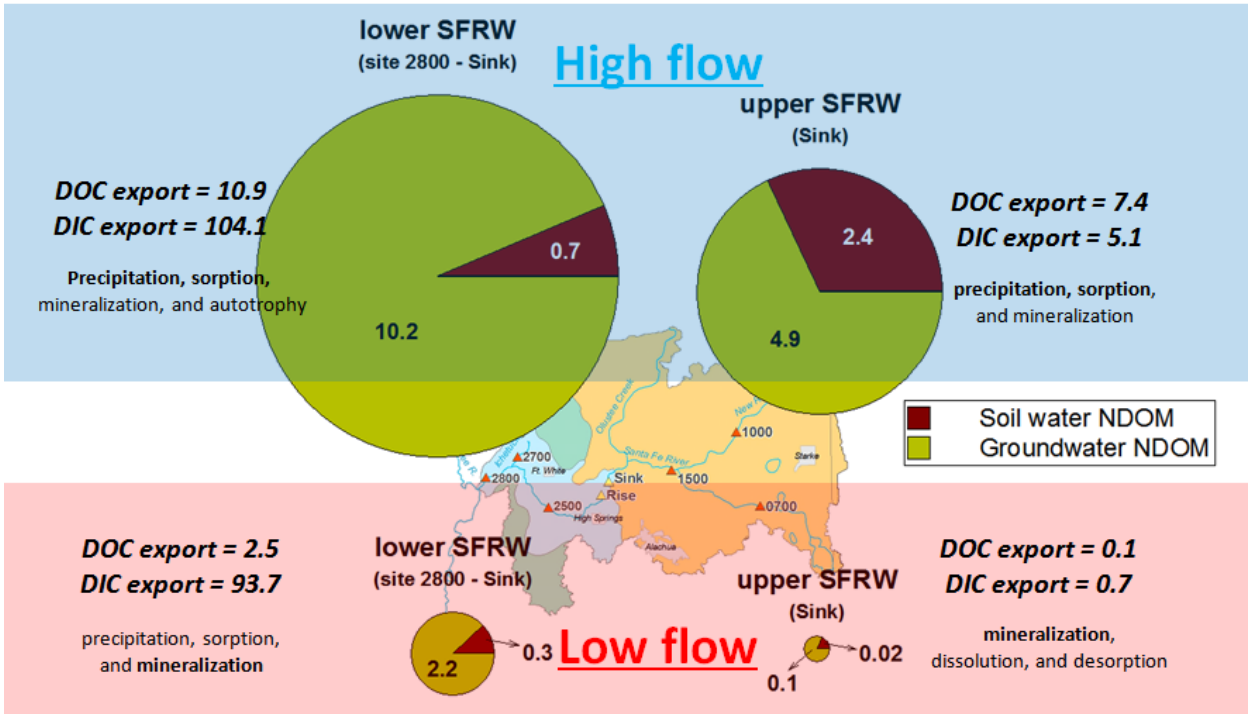

Figure 2-10. Daily carbon export (in ton/day) at representative sites in the upper and lower watershed. Export of organic carbon by presumed source are represented in four pie charts. Export of inorganic carbon are shown relative to each organic carbon export, along with presumed dominant biogeochemical processes that contribute to gain or loss of C from the river, with the major ones in bold fonts.

CHAPTER 3
A WINDOW INTO THE ORGANIC AND INORGANIC CARBON DYNAMICS OF A KARSTIC AQUIFER (O'LENO SINK-RISE SYSTEM, FLORIDA, USA)

Background

Karstic aquifers are important geomorphic features as they cover 25% of the global land surface and provide 25% of the drinking water supplies to all humans (Ford and Williams, 2007). Because of their typically high permeability (Worthington, 1994) and thus, close connectivity to the surface, they receive relatively large fluxes of natural dissolved organic matter (NDOM, Lau and Mink, 1987) and associated nutrients. Likewise, karstic aquifers are susceptible to contaminates from the surface, whose fate and transport is largely controlled by the water-rock-microbe interactions in the subsurface. Karstic areas may also be an important but overlooked part of global carbon (C) cycling. As the biggest C reservoir on the Earth, carbonate rocks contain about 6.1×10^7 billion tons of C, which is a few thousand times greater than the amount in the ocean, the next larger reservoir (Falkowski et al., 2000; Houghton and Woodwell, 1989). The annual C uptake by karstic aquifers has been estimated to be up to 0.6 billion tons of C, which is about one ninth of the amount annually released globally by combustion of fossil fuels (Quay et al., 1992).

It has been recently recognized that the flow in a karstic aquifer includes conduits, fractures, and intergranular porosity of the matrix (Martin and Dean, 2001; Screaton et al., 2004). A better understanding of flow in a karstic aquifer together with NDOM and other solutes it carries requires understanding flow in multiple portions of the aquifer. However, most well-studied aquifers are those with low intergranular porosity and permeability, where flow is dominantly via conduits. Few studies have focused on karstic aquifers with permeable and porous matrix rocks such as the upper Floridan

aquifer, which retains up to 20% intergranular matrix porosity (Randazzo and Jones, 1997).

NDOM, derived mainly from microbes and plants and their degradation products, is complex and heterogeneous in nature with a wide range of molecular masses and chemical structures (Findlay and Sinsabaugh, 2003; Frimmel, 1998). Through its interaction with other aquifer components including rocks, metals, and microbes, NDOM plays an important role in controlling the biogeochemistry and hydrogeology in the subsurface. For example, NDOM can act as a proton donor or acceptor buffering pH (Frimmel, 1998; Jiang and Kappler, 2008; Ratasuk and Nanny, 2007), influence mineral precipitation and dissolution or fuel microbial biogeochemical reactions (Findlay and Sinsabaugh, 2003; Schlautman and Morgan, 1994). The presence of NDOM considerably influences the mobilization and fixation of heavy metals such as As (Lee et al., 2005; Petrovic et al., 1999) and thus, may be a controlling factor in groundwater quality in the course of hydrogeologic projects such as aquifer storage and recovery (ASR) and aquifer recharge (AR; Arthur, 2002; Pavelic et al., 2005). Knowledge of NDOM and its behavior in groundwater is limited, however, due to the complexity of these systems with and spatiotemporal hydrological variability, multiple coupled biotic-abiotic interactions which may serve as sources and sinks of NDOM, as well as methodological difficulties related to sampling the subsurface.

Among the abiotic interactions that may take place in karstic aquifers are sorption and dissolution/precipitation reactions of minerals. Sorption of NDOM onto inorganic solid surfaces significantly alters the physiochemical properties of the underlying solid whose behavior may become dominated by the adsorbed OM (Davis, 1982). Jin and

Zimmerman (2010) recorded significant adsorption of soil OM, as well as desorption of indigenous OM from carbonate rocks of the Floridan aquifer system. Organic compounds have also been shown to enhance carbonate mineral dissolution or at least inhibit precipitation (Inskeep and Bloom, 1986; Wu and Grant, 2002). At other times, OM sorption has been shown to inhibit carbonate dissolution possibly due to surface protection, as well as enhance their precipitation (Hoch et al., 2000; Jin and Zimmerman, 2010; Lin and Singer, 2005), Enhanced carbonate dissolution is an environmental concern as it may lead to geological hazards such as land surface subsidence (Wu, 2003).

Subsurface microbes produce, consume, and transform NDOM and in doing so, mediate biogeochemical redox reactions that alter inorganic species (Chapelle et al., 2002; Lovley and Chapelle, 1995). One simplifying assumption in the study of subsurface microbial metabolism is the almost complete reliance on NDOM supplied from the surface (Hancock et al., 2005). Concentrations of dissolved organic carbon (DOC) and terminal electron acceptors such as O_2 and NO_3^- should decrease along water flow path from recharge areas due to microbial decomposition of NDOM, while the products of NDOM mineralization, such as dissolved inorganic carbon (DIC) should display concomitant increases. Strong attenuation of DOC along groundwater flow paths has been observed in many previous studies (Alberic and Lepiller, 1998; Aravena et al., 2004; Lindroos et al., 2002; McCarthy et al., 1996; Pabich et al., 2001; Rauch and Drewes, 2004). Changes in DOC concentrations along flow paths may be employed to identify sources and movement of groundwater (Batiot et al., 2003; Lee and Krothe, 2001). However, changes in DOC concentrations can also result from mixing of multiple

sources, mineral dissolution/precipitation and other abiotic reactions. Because of the number of processes that may change concentrations, a multiple tracer approach that combines the DOC, DIC and major ion concentrations, as well as stable isotopes and OM composition may be useful in discriminating among the various possible processes.

This study uses this multiple tracer approach to examine the relative magnitudes of source-water mixing, abiotic and biotic processes that control the quantity and quality of organic and inorganic C over a period of about 6 y in the O'Leno Sink-Rise portion of the Santa Fe River in north Florida. The Sink-Rise system is an ideal location for this type of study for a number of reasons. As the Santa Fe River traverses the Cody Scarp that divides the upper Floridan aquifer into confined and unconfined portions, the shallow overlying formations at this location make sampling of the shallow and deep and conduit and matrix portions of the aquifer logistically feasible and provide contrast to examine hydrogeological influences on NDOM dynamics. The large seasonality in precipitation (and NDOM flux) allows for a clear separation between processes occurring during high and low flow periods. Lastly, a number of previous hydrological and hydrogeological studies carried out at this site (Langston et al., 2012; Martin and Dean, 2001; Moore et al., 2009; Moore et al., 2010; Ritorto et al., 2009; Screaton et al., 2004) provide the necessary framework upon which to examine the biotic and abiotic NDOM transformation processes which occur in the complex system of karst aquifers.

Study area

The Santa Fe River in north Florida (Figure 3-1) flows westward from Lake Santa Fe and surrounding wetlands, for about 40 km until it reaches the Cody Scarp, where it sinks into a 36-m deep sinkhole at the River Sink in O'Leno State Park. The river flows ~7 km underground through a network of conduits in the karstic upper Floridan aquifer

(UFA) until it reemerges at the River Rise, a first-magnitude spring, marking the start of the lower Santa Fe River which flows to the Suwannee River (Martin and Dean, 2001; Moore et al., 2009). In this region, the UFA extends from the Upper Eocene Ocala Limestone to the lower confining unit of the Lower Eocene Cedar Key Formation (Miller, 1986). It is about 430 m thick but unconfined at the surface, only covered by a thin veneer of unconsolidated sediments (Miller, 1986). Porosity and matrix permeability within the Sink-Rise system have been reported as ~30% and 10^{-13} m^2, respectively (Budd and Vacher, 2004; Florea and Vacher, 2006).

Previous work has shown that the water discharging at the Rise varies in composition from that similar to the Santa Fe River at the Sink to that of the groundwater (Martin and Dean, 2001; Moore et al., 2009; Screaton et al., 2004) i.e. aquifer water sampled in deep wells which have had no recent contact with the surface or water components recently at the surface. During periods of high flow of the Santa Fe River, discharge at the Rise mostly derives from water entering the conduit system at the Sink, while during low flow, discharge at the Rise largely comes from groundwater draining from the surrounding aquifer matrix into the conduit system (Martin and Dean, 2001). A more detailed study of deep water inorganic chemistry variation identified three endmember water types in the subsurface including that from: 1) diffuse recharge through a thin vadose zone, 2) water upwelling from deep within the aquifer, and 3) allogenic recharge, or concentrated point inputs such as sinking streams (Moore et al., 2009). Diffuse recharge and upwelling deep water was calculated as providing up to 50% of the Rise discharge. The exact contribution of each source, however, depends upon head gradients between the conduit and surrounding aquifer matrix, which are

influenced by variations in precipitation, evapotranspiration and river stage (Moore et al., 2009).

Methods

Field sampling

Both surface water and groundwater samples were collected during 44 sampling trips between March 2005 and May 2011 as well as a high frequency sampling campaign during a storm event of March 2008 (Figure 3-2). Effort was made to sample during extremes of both ‘dry’ and ‘wet’ periods, based on consideration of both precipitation and hydrograph patterns. Surface water samples were collected at three sites (the Sink, the Rise and Sweetwater Lake) in the O’Leno State Park, FL (Figure 3-1). Groundwater samples were collected from nine groundwater monitoring wells, including both five deep and four shallow wells. Four of the deep wells (W4, 5, 6 and 7) were paired with shallow wells (W4a, 5a, 6a and 7a) at the same site. Deep wells were drilled to approximately the depth of the conduits (~30 meters below ground surface, or mbgs), while the shallow wells were drilled to the average depth of the water table (~10 mbgs). Detailed information about the location of wells can be found in Appendix G.

Surface water samples were collected from the shore using a peristaltic pump (Geotech Geopump 2) attached to tubing lowered to ~1 m below the surface with the end extended on a pole close to the spring boil or the deepest part of the sinkhole. Groundwater samples were collected using a Grundfos II submersible pump attached to tubing and lowered to a depth of approximately three feet below the water level in the well. Prior to sampling each well, water level was measured and recorded. Before recording values of field parameters or collecting groundwater or surface water samples, all tubing was flushed with at least 2 L of ambient water, which represented in excess of

four times the tubing volume. Following flushing, field parameters including specific conductivity (SpC), pH, dissolved oxygen (DO) and water temperature were recorded from an YSI multiprobe (model 556) placed in a free-flow cell constructed from a 500 mL PVC bottle.

Samples for DIC and C stable isotope analyses were collected unfiltered, in glass vials leaving no airspace, and immediately preserved with $HgCl_2$. All other samples were filtered in the field with 0.45 µm pore size Geotech engineering dispos-a-filters. Samples for DOC analysis were collected in 40 mL amber glass vials that had been pre-combusted (450 °C, 4 h), and immediately preserved with 1M HCl to a pH ~3. Samples for anion and alkalinity (Alk) analyses were collected in high density polyethylene bottles with no preservatives added. Samples for cation analyses were collected in 20 mL acid-washed bottles and preserved with trace-metal grade nitric acid to a pH < 2. All the samples were stored on ice and in the dark until they were delivered to the laboratory each day.

Chemical analyses

The DOC concentrations of the acidified samples were measured on a Shimadzu TOC-5000A via high temperature catalyzed combustion and measurement of CO_2 by IR detection, after sparging for 2 minutes with carbon-free air to remove inorganic carbon. For samples collected in 2007 and 2008, the DIC concentration was measured on unacidified samples using the same TOC analyzer. For both DOC and DIC, three to five injections of a 60 µL sample were measured. Only data with <5% coefficient of variance was accepted. For samples collected before 2007 and after 2008, DIC concentrations were measured on an automated coulometer (UIC). Stable isotopes of the DIC ($\delta^{13}C_{DIC}$) were measured using a ThermoFinnigan MAT 252 mass spectrometer. Isotopic results

are expressed in standard delta notation relative to Vienna Peedee Belemnite (VPDB). Analytical precision was ±0.1‰.

For samples collected from March 2005 to April 2007, concentrations of major ions (Na^+, K^+, Ca^{2+}, Mg^{2+}, F^-, Cl^-, and SO_4^{2-}) and alkalinity were analyzed by a NELAC-certified laboratory (Advanced Environment Laboratories, Inc., Gainesville, FL) in accordance with protocol developed by the U.S. Environment Protection Agency (USEPA, 1983). These results have been reported previously (Martin and Moore, 2007; Moore et al., 2009). For samples collected after April 2007, concentrations of major ions and alkalinity were measured by Dr. P. Moore in the Department of Geological Sciences at University of Florida. Concentrations of major ions were measured on an automated Dionex DX500 ion chromatograph and alkalinity was measured (within 24 hours of sample collection) by titration at room temperature. Most (221 out of 248) samples collected during the 6-year study period have charge balance errors of less than ±5%. Saturation indices with respect to calcite and dolomite ($SI_{calcite}$ and $SI_{dolomite}$) were calculated using the geochemical code, PHREEQCI, Version 2.18.3-5570. Thermodynamic data were provided by the *phreeqc.dat* database. Partial pressure of CO_2 (P_{CO2}) for each sample collected was calculated using the same geochemical code and database.

Hydrologic data

Rainfall and river stage data were obtained from Suwannee River Water Management District data website (SRWMD, http://www.srwmd.state.fl.us/documentcenterii.aspx). Daily precipitation in the O'Leno State Park is represented by the data from SRWMD rain station # 240 (29°55'12"N, 82°36'27"W) collected by an automated rain gauge. Detailed information on the

monitoring of stage of the Santa Fe River at the River Rise using an automatic Van Essen CTD Diver pressure transducer has been described earlier (Martin and Moore, 2007; Moore et al., 2009; Screaton et al., 2004).

Results

The 6-year period of surface water and groundwater monitoring captured a great deal of hydrologic and biogeochemical variability in the Sink-Rise system. The hydrologic, organic/inorganic, and isotopic variations are presented in the following in aim to shed light on the C dynamic in this karstic system.

Hydrologic conditions

During the study period (March 2005 to May 2011), the Rise stage ranged from 9.7 to 14.4 masl (meters above sea level, mean = 10.5 ± 0.5 masl) and generally followed the variation in precipitation (Figure 3-2). A 1-3 day lag between rain event and rise in river stage was observed. Although the wet period in north Florida is usually from June through September, there was quite a bit of inter-annual variation during the study period with 2005 and early 2006 being particularly wet and summer 2006 through 2008 being almost drought-like conditions.

For convenience, the 44 sampling campaigns were divided into ‘low flow’ (20) and ‘high flow’ (24) conditions (Figure 3-2). The River Rise stage ranged from 9.9 to 10.6 masl (10.2 ± 0.2 masl) during low flow and from 10.7 to 12.3 masl (11.0 ± 0.4 masl) during high flow conditions. For statistical purposes, the multiple campaigns of the March 2008 storm event high resolution sampling are treated as a single high flow data point of 3/21/08.

Organic carbon concentration variations

Long-term and high resolution time series DOC and DIC data for two surface water sites (the Sink and the Rise) and three well sites (W4, W4a and W7), are representative of the distinct chemical trends observed and are shown in Figure 3. Similar graphs with the complete DOC and DIC data set collected is presented in Appendix H. Surface water DOC concentrations ranged from 1.3 to 51.7 mg/L (mean = 31.4 ± 16.4 mg/L, n = 89) and were significantly ($p < 0.001$) greater and more temporally variable than that of groundwater samples (excluding those from W7 and W7a), ranging 0.1 to 5.9 mg/L (mean = 1.7 ± 1.1 mg/L, n = 94) (Figure 3-3A). Concentrations of DOC in surface water co-varied with hydrologic conditions: high DOC during high flow (ranging 18.5 to 49.3 mg/L, mean = 34.0 ± 11.4 mg/L, n = 14) and significantly ($p < 0.001$) lower during low flow (ranging 1.3 to 44.0 mg/L, mean = 10.3 ± 10.5 mg/L, n = 27). No such correlation between DOC levels in groundwater and hydrologic conditions was found. Groundwater DOC levels were lower (excluding those from W7 and W7a) and were not significantly different ($p = 0.34$) during high (ranging 0.3 to 5.9 mg/L, 2.0 ± 1.3 mg/L, n = 28) and low flow (ranging 0.2 to 4.0 mg/L, 1.7 ± 1.1 mg/L, n = 24). Deep groundwater (excluding W7) DOC were also not significantly different ($p = 0.49$) during high (1.8 ± 1.2 mg/L, n = 22) and low flow (1.5 ± 1.0 mg/L, n = 15).

Shallow groundwater well DOC concentrations (ranging 0.3 to 5.4 mg/L, 2.2 ± 1.2 mg/L, n = 33) were significantly ($p < 0.01$) higher than their deep well counterparts (ranging 0.1 to 5.9 mg/L, 1.5 ± 1.0 mg/L, n = 61), except for W5 (2.1 ± 1.2 mg/L, n = 16) and W5a (1.4 ± 0.5 mg/L, n = 11). For example, DOC in W4 (deep) ranged from 0.1 to 1.9 mg/L (0.7 ± 0.5 mg/L, n = 16) while that in W4a ranged from 0.3 to 3.3 mg/L (1.7 ±

1.1 mg/L, n = 11). At any given sampling period, DOC in W4a was about 1.0 mg/L greater than W4. Even more evident was W6 (1.7 ± 0.8 mg/L, n = 16) and W6a (3.4 ± 0.8 mg/L, n = 11). At any given sampling period, W6 DOC was approximately 1.7 mg/L greater than W6a. Neither shallow groundwater DOC nor deep groundwater DOC co-varied with hydrologic conditions.

Concentrations of DOC at W7 and W7a ranged from 8.3 to 13.4 mg/L (11.9 ±1.2 mg/L, n = 16) and 3.1 to 7.8 mg/L (5.9 ± 1.7 mg/L, n = 11), respectively. Groundwater at the two sites was distinct from other groundwater with significantly ($p < 0.001$) high DOC, and higher DOC concentrations in deep versus shallow water ($p < 0.001$). This suggests that W7 and W7a may have a unique water source or more specifically, a deep DOC source.

During the March 2008 high resolution sampling, DOC concentration remained high in surface water (Figure 3-3B, 42.6 ± 4.7 mg/L, n = 48). The peaks in DOC concentrations at the Sink and the Rise occurred simultaneously and were 3 days following the peak in river stage. On the other hand, groundwater DOC (except for those from W7 and W7a) were constantly low (1.6 ± 1.0 mg/L, n = 42). Shallow groundwater well DOC concentrations (2.0 ± 1.2 mg/L) were higher than their deep well counterparts (1.2 ± 0.6 mg/L), except at W5 and W5a and W7 and W7A.

Inorganic carbon concentration variations

Surface water DIC ranged from 0.0 to 37.6 mg/L (11.9 ± 12.8 mg/L, n = 83) and was significantly ($p < 0.001$) lower and showed less variation than DIC in groundwater which ranged from 21.0 to 96.5 mg/L (48.2 ± 12.7 mg/L, n = 117) (Figure 3-3C). Surface water DIC concentrations were significantly ($p < 0.001$) lower during high flow (4.5 ± 3.9 mg/L, n = 10) than during low flow (28.2 ± 8.1 mg/L, n = 28) conditions. Groundwater

DIC levels were also significantly ($p < 0.01$) lower during high flow (42.5 ± 10.2 mg/L, n = 23) than during low flow (51.2 ± 11.8 mg/L, n = 40).

Similar to DOC patterns, DIC concentrations in shallow well samples (ranging 31.0 to 96.5 mg/L, 53.8 ± 14.4 mg/L, n = 48) were generally higher than their paired deep wells samples (ranging 21.0 to 67.9 mg/L, 44.3 ± 9.6 mg/L, n = 69), except for W7 (46.6 ± 9.7 mg/L, n = 14) and W7a (40.5 ± 8.2 mg/L, n = 12). For example, DIC in W4 ranged from 32.5 to 61.3 mg/L (46.3 ± 7.5 mg/L, n = 14) while that in W4a ranged from 44.5 to 74.8 mg/L (56.3 ± 8.4 mg/L, n = 12). And more dramatically, DIC in W5a (71.5 ± 9.8 mg/L, n = 12) was much greater than that in W5 (34.1 ± 8.5 mg/L, n = 14).

During the March 2008 high resolution sampling, a drop in groundwater DIC concentration occurred simultaneously 1 day following the peak in river stage (Figure 3-3D). On the other hand, surface water DIC remained relatively constant (3.5 ± 3.2 mg/L, n = 45).

Stable carbon isotopic variations

Overall, surface water $\delta^{13}C_{DIC}$ ranged -18.7‰ to -10.2‰ (mean = -12.7 ± 2.5‰, n = 27) and exhibited greater temporal variation and significantly ($p < 0.01$) lighter $\delta^{13}C_{DIC}$ signature than groundwater (excluding those from W2), ranging -15.6‰ to -12.1‰ (mean = -14.4 ± 0.9‰, n = 18) (Figure 3-4). Surface water $\delta^{13}C_{DIC}$ was significantly ($p < 0.001$) heavier during low flow (-11.6 ± 0.9‰, n = 21) compared to high flow (-13.8 ± 1.9‰, n = 12) conditions whereas groundwater showed no evident temporal variation (high flow: -13.6 ± 2.1‰, low flow: -13.8 ± 1.9‰). Groundwater from shallow and deep wells (excluding W2) displayed similar $\delta^{13}C_{DIC}$ signatures (-13.8 ± 1.5‰, n = 25, and -13.3 ± 1.6‰, n = 25, respectively). Groundwater from W2 displayed distinct $\delta^{13}C_{DIC}$ values (ranging from -11.6‰ to -4.0‰, -7.3 ± 3.0‰, n = 7). The unique $\delta^{13}C_{DIC}$

characteristic suggests W2 may have a water source that is different from other sites. The same $\delta^{13}C_{DIC}$ signature patterns were found during the March 2008 storm event, that is, generally light surface water and similar shallow and deep groundwater $\delta^{13}C_{DIC}$ signatures.

Discussion

The results show significant spatiotemporal variations in organic and inorganic C concentration and composition in the O'Leno Sink-Rise system. On the gross scale, the data clearly suggest two endmember water types, a DOC-rich/DIC-poor/$\delta^{13}C_{DIC}$-depleted surface water component, and a DOC-poor/DIC-rich/$\delta^{13}C_{DIC}$-enriched groundwater component. The former may be sourced from swamps or soil water and enters the subsurface via sinkholes or through the vadose zone, while the latter arrives via the upper Floridan aquifer. A large portion of the spatiotemporal variations in organic and inorganic C concentration in the Sink-Rise system can be simply attributed to variable mixing of these two water sources because of changes in the hydrological gradients. The DOC-rich source is of relatively greater quantity during high flow periods and the DIC-rich source more important in the groundwater with no preference for either flow period.

While larger scale trends in water sources and mixing can be discerned from examination of DOC, DIC and $\delta^{13}C_{DIC}$ signatures, the data must be examined in finer detail to understand the quantitative proportions in which these water sources mix, as well as to identify any DOC or DIC consumptive or productive (biogeochemical) processes occurring within the Sink-Rise system. In the following discussion, several biogeochemical processes that are most likely to occur are outlined. Then, a quantitative source water mixing model is constructed to investigate whether any of the

observed variations in organic and inorganic C can be attributed to these biogeochemical processes. The March 2008 storm event is also examined to understand how water chemistry, and in particular, organic and inorganic C, evolves in the Sink-Rise system in response to a sudden influx of DOC-laden water.

Biogeochemical processes affecting C dynamics in the Sink-Rise system

While it is recognized that numerous processes could influence C transformation in the Sink-Rise system, three pair of general biogeochemical processes were identified that are deemed mostly likely to transform C at the time and space scales examined: microbial mineralization/autotrophic production of NDOM, dissolution/precipitation of carbonate minerals, and NDOM-mineral sorption/desorption (Drever, 2002; Findlay and Sinsabaugh, 2003; Findlay et al., 2003; Frimmel, 1998).

During mineralization, NDOM is degraded to inorganic components such as DIC using an oxidant such as oxygen or sulfate (Schwarzenbach et al., 2003). Mineralization of NDOM is also likely to add isotopically light biogenic C to the water, shifting $\delta^{13}C_{DIC}$ toward more negative values ranging -30 to -25‰ (Clark and Fritz, 1997). An increase in water acidity caused by NDOM mineralization could drive dissolution of carbonate minerals (Alberic and Lepiller, 1998; Li et al., 2010). By contrast, autotrophic production may increase concentrations of DOC and oxidants, while decreasing DIC and raising water pH and $\delta^{13}C_{DIC}$ due to preferential uptake of light C possibly leading to precipitation of carbonate.

Dissolution of carbonate increases levels of Ca^{2+}, Mg^{2+}, Alk, and SpC of the water. The $\delta^{13}C_{DIC}$ value of the water is also likely to increase, as the C isotopic signature shifts toward a carbonate character (~0‰, Clark and Fritz, 1997; Randazzo and Jones, 1997). Concentrations of H^+ in the water, however, would be expected to decrease due

to reaction with carbonate minerals. Dissolution of carbonate rock may also release indigenous OM incorporated in the structure of the carbonate minerals (Jin and Zimmerman, 2010). Conversely, precipitation of carbonate minerals can incorporate or 'sorb' NDOM, reducing DOC concentration in water without altering DIC and $\delta^{13}C_{DIC}$ values. Fractions of NDOM that are higher molecular weight, more acidic, and possibly more refractory tend to be preferentially sorbed by carbonate minerals (Jin and Zimmerman, 2010).

As shown in Chapter 2, all these biogeochemical processes have been shown to occur in karst areas, and may alter both the quantity and quality of C. The spatiotemporal occurrences and relative magnitudes of these processes, therefore, require examination to understand C dynamics and the changes in water chemistry they control in the subsurface.

Water source mixing model

In order to identify the times and locations of the occurrence of various biogeochemical processes and their relative magnitudes, the dominating effects of mixing of water from different sources in the study area must be removed. The quantitative mixing model presented in Chapter 2 proved its ability to identify the local biogeochemical production or consumption of DOC or DIC in the Santa Fe River system.

Three endmember water sources were previously identified in the O'Leno Sink-Rise system by Moore et al. (2009) using inorganic species distribution: diffuse recharge, allogenic recharge, and deep water recharge. A similar approach is used here, as groundwater, soil water, and deep water endmembers are assumed to represent the diffuse recharge, allogenic recharge, and deep water recharge, respectively, based on the similarity of C characteristics.

The groundwater endmember is best represented by water at W4, as it resembles most groundwater of the UFA and reflects rain water equilibrated with the Ocala Limestone (Moore et al., 2009; Sprinkle, 1989). This water source contains low DOC concentrations, elevated DIC concentrations (Figure 3-3 and Appendix F) and relatively heavy $\delta^{13}C_{DIC}$ values (Figure 3-4). In this study, the composition of water collected from W4 during high flow on 3/28/08 was used as the groundwater endmember for model calculations. This sample is selected because it has generally the highest concentrations in both Na^+ and Cl^- among 22 samples collected from W4, indicating that it may have undergone the least dilution by other water sources.

The soil water endmember is best represented by the River Sink water during high flow conditions, reflecting evolved rain water surface runoff with less contact with carbonate rocks. It was characterized by elevated DOC, low DIC (Figure 3-3 and Appendix F) and relatively light $\delta^{13}C_{DIC}$ values (Figure 3-4). Moore et al. (2009) reported the fraction of the Sink endmember to be weakly correlated with river discharge in samples collected from the Rise. Thus, water from the Sink during higher flow conditions is less likely to be diluted by other water sources. The sample collected from the Sink on 3/28/08 generally displays the highest concentrations in both Na^+ and Cl^- among all 34 samples collected from the Sink, and so was selected to represent the composition of the soil water endmember for model calculations.

The deep water endmember is best represented by water collected at W2 (Moore et al., 2009). Similar to the groundwater endmember, this deep water has low DOC and high DIC concentrations (Figure 3-3 and Appendix F), but it has elevated SO_4^{2-}, Ca^{2+} and Mg^{2+} concentrations (Appendix F, Moore et al., 2009; Moore et al., 2010) and the

most enriched $\delta^{13}C_{DIC}$ signature in the Sink-Rise system (Figure 3-4). Moore et al. (2009) found the fraction of deep water was inversely correlated with river discharge and suggested that this endmember should be best represented by W2 water during lower flow conditions. Water collected from Well 2 on 1/17/2007 was used as the deep water endmember for the Sink-Rise system, as this sample was most enriched in major ions among all the samples collected. The water chemistry of the three assigned endmembers is provided in Appendix F.

Concentrations of Na^+, Cl^- and SO_4^{2-} in each sample were used to estimate the proportions of the three water sources in each sample. The ions Na^+, Cl^- were chosen because of their expected conservative behavior (Martin and Dean, 2001). These elements show a good linear correlation ($R^2 = 0.80$, $p < 0.0001$, Appendix I) with an average molar Na/Cl ratio of 0.87 ± 0.32 (n = 248), similar to that of seawater (0.86). This ratio suggests the source of Na^+ and Cl^- is from entrained sea spray in precipitation (Grubbs, 1998) and the good correlation between Na^+ and Cl^- reflects little diagenetic alteration to their concentrations. SO_4^{2-} was included in the model as the third chemical species in order to better distinguish the contribution of the deep water endmember. The upward vertical flow of deep water was estimated to be ~1 m/y (Moore et al., 2009), but because of its distinct chemical composition (Appendix F), could strongly influence water composition in the Sink-Rise system. For instance, deep water SO_4^{2-} concentration was approximately 33 times higher than allogenic recharge water and Ca^{2+} and Mg^{2+} was about 5 and 18 times higher, respectively. In addition, SO_4^{2-} was chosen over other ions such as Mg^{2+} and Ca^{2+} because, in the study area, because DO

was always present in the water samples, it was less likely to be involved in biogeochemical redox reactions.

The mixing model was based on mass-balance calculations assuming the following relationships:

$$f_{soil} + f_{gw} + f_{deep} = 1 \quad (3\text{-}1)$$

$$SO4_n = f_{soil} SO4_{soil} + f_{gw} SO4_{gw} + f_{deep} SO4_{deep} \quad (3\text{-}2)$$

$$Na_n = f_{soil} Na_{soil} + f_{gw} Na_{gw} + f_{deep} Na_{deep} \quad (3\text{-}3)$$

$$Cl_n = f_{soil} Cl_{soil} + f_{gw} Cl_{gw} + f_{deep} Cl_{deep} \quad (3\text{-}4)$$

where *f* is the volumetric fractions of each endmember: 'soil', 'gw', and 'deep' representing soil water, groundwater, and deep water, respectively. $SO_{4\text{-}n}$, Na_n and Cl_n are the concentrations of SO_4^{2-}, Na^+ and Cl^- in any given water sample *n*. These equations were solved simultaneously yielding the fraction of each endmember in each sample.

Source water mixing patterns: Results of this mixing model for all water samples are shown in Figure 3-5. Surface waters (i.e., the River Sink, River Rise and Sweetwater) were made up of all three endmembers, although generally contained < 10% of the deep water endmember. Surface water generally received greater soil water endmember contributions during high flow (60 ± 25%) than low flow (2 ± 7%). Correspondingly, contributions of groundwater were lower during high flow (38 ± 25%) than low flow (87 ± 8%). In contrast, the relative contributions of each endmember to well-water samples, whether in shallow or deep wells, remained relatively stable, with the groundwater endmember by far the dominant contributor. Approximately 86 ± 26% and 89 ± 20% of the well-water was derived from groundwater and 13 ± 26% and 10 ± 20% could be attributed to a soil water source during high flow and low flow,

respectively. Water collected from W4a, W5a, and W7 displayed higher contributions from the soil water endmember (15.7%, 31.0% and 47.0% on average, respectively), than water from other well sites, regardless of flow conditions, perhaps indicating higher connectivity with the surface at those sites. The deep water endmember usually made only limited contributions to both surface water (1 ± 2% during high and 11 ± 7% during low flow) and well-water (1 ± 2% during high and 1 ± 3% during low flow). Water at W2 exhibited a much greater contribution from the deep water endmember source than from the groundwater endmember compared to other sites (92 ± 14% during high flow and 88 ± 17% during low flow).

These source water mixing patterns show that, when Santa Fe River flow increases, the River Rise water had greater soil water, less groundwater and deep water contributions. As found here, Moore et al. (2009), using a similar modeling approach, but based on only Mg^{2+} and SO_4^{2} ions over the period from March 2003 to April 2007, reported that discharge at the River Rise was positively (though only weakly) correlated with a soil water (referred to as allogenic recharge) endmember fraction, but was inversely correlated with a deep water (deep recharge) endmember fraction.

The compositions of River Rise water predicted by this and Moore et al. (2009) were also compared during the overlapping sampling periods (March 2005 – April 2007). Although both studies find similar contributions of the deep water endmember, and similar temporal trends in endmember contributions, there are some discrepancies in the quantitative contributions of the other two endmembers. During high flow conditions, Moore et al. (2009) found that the soil water endmember contributed to 60%-70% of the River Rise water, which was ~20% higher than the estimation in this study. During low

flow conditions, the estimated soil water endmember fractions in Moore et al. (2009) were ~50% lower, on average, than those in this study.

These discrepancies could be attributed to different molar ratios of Na^+/Cl^- and Mg^{2+}/SO_4^{2-} in the River Rise water samples collected. The soil water endmember has a Na^+/Cl^- molar ratio of 0.84 and a Mg^{2+}/SO_4^{2-} molar ratio of 0.87. The smaller deviation from these values in a particular sample indicates greater contribution of soil water in that sample. During high flow periods, Na^+/Cl^- molar ratios in the River Rise water (0.83 ± 0.14) were ~4% lower than that in the soil water endmember, while Mg^{2+}/SO_4^{2-} ratios in the River Rise water (0.71 ± 0.80) were only ~2% lower. The smaller deviation in Mg^{2+}/SO_4^{2-} ratios may explain for the ~20% more soil water contribution that Moore et al. (2009) than in this study. The greater deviation of ion ratios (~15% for Na^+/Cl^- and ~95% for Mg^{2+}/SO_4^{2-}) during low flow periods, on the other hand, may be responsible for the larger discrepancies regarding soil water contribution during low flow periods in the two studies.

In order to evaluate the stability and quality of the mixing model, a series of sensitivity analyses were performed, in which the chemistry of each endmember was altered slightly (each ions concentration adjusted by a by a single standard deviation) and the response in source contributions was noted (see Chapter 2 for details). The sensitivity analysis showed that the proportion of surface water and groundwater endmembers could be quite sensitive to small changes in Cl^- or Na^+ concentration (changing up to 19%), particularly during high flow periods. Otherwise, the model was generally insensitive to small changes in endmember chemistry.

Biogeochemical processes in the Sink-Rise system

Using the model-estimated fractions of each water endmember, one can predict a water sample's composition (e.g., DOC, DIC, Ca^{2+}, DO, pH etc.) if is controlled solely by mixing of the different endmembers. The difference between the predicted and actual measured value of any chemical component (Δ) can be attributed to a biogeochemical process which causes a gain (positive Δ value) or a loss (negative Δ value) of the component.

A plot of ΔDOC versus ΔDIC values suggests the occurrence and relative magnitude of various biogeochemical C-cycling processes within the Sink-Rise system during the study period (Figure 3-6). Generally speaking, samples that plot within Quadrants I and IV, have gained DOC, perhaps from autotrophic production or by NDOM released from dissolving aquifer materials, the former being more likely in those samples that have also lost DIC (Quadrant IV). Those that plot in Quadrants II and III have lost DOC, either via microbial NDOM mineralization or NDOM-mineral sorption, the former being more likely in those samples that have also gained DIC or lost an oxidant (Quadrant II) and the latter perhaps indicated by those with little change in DIC.

The DIC gain (Quadrants I and II) could originate from either NDOM mineralization or carbonate dissolution. Since the Sink-Rise system was dominated by supersaturated P_{CO2} conditions (data not shown), DIC gain by atmosphere CO_2 absorption can be ruled out. Loss of DIC (Quadrants III and IV), could occur through either microbial autotrophic activities or carbonate precipitation. Loss of DIC through degassing to the atmosphere (Hoffer-French and Herman, 1989; Li et al., 2010) or uptake by phytoplankton or subaquatic vegetation (de Montety et al., 2011) is possible in surface water, while they are considered to be unlikely in the subsurface portions of the system. Spatiotemporal

trends and the association of specific samples with biogeochemical processes are discussed further in the following.

Quadrants IV: Nearly all water samples plotted within Quadrants II or IV or near the origin. More samples plot in Quadrant IV than any other (excluding those close to origin, discussed separately) and representatives of all hydrologic conditions and all sample locations (Figure 3-6). Evidence of carbonate dissolution was found, as most samples exhibited positive ΔpH (35 of 44) and ΔCa (40 of 47). Carbonate dissolution is also supported by negative $SI_{calcite}$ and $SI_{dolomite}$ in most samples. Samples in Quadrant IV may also have gained DOC via desorption of NDOM from carbonate rocks, as carbonate dissolution and NDOM-mineral desorption are often linked (Jin and Zimmerman, 2010).

In addition, positive ΔDOC and negative ΔDIC in all samples suggest the occurrence of autotrophic production. Because of the negative ΔDIC, DIC loss by autotrophic production must have occurred at a greater rate than DIC gain by carbonate dissolution. Autotrophic production is likely of different microbial metabolisms in surface water versus groundwater. In the surface water, autotrophic production largely occurred via oxygenic photosynthesis, as the production of oxygen (ΔDO = 2.1 ± 2.1 mg/L) was found in 33 surface water samples. Greater rates of autotrophic production occurred during high flow versus low flow periods, evidenced by greater high flow OM production (ΔDOC = 20.5 ± 4.1 mg/L versus 9.5 ± 10.2 mg/L for low flow), greater DIC consumption (ΔDIC = -23.7 ± 9.3 mg/L versus -19.7 ± 8.1 mg/L for low flow), greater oxygen production (ΔDO = 3.0 ± 2.4 mg/L versus 2.0 ± 2.1 mg/L for low flow), and lighter $\delta^{13}C_{DIC}$ (-18.5 ± 0.3‰ versus -11.8 ± 1.2‰ for low flow). Previous studies

(Heffernan et al., 2010; Kurz et al., 2004) have shown that subaquatic vegetation was mainly responsible for surface water photosynthesis, as it occurred to a larger extent in the more clear portion of the watershed below the Rise and water chlorophyll-a concentrations were extremely low. This finding is supported by this study.

Unlike surface water, groundwater samples (particularly those from deep wells) showed no oxygen production ($\Delta DO = -0.5 \pm 0.9$ mg/L), suggesting that chemolithoautotrophy was responsible for majority of the subsurface autotrophy. One type of chemolithoautotrophy that has been reported to occur in a karstic cave ecosystem is sulfur oxidation (Sarbu et al., 1996). In the Sink-Rise system, carbonate dissolution which might be induced by the production of sulfuric acid (discussed later) and DIC consumption in the deep aquifer are consistent with sulfur oxidation. In fact, water from one of the deep wells (W2) presented a strong odor of H_2S and high SO_4^{2-} concentrations (414.3 ± 77.4 mg/L), indicating the possibility of sulfur-based metabolism. However, this hypothesis is contradicted by the neutral pH (7.0 ± 0.3) found in most deep groundwater samples collected, as acidic conditions are a preference of sulfur oxidizers (Konhauser, 2007). Moreover, the neutral pH condition may also rule out N oxidizing and Fe oxidizing as the main chemolithoautotrophic pathways, because the former generates nitric acid and the latter only occurs under pH < 3 (Konhauser, 2007). Methane oxidation has been reported to occur in the UFA, based on the isotopic composition (^{13}C, ^{14}C, and ^{15}N) of tissues from a troglobitic macrofauna collected from Dougherty plain, southwest Georgia (Opsahl and Chanton, 2006). However, this process is not supported in the Sink-Rise system because this metabolism does not

produce DIC and thus, is not indicated by the negative ΔDIC values and no highly depleted isotopic signatures were recorded.

The most likely chemolithoautotrophic pathway in the deep aquifer of the Sink-Rise system appears to be hydrogen oxidation. There are both aerobic and anaerobic forms of this metabolism, the best know of which reduces inorganic carbon to methane. Methanogenic bacteria are known to be ubiquitous in the biosphere's anaerobic habitats (Konhauser, 2007), especially where geothermal hydrogen gas is present (Lovley and Chapelle, 1996). Moore et al. (2009) noticed water from W2 has a unusually high temperature (25.0 ± 4.1°C) and implied that at least part of the study area might be geothermally active.

Quadrant II: Quadrant II has the second most samples (Figure 3-6). The NDOM mineralization suggested by negative ΔDOC and positive ΔDIC is also supported by the negative ΔDO in most of the samples (9 of 13). Mineralization of NDOM is also consistent with the negative ΔAlk (7 of 13) and negative or close to negative ΔpH (9 of 13) of most of the samples.

Carbonate dissolution, which may result from NDOM mineralization due to acidity production (Alberic and Lepiller, 1998; Li et al., 2010), may also have occurred as most samples in this quadrant display positive ΔCa (12 of 13), ΔSpC (11 of 13). Carbonate dissolution is also consistent with the negative $SI_{calcite}$ and $SI_{dolomite}$ values in all samples. But since dissolution of Floridan aquifer materials may result in NDOM-mineral desorption, the DOC loss due to DOC mineralization may be offset (Jin and Zimmerman, 2010).

Most of the 13 samples in Quadrant II were collected during low flow periods, either from shallow wells (4) or deep wells (6). Besides, deep aquifer displayed higher production of DIC (ΔDIC = 24.3 ± 17.4 mg/L) and higher consumption of DOC (ΔDOC = -11.9 ± 9.7 mg/L) and DO (ΔDO = -2.7 ± 2.2 mg/L) relative to shallow aquifer (21.0 ± 12.2 mg/L, -7.3 ± 4.9 mg/L, and 0.1 ± 2.5 mg/L, respectively), suggesting that NDOM mineralization occurred at a greater rate in deep aquifer. These findings contradict the expectation that labile NDOM is supplied from the surface, carried by allogenic recharge. Simon et al. (2001) also recorded lower respiration rates in a karstic aquifer during high flow periods. They attributed this to the scouring of aquifer mineral surface biofilms and importing inactive soil microbes into the aquifer during a flood. On the other hand, high respiration rate during low flow condition could result from the lowering of inactive cell density during flood recession (Simon et al., 2001). I propose that, in the Sink-Rise system, NDOM carried by allogenic water is relatively refractory (most soil-derived, see Chapter 2) compared to that generated from deep subsurface autochthonous sources or, perhaps, released by carbonate dissolution. It is and the latter, along with diffuse internal aquifer flow patterns which drives the activity of subsurface heterotrophic microbes.

Quadrant I and samples close to the origin: Fourteen samples, including most of those within Quadrant I, display small deviations in DIC and DOC that are within 4 mg/L of the origin (Figure 3-6). This indicates that the chemistry of these water samples do not deviate greatly from that expected by the mixing model endmember water sources, and thus, may have experience only minor biogeochemical modifications. However, all these samples show positive ΔCa concentrations, as well as negative

$SI_{calcite}$ and $SI_{dolomite}$ values, suggesting ions were mobilized from aquifer materials during carbonate dissolution. NDOM carbonate dissolution by mineral desorption may have produced the small positive ΔDOC values recorded for most of the samples.

Most of the 14 samples were collected from deep wells and during low flow conditions when flow direction is from the aquifer matrix into the conduits (Martin and Dean, 2001; Moore et al., 2009; Screaton et al., 2004). Many of these samples were collected from deep wells W2 and W6. Carbonate dissolution at W2 is not surprising, as one study attributed the elevated ion concentrations in W2 water to the dissolution of gypsum or anhydrite in the lower portions of the aquifer (Moore et al., 2009). Greater carbonate dissolution at W6 relative to other sites, on the other hand, highlights the heterogeneity of karst aquifer.

Spatiotemporal variations in biogeochemical processes

Net autotrophy (NDOM production) is apparent in many surface water and some groundwater samples. Unlike autotrophic production in the surface water that mainly occurs via subaquatic vegetation photosynthesis, autotrophic production in groundwater occurs via chemolithoautotrophy. Other researchers have also reported that subsurface chemolithoautotrophic microbes generate autochthonous OM in cave and karstic systems, some of which support food webs largely based on autochthonous NDOM produced from chemolithoautotrophically (Birdwell and Engel, 2009; Engel et al., 2004; Farnleitner et al., 2005; Sarbu et al., 1996; Vlasceanu et al., 2000). For example, Farnleitner et al. (2005) presented evidence for the existence of autochthonous microbial endokarst communities in the spring water of an alpine karst aquifer. By examining the fluorescent character of NDOM in a karstic aquifer in central Texas, Birdwell et al. (Birdwell and Engel, 2009) concluded that the dominant source of NDOM

was in situ chemolithoautotrophic production. And a study on the Movile Cave in southern Romania showed that autochthonous NDOM produced by sulfide-oxidizing bacteria was the food base for 48 species of cave-adapted terrestrial and aquatic invertebrates (Sarbu et al., 1996).

In the Sink-Rise system, no evident temporal pattern was observed for subsurface chemolithoautotrophy, as would be expected of a system independent of surface C source or oxidant supply. However, there certainly was spatial variability as DOC production near W7 and W7a ($\Delta DOC = 6.4 \pm 1.9$ mg/L) was roughly six times higher than that found elsewhere. Chemolithoautotrophic production, thus, also explains the exceptionally high DOC concentrations in water from W7 and W7a (Figure 3-3).

Net NDOM mineralization was found to occur in both shallow and deep aquifer samples and to a greater extent during low flow periods and in the deeper aquifer. Prevailing thought is that karst aquifers are heterotrophic ecosystems fueled by OM largely imported from the surface (Hancock et al., 2005; Simon et al., 2001). For instance, significant NDOM mineralization was detected within a karstic aquifer in France, where the NDOM in the aquifer was mainly supplied by surface stream sinks (Alberic and Lepiller, 1998). In the Sink-Rise system, the lack of a NDOM mineralization increase during high flow periods, for most subsurface sites, and the greater rates in the deeper portion of the aquifer, suggests no strong dependence on surface NDOM supplies. On the other hand, the mineralization of NDOM at shallow well sites is unlikely to be supported by NDOM that produced by deep-sourced autochthonous NDOM and a few shallow aquifer sites did show greater mineralization during high flow periods (see

below). A study with more detailed organic geochemical analyses is needed to better understand distributions in NDOM sources in supporting subsurface microbial activity.

Carbonate dissolution in the Sink-Rise system appears to be spatially and temporally pervasive, as the model indicates that almost all samples collected indicate some contribution of the products of carbonate dissolution. Overall, it is not surprising to find carbonate dissolution, as this has been noted in previous studies of the Sink-Rise system (Martin and Dean, 2001; Moore et al., 2010) as well as in other karstic systems (e.g., de Montety et al., 2011; Dreybrodt, 1990; Li et al., 2010). For instance, Moore et al. (2010) determined carbonate dissolution in the Sink-Rise system to be episodic and calculated a conduit wall retreat rate of 7×10^{-7} m/day due to dissolution. Carbonate weathering rates in temperate karstic region has been estimated to be as much as 133 ton/km^2/y in southwestern China (Li et al., 2010) and 151 - 176 ton/km^2/y in northern England (Pentecost, 1992).

But the finding of this study contradict the commonly held view that the carbonate dissolution occurs primarily during high flow periods when surface water flow into the aquifer bringing organic acids and soil CO_2 (Gulley et al., 2011). Instead, it is found that, in this system, dissolution of carbonate minerals is pervasive, driven perhaps by mineralization of autochthonous NDOM, as the greatest net carbonate dissolution occurred in the deep aquifer and during low flow periods. These findings suggest a greater importance of subsurface biogeochemical processes on karst and aquifer evolution than is commonly recognized. The presence of subsurface chemolithoautotrophy would thus play a role in the development of secondary porosity and permeability, which controls an aquifer's hydrological properties, the transport of

subsurface contaminants and has important implication for the formation of petroleum reservoirs.

Evidence for NDOM-mineral desorption was found in the Sink-Rise system. It occurred in similar spatiotemporal patterns to carbonate dissolution, i.e. the greatest rates in deep aquifer and during low flow periods. Although net carbonate precipitation and NDOM-mineral sorption were not directly detected by the model, they might have occurred at smaller rates in the Sink-Rise system, as our model detects only the net result of paired processes. Other studies have reported that carbonate precipitation and NDOM-mineral sorption can have large influence on C dynamics in other karstic systems. For example, carbonate precipitation was found to account for 88% of DIC loss in the karstic Ichetucknee Spring Run in north Florida (de Montety et al., 2011), while NDOM-mineral sorption may cause 23% DOC loss in injected surface water during an artificial recharge (AR) operation in southern Finland (Kortelainen and Karhu, 2006).

Water chemistry variation during the March 2008 storm event

During the entire storm event (3/11 to 4/1), concentrations of two conservative ions (Na^+ and Cl^-) in surface waters were inversely correlated with River Rise stage ($R^2 = 0.8$, $p < 0.0001$ and $R^2 > 0.6$, $p < 0.001$, respectively, Figure 3-7). It is likely that this was caused by dilution of surface water with storm water runoff water depleted in major ions. Rainwater in northern Florida has concentrations of Na^+ and Cl^- (0.3 ± 0.2 and 0.6 ± 0.3 mg/L, respectively, Katz et al., 1998) that are roughly 30 times lower than that of allogenic recharge water and 15 times lower than that of diffuse recharge water, as defined here by endmember source waters (Appendix F). In addition to Na^+ and Cl^-, surface water displayed decreases in concentrations of many other solutes including

DIC (Figure 3-3D), Ca^{2+}, K^{+}, and SO_4^{2-} as well as SpC (Figure 3-7D) during the ascending hydrograph limb (3/11 to 3/14) that may be due to dilution by runoff. The unexpectedly low Cl^{-} concentration on 3/11 at the Sink is hard to explain other than by measurement error.

Because the current mixing model does not include a water source endmember representing the storm water runoff, it was unable to identify reasonable variations in water sources and biogeochemical processes during the storm event. Nevertheless, using conservative ions (Na^{+} and Cl^{-}) and other ancillary geochemical parameters, one may still surmise the relative contributions of different water source as well as their evolution during the storm. For instance, during the descending limb (3/14 to 4/1), gradual increases in concentrations of Na^{+}, Cl^{-}, DIC, and SpC suggest that storm water runoff became a progressively less important water source beginning 3/14, about one week after the rain event ended (3/7). Although diluted by runoff, surface water still displayed levels of DOC as high as any observed during the 6-year study (Figure 3-3B). This indicates either that the runoff water contained DOC or that a large portion of the storm water quickly infiltrated the soil, picked up an abundance of DOC, and then discharged into the surface water. The former is considered unlikely in that runoff water lacked ions that would likely have been gained along with DOC if it had significant contact with soil or detritus.

The storm event was found to have had less obvious effect on the groundwater geochemistry. Concentrations of Na^{+} and Cl^{-} in both deep and shallow groundwater decreased during the storm event relative to average non-storm conditions. The decrease in shallow groundwater Na^{+} and Cl^{-} concentrations (1.6 ± 1.2 mg/L and 2.0 ±

0.9 mg/L, respectively) was about two to three times greater than for deep groundwater (0.9 ± 0.5 mg/L and 0.6 ± 0.4 mg/L, respectively). Though the magnitude of this shallow aquifer water dilution was ~10 times less than that of surface water (Na^+ and Cl^- concentration decreases of ~5-10 mg/L), the change in concentration of these conservative ions relative to non-storm concentrations was significant. However, for every groundwater well sites, variations in DOC concentrations during the storm event were no different from those during the non-storm conditions. The greatest solute concentration decrease during the ascending hydrograph limb was that of DIC (Figure 3-3D), which might have been effected by biogeochemical reactions. During the descending limb, most geochemical parameters including DOC, DIC, Na^+, Cl^-, and SpC for every groundwater sites largely remained constant or shifted only slightly.

The greater decreases in Na^+ and Cl^- concentrations in shallow aquifer waters relative to deep aquifer during the storm indicate that, as one would expect, the shallow aquifer is more closely connected to the surface and more likely to be affected by dilution by diffuse recharge. By monitoring the SpC and water level in the Santa Fe River Sink-Rise system, Langston et al. (2012) also pointed out that diffuse recharge are the main influences on well-water during storm events. They found that diffuse recharge flow horizontally during storm events and does not mix rapidly within the aquifer. Interpretive numerical simulations suggest that diffuse recharge can even impact the intrusion of allogenic water from the conduit and thereby reducing influx from the conduit to the aquifer matrix (Langston et al, 2012). In this study, the influence of diffuse recharge is most evident in two shallow wells sites, W4a and W5a, where water displayed greater decreases in concentrations of Na^+ (2.4 mg/L and 2.6 mg/L,

respectively) and Cl^- (1.9 mg/L and 1.3 mg/L, respectively) than other shallow groundwater sites. This finding indicates that water chemistry at W4a and W5a responds to surface events at shorter timescales response compared to other well sites, emphasizing the heterogeneity of karstic aquifer.

It is difficult to identify changes in biogeochemical processes caused by the storm without quantitative estimates of changes in source water contributions and their compositions during this event. It is not expected that any change in biogeochemical processes would have occurred at deep aquifer sites due to the storm event because there was no evidence of a change in source water composition. In contrast, the influx of DOC-rich and DIC-poor surface water to shallow aquifer sites might be expected to increase mineralization of this newly supplied NDOM or to increase carbonate dissolution due to an influx of undersaturated water. However, no significant DOC increase was found at any shallow aquifer site during the storm, suggesting that the newly supplied NDOM was either mineralized or mineral-sorbed along the flow paths.

Concentration of DO in W4a water increased dramatically starting 3/17 (Fig. 7E), suggesting that NDOM-mineral sorption rather than NDOM mineralization occurred. The absence of NDOM-mineralization along the flow path for W4a during the storm is supported by higher $\delta^{13}C_{DIC}$ at W4a during the storm (-12.8 ± 1.3‰ and 4.6 ± 1.7 mg/L) compared to non-storm periods (-14.4 ± 0.1‰ and 3.4 ± 0.7 mg/L). Unchanged DO at other shallow well sites suggests complete consumption of the supplied DO during NDOM mineralization along their flow path. However, water from shallow well sites other than W4a also displayed higher $\delta^{13}C_{DIC}$ and DO during the storm (-13.6 ± 1.7‰ and 1.9 ± 1.3 mg/L) than non-storm period (-14.6 ± 1.2‰ and 0.6 ± 0.3 mg/L),

suggesting that storm did not boost microbial respiration in shallow groundwater. This finding agrees with the earlier conclusion that NDOM mineralization is more prevalent during low flow periods.

There may be evidence for carbonate dissolution in shallow aquifer during the storm event, since all shallow groundwater samples collected during the storm were undersaturated with respect to carbonate minerals ($SI_{calcite}$ = -0.6 ± 0.4 and $SI_{dolomtie}$ = -1.1 ± 0.4). Greatest carbonate dissolution might have occurred at W5a, since the water from there displayed Mg^{2+}, DIC and SpC values that were about 33%, 55%, and 29% higher than water from other shallow well sites. Lower $SI_{calcite}$ (-0.8 ± 0.2) in W5a water than water from other shallow wells (-0.6 ± 0.4) also supports this conclusion. However, at shallow groundwater site as a whole, Ca^{2+}, DIC and SpC were found to be about 91%, 5%, and 9%, respectively, lower during the storm period versus non-storm conditions, suggesting a lessening of dissolution by the storm. This may have occurred because much of the water entering the matrix was derived from runoff rather than the more typical allogenic water which passes through soil layers picking up CO_2.

Conclusions

Much of the spatiotemporal variations of organic and inorganic C observed in the Sink-Rise system during the 6-year sampling period could be ascribed to mixing of three water sources identified as allogenic recharge, diffuse recharge and deep water. By taking into account the effects of mixing, evidence for biogeochemical processes such as autotrophic production, NDOM mineralization, and carbonate mineral dissolution was found in different portions of the system. In general, surface waters in the Sink-Rise system could be characterized as net autotrophic while the groundwater was net heterotrophic except for portions of the deep aquifer where chemoautotrophy was

identified. The biogeochemical processes observed, however, are likely to be linked together. For instance, both surface and deep autotrophic production fuels subsurface NDOM mineralization, which can render the water more acidic and drive carbonate dissolution. The dissolution of aquifer materials can release indigenous NDOM, some of which may serve as fuel for further microbial metabolism. Temporal variations in these biogeochemical processes were also identified such as both NDOM mineralization and carbonate dissolution tend to occur during low flow periods. However, temporal biogeochemical variations were difficult to identify during the March 2008 storm event, due to influx of new water sources of unknown composition to a few shallow aquifer locations.

This study also highlights the heterogeneity of aquifer water sources and biogeochemical processes and has implications for the management of hydrogeologic projects such as ASR and AR, development of secondary porosity and efforts to remediate groundwater contaminants. For instance, the surface water injected into an aquifer during ASR and AR may carry solutes including NDOM, and it is clear from this study that NDOM can significantly alter subsurface biogeochemical processes such as result in dissolution of karstic aquifer. This study also shows that karstic subsurface geomorphology can be not only modified via abiotic processes as commonly known, but also via various biogeochemical processes where NDOM and microbes are greatly involved. In addition, the results of this study may benefit contaminant remediation operations in karstic aquifer by advancing our knowledge of the subsurface biogeochemistry. For instance, this study shed light on the possible mechanisms of

secondary porosity development and subsurface NDOM production, both greatly influences the fate and transport of the aquifer contaminant.

The source water mixing model developed proved to be a powerful tool to evaluate C dynamic processes and their spatiotemporal distributions in this complex surface-groundwater exchange system. However, the mixing model was limited in its ability to predict variations of water sources and biogeochemical processes during intense storm events. Future high resolution sampling during an intense storm should include collection and geochemical measurement of stormwater runoff, for inclusion in the model as a fourth water source endmember. Future work is also needed that will simultaneously examine spatiotemporal variation in additional chemical proxies such as nutrients, metals (e.g., iron), multiple stable isotope (^{13}C, ^{14}C, and ^{15}N) and molecular-level NDOM composition to better identify the occurrence and quantify rates of biogeochemical processes. Subsurface chemolithoautotrophic pathways also require better characterization, perhaps isotope and molecular genetic tools.

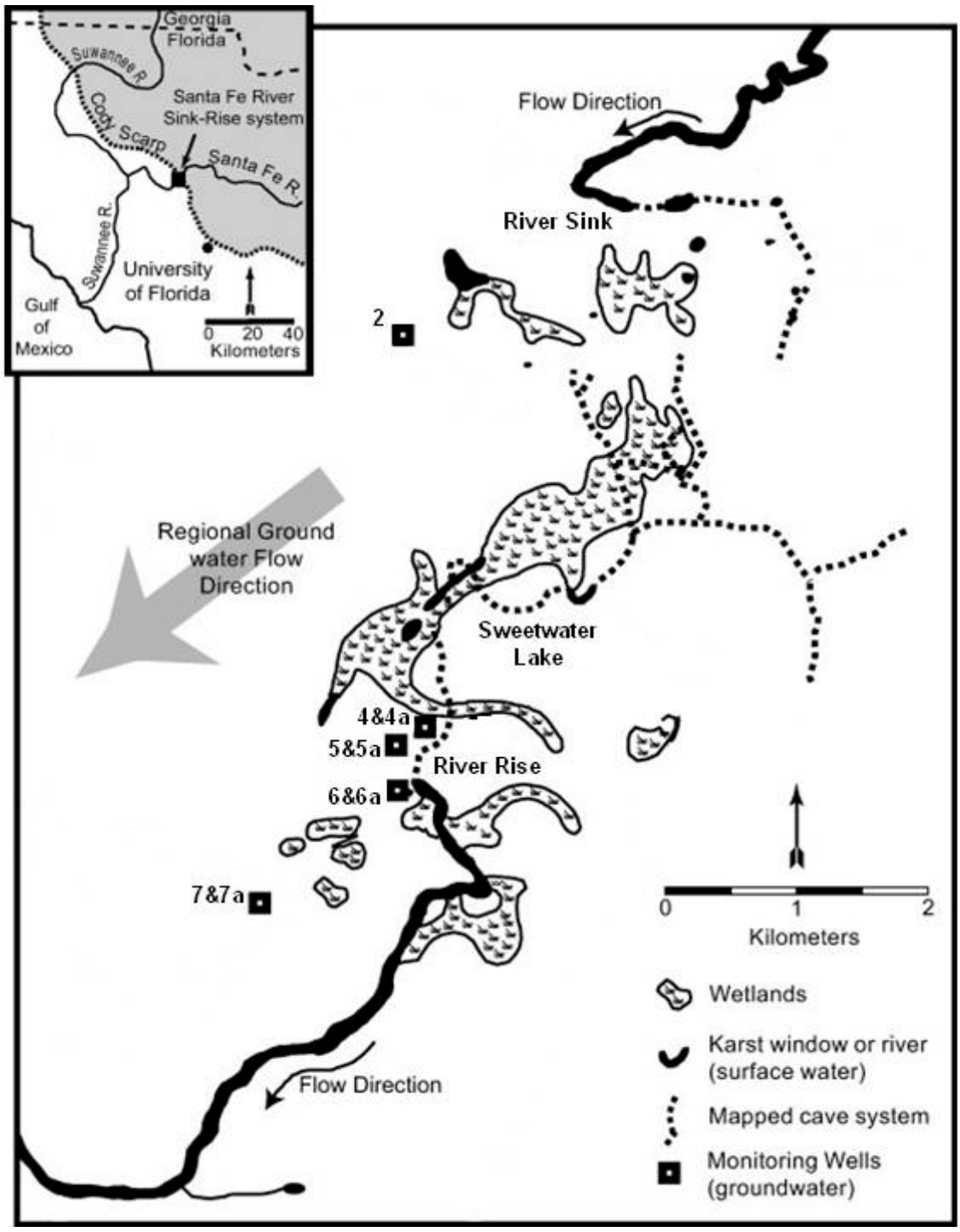

Figure 3-1. Study area showing surface water sampling locations (Santa Fe River Sink, River Rise, Sweetwater Lake), deep groundwater monitoring wells (2, 4, 5, 6 and 7) and paired shallow water wells (4a, 5a, 6a, 7a). Inset shows regional setting; shaded where the upper Floridan aquifer is confined by the Hawthorn Group, unconfined to the southwest.

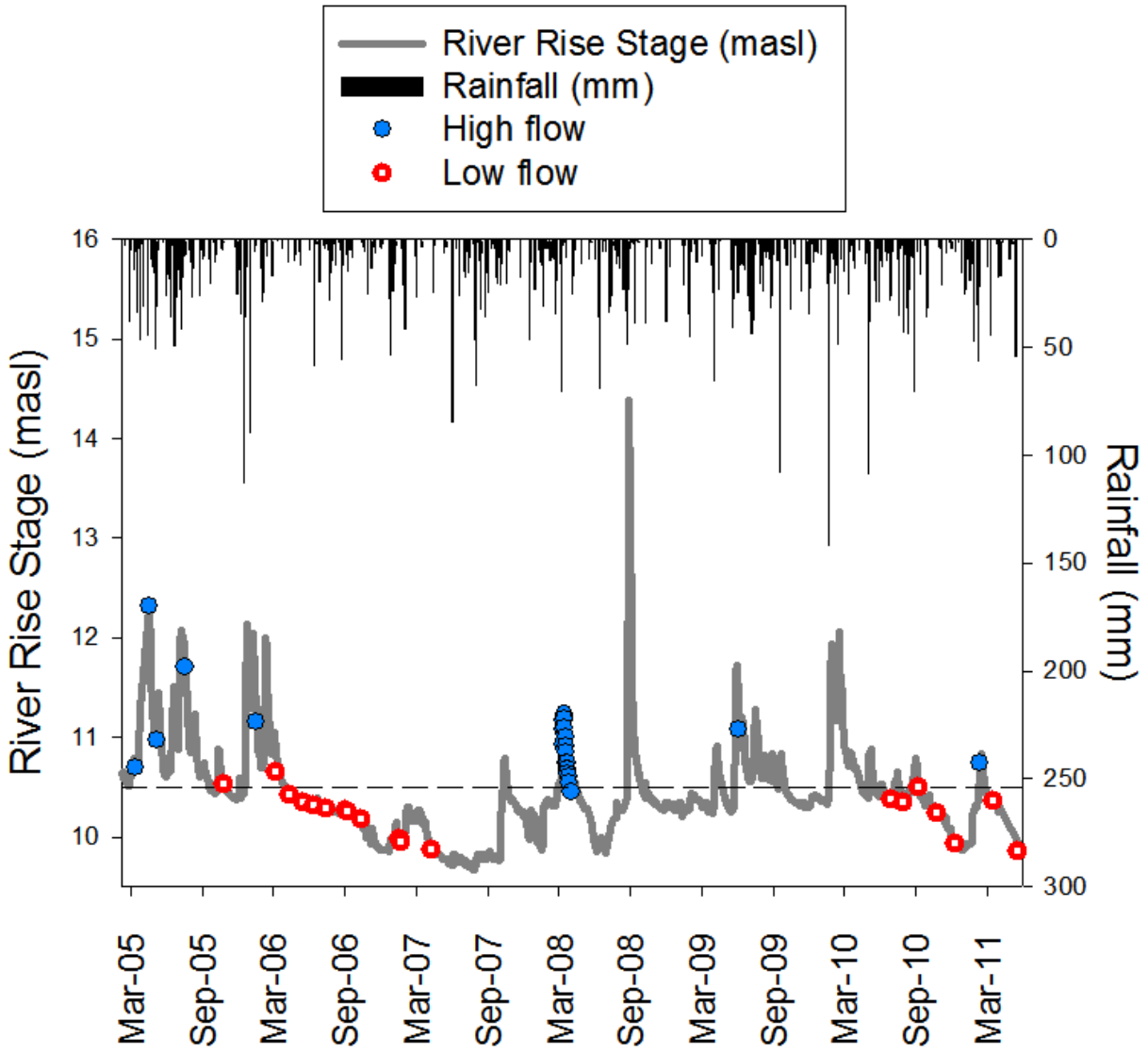

Figure 3-2. Stage of the Santa Fe River at the River Rise (in meters above sea level, masl), rainfall within O'Leno State Park, and sampling episodes designated as 'wet' (open circle) or 'dry' (closed circle). The dashed line indicates the average River Rise stage of 10.5 masl during the 6-year sampling period.

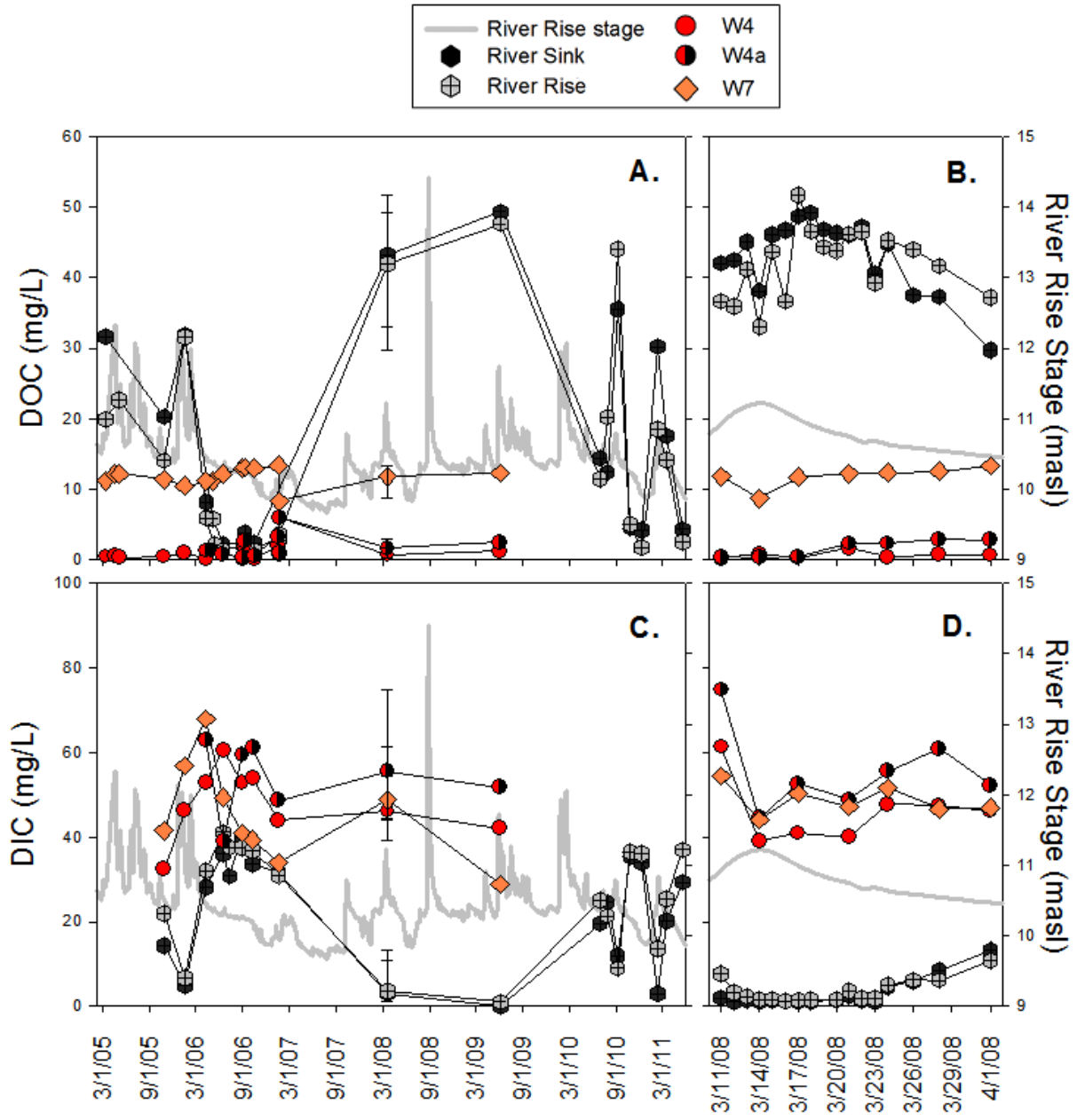

Figure 3-3. Time series data of DOC during (A) six-year study period and (B) March 2008 flood event, and DIC during (C) study period and (D) March 2008 flood event. Shown are two representative surface water sites (River Sink and River Rise, hexagon symbols) and three representative wells sites (W4, W4a and W7).

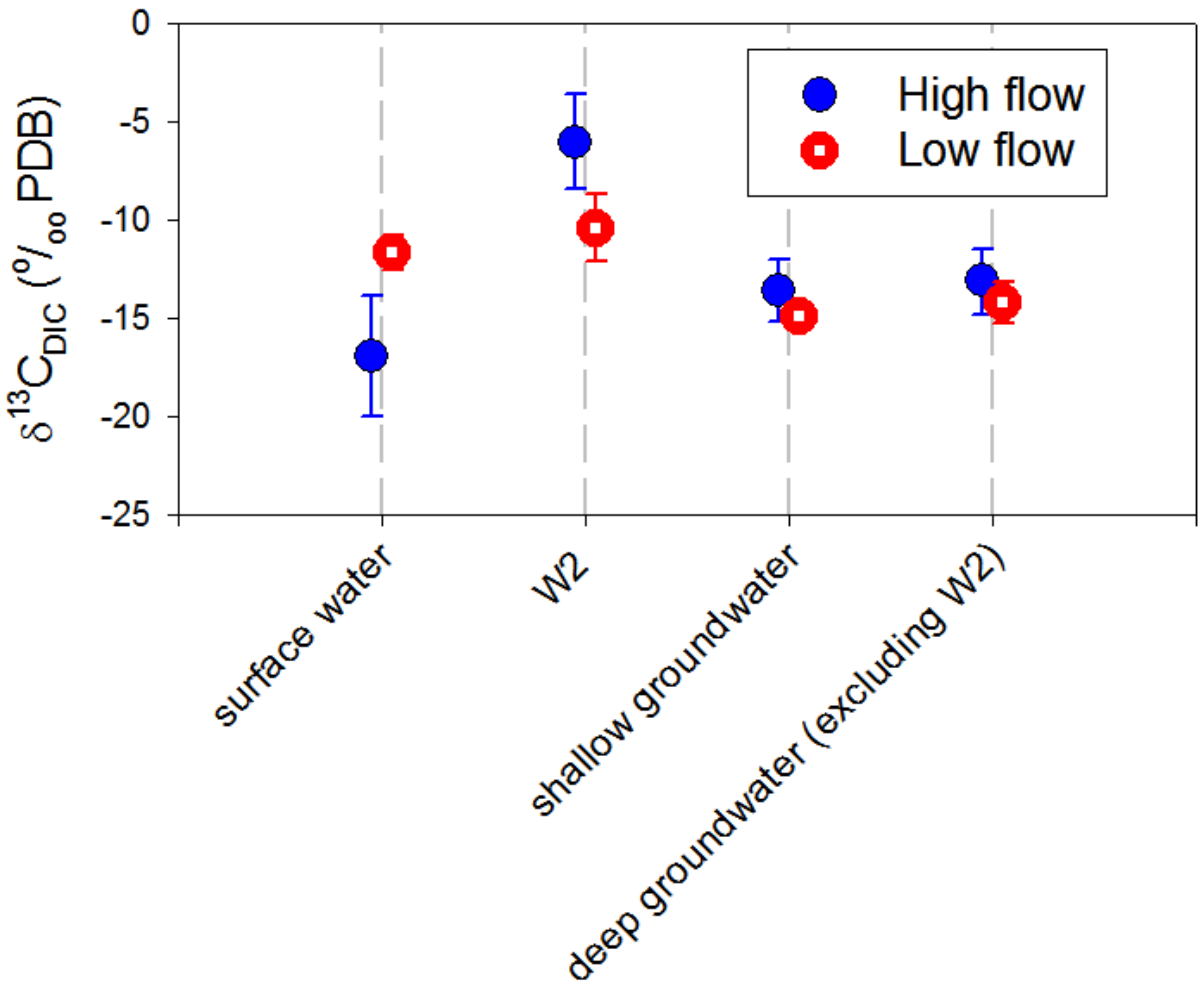

Figure 3-4. Stable carbon isotope data for samples from surface water and groundwater sites during high flow and low flow periods. Error bars represent the standard deviation of $\delta^{13}C_{DIC}$ measured over time.

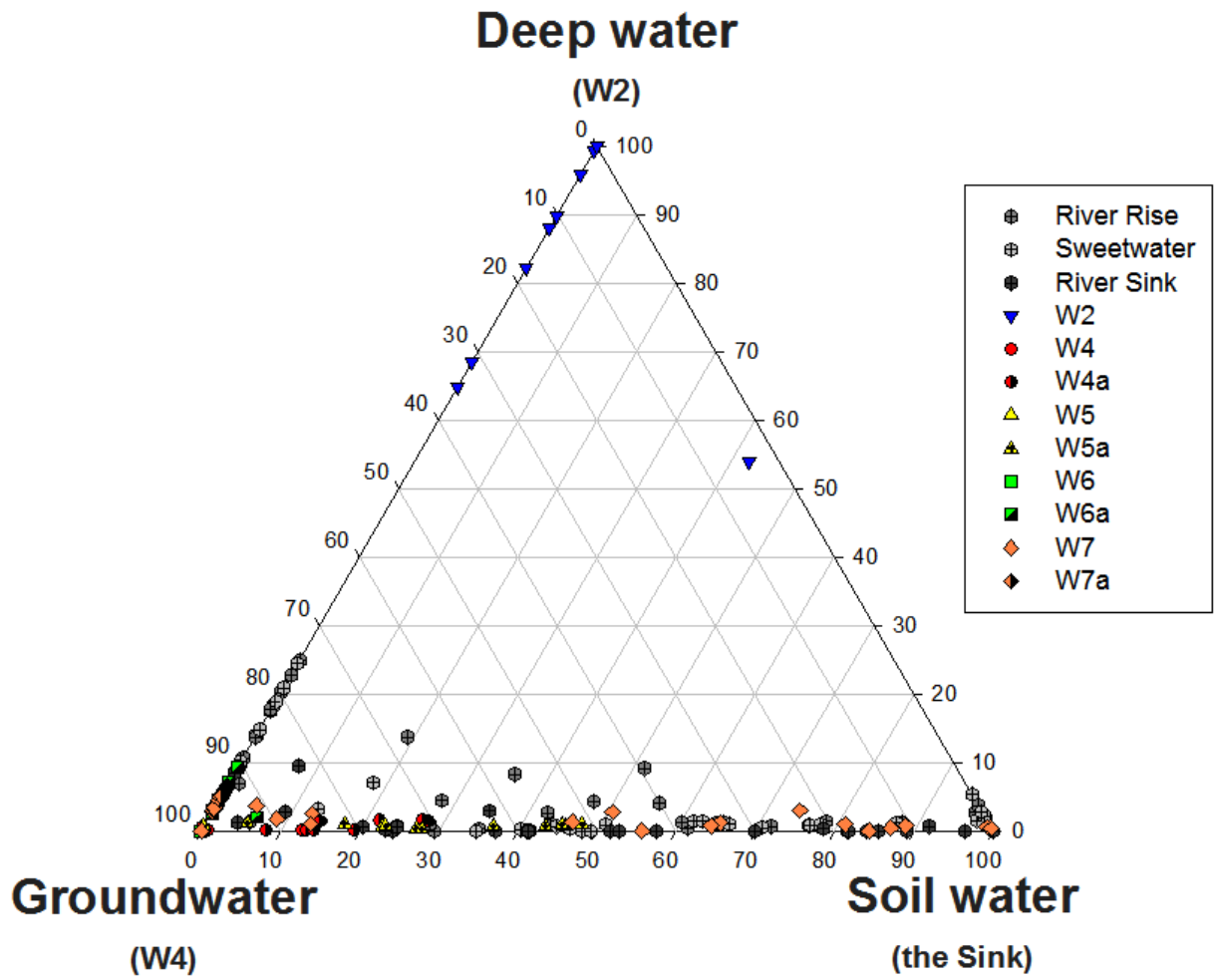

Figure 3-5. Results of the water source mixing model shown as the fraction (in %) of diffuse recharge, allogenic recharge, and deep water recharge theoretical endmembers in each sample collected in the Sink-Rise system over the six-year study period.

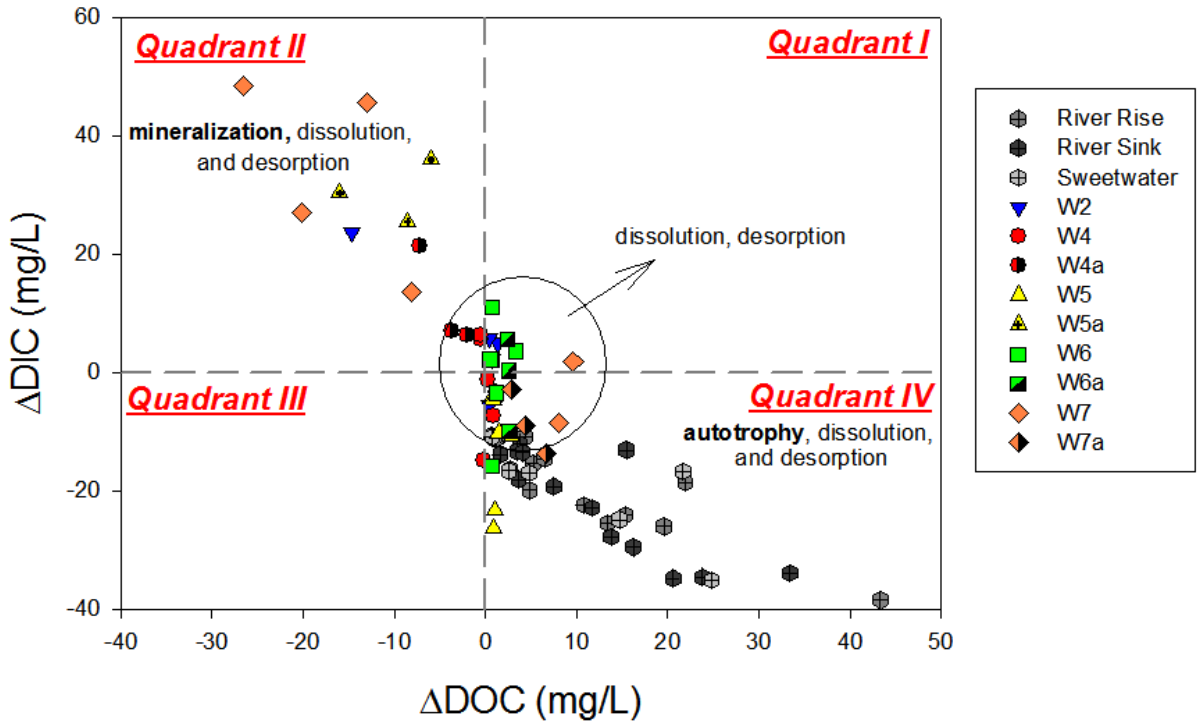

Figure 3-6. Differences between the model-predicted and measured dissolved inorganic and organic carbon concentrations (ΔDIC and ΔDOC, respectively) in samples from the Sink-Rise system during the 6-year study period. Possible biogeochemical processes responsible for shifts are listed in each quadrant, with the major ones indicated by ancillary geochemical evidence in bond fonts.

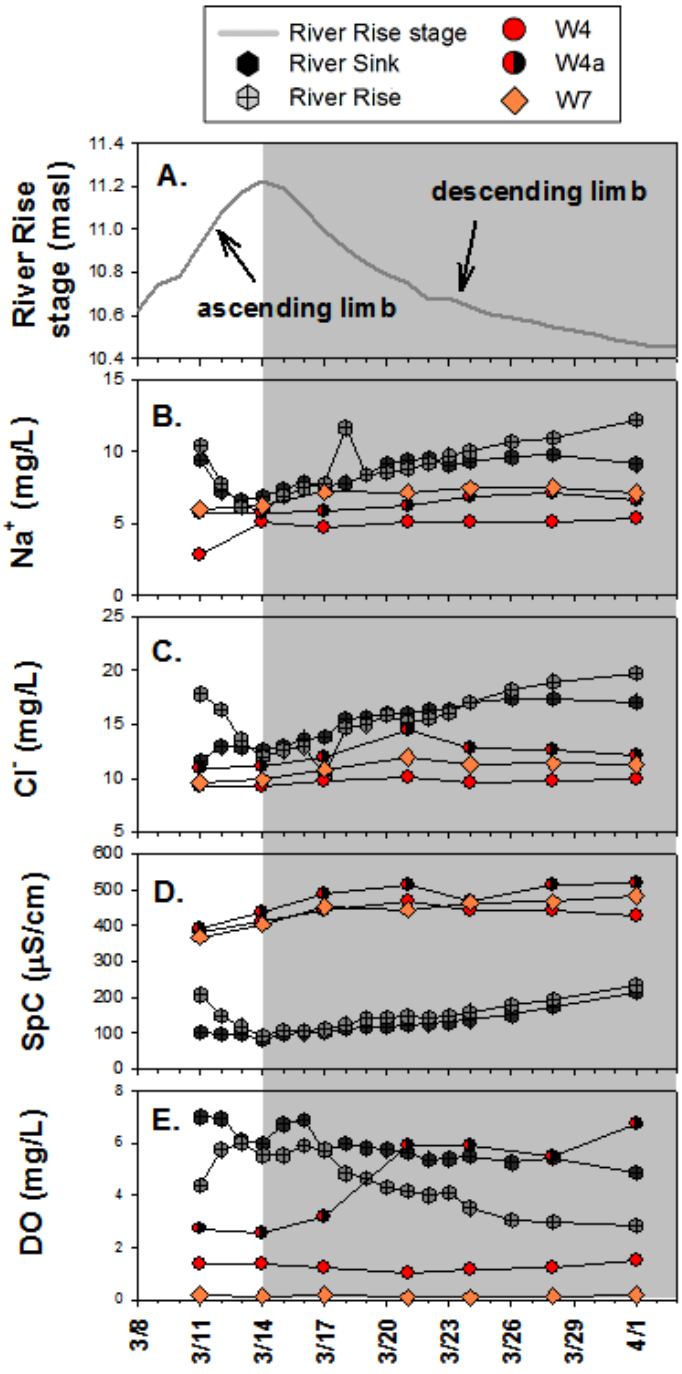

Figure 3-7. High resolution storm event time series measurements of (A) River Rise stage, (B) Na^+, (C) Cl^-, (D) specific conductivity, and (E) dissolved oxygen. The storm event was divided into two hydrologic periods, indicated by shading. Shown are two representative surface water sites (River Sink and River Rise, hexagon symbols) and three representative wells sites (W4, W4a and W7).

CHAPTER 4
THE INFLUENCE OF NDOM AND MICROBIAL PROCESSES ON ARSENIC RELEASE DURING ASR OPERATIONS IN THE FLORIDAN AQUIFER

Background

The mobilization of subsurface arsenic (As) poses a serious threat to human health, particularly in a region such as Florida where the population is heavily dependent on highly porous karstic aquifers for drinking water (Nordstrom, 2002). The mobilization of As during aquifer storage and recovery (ASR) and aquifer recharge (AR), which involve injecting water into an aquifer, has become the primary regulatory constraint for implementing these alternative water storage and supply strategies. The feasibility of these direct recharge projects has come into question due to the occurrence of As above the maximum contaminant level (10 µg/L) at ASR sites in Florida (Arthur, 2002).

Natural dissolved organic matter (NDOM) may control the biogeochemistry and the chemical composition of groundwater through its interaction with other aquifer components including rock minerals, metals and microbes (Findlay and Sinsabaugh, 2003; Frimmel, 1998; Ratasuk and Nanny, 2007; Schlautman and Morgan, 1994). In particular, NDOM has been reported to play an important role in governing the mobility, bioavailability and transport of metals in the subsurface (Han and Thompson, 2003; Lee et al., 2005; Petrovic et al., 1999).The influence of NDOM on As mobility and transformation has drawn wide attention recently and a number of studies have demonstrated strong correlations between NDOM and As release from aquifer materials (Anawar et al., 2003; Chen et al., 2006; Kalbitz and Wennrich, 1998; Meharg et al., 2006; Redman et al., 2002; Wang and Mulligan, 2006). However, most of these studies were targeted at Bangladesh aquifers where As is bound to Fe oxides (Mladenov et al.,

2010; Rowland et al., 2006). Less research has been conducted on As mobilization during ASR and AR in karstic aquifers such as the Floridan where As is primarily thought to be associated with pyrite (Jones and Pichler, 2007; Price and Pichler, 2006). For instance, Arthur et al. (2002) attributed the mobilization of As to the oxidation of As-containing minerals such as pyrite when high DO water was injected into reduced aquifer waters during ASR. Selective leaching and/or mineral dissolution may also release As into the aquifer (Arthur, 2002). Although injection water used in ASR and AR operations can be high in NDOM and Floridan aquifer materials contain indigenous OM that can be readily released during carbonate rock dissolution (Jin and Zimmerman, 2010), no study, to our knowledge, has been conducted to elucidate how NDOM may influence As mobilization during AR and ASR in the Floridan Aquifer.

The main objective of this study was to advance our understanding of the influence of NDOM, as well as microbial processes, on the mobilization of As from Floridan Aquifer carbonate rocks during AR and ASR. One or more of three mechanisms are hypothesized to be most likely responsible for As mobilization during ASR operation: oxidative dissolution, reductive dissolution, and As desorption. These three mechanisms were tested by manipulating redox conditions and solution chemistry in a laboratory system during different experimental phases (i.e. water type and headspace in the reaction vessels). In addition, the possible influences of biogeochemical reactions on As release were examined by treatment additions of NDOM, acetate and microbes. A labile organic matter source (Na-acetate) was added to test whether As is mobilized via microbially-mediated reactions. A refractory organic matter source (soil NDOM extracts) was added to test whether it promotes As release

via ligand-exchange complexation mechanisms or as a microbial substrate, or inhibits release via surface adsorption. Soil microbes were added to selected treatments to test whether As mobilization was limited by unfavorable storage conditions or a limited population of subsurface microbes.

Material and methods

A three-phase laboratory incubation experiment was conducted in sealed reaction vessels in an effort to determine the mechanism and influence of biogeochemical processes of As release in the Floridan Aquifer. First, homogenized Floridan Aquifer carbonate core materials were first equilibrated with native groundwater (NGW) to simulate a pre-injection condition in the aquifer. Then the surface water injection process was simulated by replacing the native groundwater in the vessels with typical ASR source water (SW) containing a fixed amount of oxygen as well as each of three treatment additions of microbes, labile OM or refractory NDOM. Finally, in the last phase, the vessels were opened to atmospheric conditions to simulate injection of an unlimited oxygen supply. Various geochemical parameters, including concentration of As, were monitored during the 110-day incubation.

Aquifer core materials

Detailed core collection and preservation procedures were described by Norton (2011). In brief, the entire thickness of the Suwannee Limestone, from 290 to 480-ft (below ground surface, or bgs), was cored at the Southwest Florida Water Management District (SWFWMD) ROMP TR 9-1 well site in Hillsborough County, FL (27º 44’ 16’’N, 82º 27’ 38’’W). To minimize atmosphere exposure during drilling, the borehole was allowed to flow under artesian pressure overnight. Upon retrieval, the cores were sealed in storage vessels constructed of 3-inch Sch. 80 PVC pipe, fitted with gas tight seals

and valves, and were immediately N_2-flushed followed by vacuum evacuation, this process was repeated three times and vessel finally sealed under positive nitrogen pressure to minimize contact with air during transport and storage.

The core section that was collected from ~447.5 to ~455 ft bgs was chosen for the incubation experiments because this depth interval represented the approximate middle section of the typical ASR storage interval for the Suwannee Limestone. Immediately before loading into incubation chambers, this selected section was crushed, homogenized, and split into ~300 g subsamples in the FGS Hydrogeochemistry Laboratory, Tallahassee, FL.

Native groundwater and source water

Detailed water collection procedures were described earlier (Norton, 2011). In brief, native groundwater (NGW) was collected from the ROMP well TR 9-2 (27°45’54’’N, 82°23’38’’W, ~5 miles northeast of TR 9-1) on June 8, 2010. Well TR 9-2 was completed with a bore-hole open to the Suwannee Limestone from 247-462 ft bgs. The samples were collected into three sealable flow-through containers constructed using 20 L Nalgene Heavy Duty Vacuum Carboys and were N_2-flushed and vacuum sealed at the well site to prevent atmosphere exposure. Typical ASR source water (SW), potable (tap) water, was collected from Bradenton High Service Pump Station (an ASR site) on July 19, 2010 using 5-gallon plastic carboys. The SW was transported to the FGS lab in Tallahassee, FL the next day. Major hydrogeochemical parameters of the NGW and SW are presented in Appendix J.

Treatment addition materials

The NDOM for incubation additions was water-extracted from a north Florida soil. This soil NDOM has been previously chemically characterized and found to be similar to

groundwater NDOM in north Florida (Jin and Zimmerman, 2010). The selection of soil NDOM was also based on the assumption that most NDOM in groundwater is likely to be soil-derived (Tipping et al., 1997). A north Florida mixed forest soil (collected at 29°36’04’’N, 82°21’42’’W) was combined with water (soil: water volume ratio=1:1) and placed on platform shaker for 4 days. The soil-water mixture was then screened using a sheet of nytex netting to remove large particulate materials before centrifugation (4500 rpm, 30 min,Young et al., 2005; Young et al., 2004). The supernatants were then filtered using medium glass fiber filter paper (Fisher, Q5), sterilized (autoclave, 1 hour), stored in the dark at 4°C, and used as a microbe-free NDOM solution (treatment 1). There was no significant change in quantity and quality of NDOM during autoclaving as determined by total organic C content and fluorescent characteristics.

The concentrated microbe solution added to the incubation experiments was obtained from the same Florida soil from which NDOM was extracted. Pellets from the centrifugation were re-suspended, filtered with coarse glass fiber filters (Fisher, P8), and incubated in the dark at 4°C. Microbe cell numbers were not counted, but DOC content of the inoculants was analyzed and was used to estimate cell numbers. No additional carbon source was added during the culturing, in order to avoid preferentially enriching certain microbial species.

Na-acetate solution was used as a labile source of organic matter that could be utilized by microbes easily and quickly. The Na-acetate solution was made by dissolving 72.80 mg Na-acetate solids into 1.5 L water and was sterilized in an autoclave. Neither NGW nor SW was sterilized or chemically modified in any way.

Incubation experiment

Incubation experiments were begun on June 9, 2010 in the FGS lab in Tallahassee, FL, after 6 months of core storage under vacuum, by combining core material, solution, and treatment additions in 2.5-L reaction vessels that could be sealed and sub-sampled through gas-tight ports. Sampling over the six week of each experimental phase was conducted three times per week for the first three weeks, and once per week for the last three weeks. At each sampling period, 40 mL were taken from each vessel, followed by the injection of 40 mL of solution of composition corresponding to the starting background solution of each vessel.

The incubations can be divided into three phases. Phase 1, or the Upper Floridan Aquifer low DO native groundwater (LDO-NGW) phase, initiated within 25 hours of NGW collection, was a 41 day period in which 300 g of core material was equilibrated with 1 L NGW in an anaerobic environment (N_2 headspace), simulating a normal subsurface condition before ASR and AR operation. Phase 2, or the 'high DO source water (HDO-SW)/ N_2 headspace' phase was initiated on day 41 and ran for 38 days. To initiate Phase 2, the incubation solution was replaced with SW, with or without experimental treatments, simulating the start of an ASR operation introducing different types of storage waters (Table 4-1). In an effort to keep the reaction vessels from become too aerobic, i.e. unrealistic groundwater conditions, a N_2 headspace was applied to each vessel upon re-filling with SW and after each sample collection which occurred every three days. At the start of Phase 3, high DO source water (HDO-SW/air headspace), an air headspace in the vessels was initiated on day 79 and was run for 31 days. To initiate this phase, caps were loosened on all the vessels to allow the head space to equilibrate with atmospheric (lab) conditions.

Table 4-1 summarizes the experimental treatments used during Phases 2 and 3. A total of 16 reaction vessels were used for different incubation treatments, including duplicates and blanks. Vessels 1-3 contained core materials and Vessels 4-6 contained purposefully unpreserved core materials. Vessel 7 contained no core materials and serves as blank control for all 16 vessels. Vessels 8 & 9, 11 & 12, and 14 & 16 contained core materials plus treatments additions 1, 2 and 3, respectively. Vessels 10, 13 and 16 served as controls containing treatment additions 1, 2 and 3, respectively, but no core material.

Treatments were diluted so that each vessel contained equal amounts (1 L) of solution at approximately the same DOC concentration (about 7.1 mg/L). Treatment 1 vessels received 500 mL SW (3.4 mg/L) and 500 mL NDOM extract (14.2 mg/L). Vessels 11-13 (Treatment 2) received 500 mL SW (3.4 mg/L), 490 mL NDOM (14.2 mg/L) and 10 mL microbes (~60 mg/L). Vessels 14-16 (Treatment 3) received 500 mL SW (3.4 mg/L) and 500 mL Na-acetate (14.2 mg/L).

Organic matter adsorption and desorption experiment

Batch sorption experiments were conducted to estimate how much indigenous OM may have desorbed from the core materials, as well as how much of the added organic components may have sorbed onto the core. The experimental design is summarized in Appendix K and included three experimental treatments; core material + distilled water, core material + humic acid, and core material + Na-acetate, as well as three corresponding controls; distilled water, humic acid, and Na-acetate with no core material.

For each treatment with core material which was prepared in triplicate, 30 mL solutions of distilled water, humic acid, or Na-acetate prepared in distilled water were mixed with approximately 10 g of core materials in 50 mL polypropylene centrifuge

tubes. Starting concentrations of NDOM (Sigma-Aldrich humic acid standard, CAS#: 1415-93-6) and Na-acetate were 7.8 mg/L and 230.0 mg/L, respectively. The centrifuge tubes were then placed horizontally on a platform shaker (300 rpm) for 1 hour at room temperature (22 ± 2 °C). A 1-hour contact time was selected to minimize the possibility of microbial reactions. At the completion of the contact period, the suspensions were centrifuged at 3000 rpm for 5 min and DOC concentrations in the supernatants were immediately analyzed.

Sorption or desorption of organic C was calculated as the difference between DOC concentrations in experimental treatments with core material present and corresponding controls with no core material present.

Chemical Analyses

Concentrations of DOC were measured on a total organic carbon analyzer (Shimadzu TOC-5000A) after acidifying to pH 1–2 with 1 M HCl and sparging for 2 min with carbon-free air to remove inorganic carbon. Each sample was measured in duplicate by the injection of 50 µL of sample three times or more if the coefficient of variation was greater than 5%.

Samples collected for As measurement were collected in 20 mL glass bottles and were immediately acidified with HCl. They were later prepared for analysis using a 3:1 dilution with 20% HCl and 1% Thiourea. Total As concentrations were measured on a Hydride Generation Atomic Fluorescence Spectrometry (HG-AFS) at University of Florida Department of Environmental Engineering Sciences. Major cations and trace metals were measured using an inductively coupled plasma mass spectrometry (ICP-MS, Perkin Elmer Optima 3000) and anions (SO_4^{2-}, NO_3^-, NO_2^-, PO_4^{3-}, F^-, Cl^-, and Br^-)

were measured using a DIONEX DX-120 ion chromatograph. Geochemical parameters including pH, ORP, DO and SpC were monitored in FGS lab using an YSI multiprobe.

Whole-rock geochemical analysis of the core material was completed by Activation Laboratories Ltd. (Ontario, Canada). Details of the sample preparation and analysis have been presented elsewhere (Norton, 2011). The mineralogy of core materials were analyzed via X-ray diffraction (XRD), scanning electron microscopy (SEM), electron microprobe analysis (EM), and energy-dispersive X-ray fluorescence elemental spectrometry (EDS) by Dr. W. Harris, at University of Florida Department of Soil and Water Sciences. Efforts to identify As associations with minor but geochemically-significant phases in the rock included selective dissolution and density fractionation. Details of these procedures have been presented elsewhere (Norton, 2011).

The OM content of the carbonate core materials was determined by a loss-on-ignition (LOI) method. Core materials were oven-dried overnight at 40°C and then granulated and sieved to < 0.3 mm. Five sets of core material were homogenized, weighed and placed in crucibles before combusting at 550°C for 4 hours (Heiri et al., 2001; Santisteban et al., 2004). The weight loss after combustion was considered as the OM content of core, and was converted to organic carbon (OC) content assuming an average of 0.5 g OC/g OM (Essington, 2004).

Results

Core material composition

Results of whole-rock geochemical analysis are presented in Appendix L. Total As was measured to be 2.0 mg/kg. The bulk core material was dominated by calcite with a minor amount of quartz (and very small but detectible amounts of feldspar and aragonite). The trace mineral components were examined by SEM, EDS, and EM

following a selective dissolution of carbonate. The results indicated the presence of pyrite in very low concentrations, as has been found by other studies of Suwannee Limestone (Budd, 2007; Price and Pichler, 2006). Although no As-bearing minerals were detected, As was identified as associated with one iron sulfide and one iron oxide particle using SEM/EDS/EM.

Loss-on-ignition and OM sorption measurements

Both OM sorption experiment and LOI measurement revealed significant indigenous OM in the core materials. The OC content of the core was determined by LOI to be 8.0 ± 0.6 g/kg core (n = 5, Appendix M). The finding of a linear correlation between LOI weights and the amount of core material combusted adds confidence to the OC calculations (Appendix M, $R^2 = 1.0$, $p < 0.005$).

The carbonate rocks of the core material were also found to desorb as well as sorb significant quantities of NDOM (Figure 4-1). When place in distilled water for 1 h, the core material desorbed 3.6 mg/kg. Losses of humic acid and Na-acetate occurred after 1 hour contact with the carbonate rock, respectively, or were16.9 mg/kg and 190.4 mg/kg, respectively, with no significant difference between the replicate treatments. This amounted to 72.0% and 27.6% of the humic acid and Na-acetate initially present, respectively. However, assuming that the same amount of indigenous OM was desorbed from the carbonate rock in the presence of the humic acid and acetate solutions as occurred in the distilled water solution, the adsorption rate for humic acid and acetate could be re-calculated as 20.5 mg/kg/h and 194.0 mg/kg/h, respectively.

Incubation experiment

Time series data for all parameters measured during the incubations are presented in Figures 4-2, 4-3 and 4-4 as well as in Appendix N with each data point

representing means of concentrations in the overlying solution of duplicate treatment vessels and error bars as the standard deviation (n = 2).

Incubation DOC Concentrations: The DOC concentrations measured during the incubation time series (Appendix N) showed high variability even among replicate treatments, and displayed no clear pattern across different treatments. This instability may have been caused by releases of indigenous OM into solution or sorption of the added DOC in the forms of soil NDOM or Na-acetate. Given the amount of DOC release or consumption measured over only 1 hr in the sorption experiments, these processes could have accounted for a possible release of 1.1 mg/L OC as indigenous DOC, or adsorption of 6.2 mg/L OC as soil NDOM or 58.2 mg/L OC as acetate. However, much more may have been released or sorbed during the much longer time period of the incubations. Another possible cause of variations is booms and crashed of microbial populations that utilize DOC for either growth or respiration.

Alternatively, some of the instability in the data may have been methodological as control treatments also displayed similar variability as those with core material. For instance, the DOC samples were not pre-filtered immediately upon collection to exclude microbes or colloidal OM, possibly adding to the DOC measured. Abiotic precipitation of dissolved OM may be another possible loss of DOC. In addition, DOC measurement sample sets were run at different time, and therefore, though standards were used, variation in instrument response may also be a factor.

Incubation Arsenic Concentrations: Time series As concentration plots (Figure 4-2), show that As concentrations were near zero (< 0.5 µg/L) in all control vessels, indicating no As contamination in the experimental solutions. Arsenic was clearly

released from the core materials into solution during the low DO equilibration period (Phase 1). In all treatments with core samples the As concentration increased to about 18 ug/L by the end of phase 1. The mass of As released represents a small fraction, about 3%, of the As present in the cores samples. At the start of Phase 2, As concentrations were lowered in all treatments due to removal of the overlying solution containing the released As and replacement with As-free SW. Both the NDOM and NDOM with microbe addition treatments maintained low As concentrations (~2 µg/L) throughout Phase 2. This low level of As release represents only about 0.3% of the As present in the core material. This reduced As release between phases 1 and 2 may indicate that much of the As associated with the core samples is not available for extraction. Arsenic levels in Treatment 3 with Na-acetate addition noticeably increased to ~8 µg/L (i.e. a release of 0.02 mg As/kg or about 1.3% of As in the core) and remained constant for the remainder of Phase 2.

At the start of Phase 3, when laboratory air was allowed to equilibrate with the reactor vessels, the concentration of As in treatment 3 returned to the levels of the other treatment vessels. In the first two weeks of Phase 3, As levels generally increased gradually by about 2 µg/L in all treatments. The increased mass release during Phase 3 is comparable to that observed between Phase 1 and 2 for all treatments other than treatment 3. The one exceptional high As concentration in the ‘no core’ control, collected on day 80 (4.77 µg/L), is likely a result of measurement error or sample contamination.

During all three experimental phases, treatments with NDOM or microbe additions had no apparent effect on As release. That is, changes in As concentration were all similar to that of treatment ‘core’, varying no more than 10%.

Dissolved Oxygen and ORP: Levels of O_2 in all vessels were generally close to 0 mg/L throughout phases 1 and 2 (Figure 4-3). An increase in DO occurred at the beginning of Phase 2 when the solution was changed from low DO NGW to high DO SW after which, DO levels returned to near zero, presumably by degassing of the solution into the N_2-flushed headspace. When the vessels were opened to the atmosphere at the start of Phase 3, DO concentrations in all treatments increased immediately to between 4.0 and 5.6 mg/L and then gradually to as high as 7.9 mg/L. During this period, DO increased faster in control treatments than in their corresponding treatments with core material indicating, perhaps, some degree of biotic or abiotic oxygen consumption in the latter.

Another, perhaps more sensitive indicator of redox condition in the incubation vessels, oxidation reduction potential (ORP) gives a somewhat different picture of redox variation in the incubation vessels (Figure 4-4). During Phase 1, ORP remained reducing but increased gradually to near zero in all vessels. At the start of Phase 2, with the change to SW, ORP increased to about +200 mV in all of the vessels as expected. However, control vessels with no core material but added NDOM or Na-acetate, along with the vessel containing Treatment 3 (core + Na-acetate), began to exhibit progressively reducing ORP. The ORP in these vessels decreased rapidly to below 0 mV within the first week; the rate of the decrease then subsided until day 69 when the ORP started to approach 0 mV. Among these four vessels, Treatment 3 with core

material maintained the lowest ORP values, reaching -182.65 mV on day 69. The lower ORP observed in Treatment 3 during Phase 2 compared to the vessel with Na-acetate and no core, may be an indication of a different microbial community present in the core material compared to the SW. After abundant oxygen was introduced at the start of Phase 3, ORP behaved uniformly in all treatments, ranging between 150 mV and 280 mV.

Discussion

The results, taken as a whole, show that releases of As, when they do occur, are mainly associated with changes in solution chemistry or redox condition. This is not surprising given that geochemical analysis of core materials showed As to be associated with iron sulfide and iron oxide, both redox-sensitive minerals. The greatest As release occurred during Phase 1, when ORP data show the experimental conditions to be the most reducing and, among the treatments, when Na-acetate was added during Phase 2 which also decreased ORP conditions. In the following discussion, the geochemical evidence supporting or negating three As mobilization mechanisms that are considered to be most likely are examined: oxidative dissolution, reductive dissolution, and As desorption. To assist the identification of treatment effects, the data is presented here in the form of ‘Δ values’, i.e. differences between each chemical parameter in a treatment vessel and their corresponding ‘no core’ control vessel (treatment solution with no core material). These ‘Δ plots’ (Figures 4-5 to 4-11) indicate whether the chemical species or environmental parameter increased (was produced or released) or decreased (was consumed or sorbed) due to mineral interaction.

Arsenic mobilization mechanisms

Oxidative As release mechanism: In this study, iron was found commonly associated with sulfur in the core material. Though pyrite was reported to be associated with As and to be a major 'source' of As in aquifer materials in southwest Florida (Arthur, 2002; Price and Pichler, 2006), the presence of pyrite (FeS_2) was not indicated by mineralogical analyses of this core. However, iron mono-sulfide and other amorphous Fe-S phases may be present, and amorphous Fe, as determined by oxalate extraction was measured as 130 mg/Kg. In addition to iron-sulfide phases, iron oxides are also likely to exist in the core material and may also contain As. Both iron-sulfide and iron oxides can be geochemically stable in reducing surroundings but can undergo dissolution in an oxidizing environment, thus releasing As. These types of reactions may occur abiotically when thermodynamically and kinetically favorable, or they may require microbial-mediation.

According to the oxidative dissolution As release mechanism, a greater amount of As would be expected to be mobilized as the solution becomes more oxidized. The As release during Phase 1 may have corresponded to the increasing ORP measured during this equilibration period, however most of the observed As increase occurred during the first few weeks when the ORP was relatively stable around -150 mV (Figure 4-2 and 4-4). Thus, oxidation was most likely to have taken place in Phases 2 and 3 when higher DO SW was in contact with the cores leading to ORP values of +200 mV and higher. In the beginning of Phase 2, As concentrations were lowered in all treatments by the removal of the released As during Phase 1 and replacement with SW (Figures 4-2 and 4-5). The As concentrations of approximately 2 ug/L are much lower than those observed in Phase 1 and represent a minimal mass release even at the

much higher ORP values. Phase 3 was more oxidized than Phase 2, and this may correspond to the slight increase in As release observed during this time for all treatments except for ‘core + Na-acetate’. However, the amount of As release during this period of high DO (Phase 3) was much lower than that which occurred during the lower DO Phase 1. As noted earlier, this may be indicative of a limited amount of easily oxidizable mineral or As associated with these mineral phases.

Considering the pH of the solution (Appendix N), As should mainly exist in the form of As^{3+}, with a small amount of As^{5+}. Thus, the oxidative dissolution mechanism may be represented using the following chemical reactions:

$$Fe(As)S_2 + 4O_2 \rightarrow Fe^{3+} + 2SO_4^{2-} + As^{3+} \quad (4\text{-}1)$$

$$Fe(As)O_xH + O_2 \rightarrow Fe^{3+} + As^{3+} + 1/2\ H_2O \quad (4\text{-}2)$$

The dissolution of minerals into solution might be expected to release ions such as Ca^{2+} Fe^{3+}, SO_4^{2-} and As^{3+} into the solution. The increase in SpC during Phase 2 and then Phase 3 suggests occurrence of oxidative mineral dissolution (Figure 4-6, Appendix N).

According to the above two chemical reactions, the occurrence of mineral oxidation might be reflected in an increase in Fe and sulfate levels. The Fe data were scarce and most of the values were below detection limit, and thus they are not conclusive. Other Fe oxide phases likely formed via precipitation directly onto rock surfaces, removing Fe from solution. Some increases in sulfate concentrations during Phases 2 and 3 may support the existence of mineral oxidation (Figure 4-7).

The only treatment with greater As release was that with added Na-acetate. But this treatment also had the lowest ORP (Figures 4-4 and 4-8), likely due to aerobic respiration of the Na-acetate. These data make it unlikely that oxidative dissolution is

the predominant As release mechanism. Future experimentation to test for this mechanism could examine As release in reaction vessels with core material and the addition of oxidants such as peroxides to regulate ORP.

Reductive dissolution As release mechanism: Although As has not been found to be associated with oxides in most studies of aquifer material, that does not mean it does not become associated with oxides either during ASR or, in our case, following core collection and manipulations. During the 6-month core storage period, even the preserved core likely underwent some degree of alteration. Minerals such as iron sulfides in the core might have been oxidized and released As, Fe, and other metals. Dissolved metals can re-precipitate locally as metal-hydroxides whose surfaces may sorb aqueous As and became a 'source' of As during later experimental stages (Mirecki, 2006). Therefore, reductive dissolution of metal-hydroxides may have been another possible As mobilization mechanism.

The highest amount of As released occurred during Phase1, while ORP data show the conditions of all cores to be the most reducing (Figure 4-2). Another possible argument in support of reductive dissolution is the fact that, among the treatments, the vessel with Na-acetate added had the lowest ORP and the greatest As release.

Arguing against reductive dissolution As release mechanism, Phase 3 was somewhat less reducing than Phase 2 (Figure 4-4) but had slightly more As production (Figures 4-2 and 4-5) as well as more ion release (Figure 4-6, Appendix N) than Phase 2 in most of the vessels. Therefore, the reductive dissolution mechanism does not satisfy all of the observed data, unless it is combined with the requirement of microbial aerobic respiration-mediated oxidation of metal-hydroxides. A direct test of the reductive

dissolution mechanism could be devised by incubating core materials under a range of ORP conditions.

Desorptive As release mechanism: According to at least one study, arsenic may be sorbed to mineral surfaces via a weak chemical association such as electrostatic or even van der Waals attraction and released by surface exchange processes (Pearcy et al., 2011). These exchanges could be initiated by changes in solution chemistry such as ionic strength or ORP, thus releasing As into solution. The desorbed As found in solution may also re-sorb onto mineral surfaces. Differently from the previous two mechanisms, desorption/adsorption of As could take place during all three phases, especially at the beginning of each phase when significant changes to the solution chemistry were imposed.

The high As release observed during Phase 1 (Figures 4-2 and 4-5) could certainly be explained by the destabilization of weakly sorbed As on mineral surfaces. The first three weeks of Phase 1 showed high As release, but after that, As levels plateaued, suggesting the depletion of weakly associated As. However, arguing against the desorptive mechanism, no As release was observed during the 1-h OM sorption experiment. A possibility is that this time period was too short for desorption to occur but sorption/desorption of As onto/from mineral phases has been shown to occur quickly, often within minutes or even seconds (Gimenez et al., 2007; Luengo et al., 2007; Wolthers et al., 2005).

Although solution chemistry in the vessels changed quite dramatically at the start of Phase 2, as evidenced by Δ plots of SpC, ORP and pH (Figures 4-6, 4-8, and 4-9, respectively), there is not a dramatic release of As or NO_3^-, Ca^{2+}, or SO_4^{2-} (Figures 4-5,

4-10, 4-11, 4-7). Unless, desorption of As was kinetically limited, perhaps due to the necessity of microbial involvement, this data does not clearly support the desorption mechanism.

The transition from Phase 2 to Phase 3 saw more ion release (As, Ca^{2+} and SO_4^{2-}) into solution. The concentrations of As went up once Phase 3 started and kept going up for about 3 weeks until achieving an equilibrium during the remaining 3 weeks of Phase 3. Again, this apparently kinetically limited process does not strongly indicate a desorption mechanism. Microbial activity and/or redox-associated As release mechanism seems more likely. However, release of weakly sorbed ions may occur by hydrolysis which would produce H^+ or OH^-. Figure 4-9 shows that pH varied greatly among the vessels and over the whole experimental period. The 'core + Na-acetate' treatment, however, generally had higher pH than other treatments relative to its control (Appendix N), possibly indicating that OH^- might exchange with mineral-sorbed AsO_3^{3-} or AsO_4^{3+} resulting in As mobilization. These observations indicate possible desorptive As release, but this mechanism cannot, alone, completely explain all the observations. Multiple release mechanisms might be involved during different periods of the experiment. Incubation of core materials in solutions with different ionic strength could be used to test for the importance of the desorptive As release mechanism.

Influence of organic matter and microbes on As release

There are a number of clear conclusions that can be made in regards to the effects of NDOM and microbes on metal release from aquifer materials. First, there was no apparent geochemical difference between treatments with 'core + NDOM' and 'core + NDOM + microbes'. Further, the addition of Na-acetate (without a microbe amendment) resulted in, what appears to be, high microbial activity. One can conclude,

therefore, that the core materials collected were not sterile or lacking in a microbial population with metabolic capabilities though removed from the subsurface environment. The indigenous microbes already present in the core or desorbed from rock into solution were biogeochemically active.

The greatest As release occurred in treatments with Na-acetate during Phase 2 and corresponded to the most reducing condition measured (lowest ORP, Figures 4-5 and 4-8). The effect of Na-acetate addition on As release is depicted by a plot of differences between As and ORP measured in treatment vessel and control with core materials but no amendment (Vessels 1-3, δ values in Figures 4-12 and 4-13). These findings of greatest As release during lowest ORP conditions strongly suggest that Na-acetate fueled a microbially-mediated reaction that either directly or indirectly mobilized ions such as As.

One possible indirect mechanism for As release is that of reductive dissolution (discussed above). That is, Na-acetate may have fueled aerobic respiration, which consumed O_2 and led to lowered ORP conditions which encouraged As-bearing mineral dissolution. However, this mechanism is not supported by the observation of greater As release in other treatments during Phase 3 when O_2 was present (as discussed above). A possible direct effect would be that Na-acetate may have fueled microbial iron reduction, thus releasing As associated with iron oxides. Again, there is ancillary evidence both supporting and conflicting with this hypothesis. In other studies, both the release of As and Fe^{3+} reduction, though decoupled, was found to be stimulated by acetate addition to incubations of West Bengal sediment (Islam et al., 2004; Van Geen et al., 2004). Because this only occurred when Fe oxides were present, this suggests

oscillations in redox conditions may be required for As release. Successive cycles of ASR are likely to produce redox oscillations.

Lastly, the labile C source could have fueled As release directly by serving as an electron acceptor during microbial reduction of the more strongly sorbed As^{5+} to the more mobile As^{3+} species. This mechanism could act in combination with the reductive dissolution and the desorption As release mechanism and may be carried out by the same class of organisms responsible for S reduction (Inskeep et al., 2002; Oremland et al., 2002).

While Na-acetate fueled aerobic respiration in the presence of core material, NDOM did so only when core material was absent. This may indicate that all the added NDOM sorbed to solid surfaces rendering it inaccessible to microbes. Alternatively, the NDOM may have been too refractory to serve as a microbial substrate. Unlike with Na-acetate, the addition of soil NDOM did not result in elevated As concentration in the solution or change the solution chemistry in any clear way. Thus, there is no evidence provided here that added NDOM has an effect on metal release, either as a chelator of metals or as a microbial substrate. No strong conclusion can be made, however, because of the apparent complete sorption of NDOM onto the core material.

Conclusions

The results of these core material incubations provided some evidence to support each of the hypothesized As release mechanisms evaluated, oxidative dissolution, reductive dissolution, and As desorption, during different portions of the incubation experiments. Evidence from As, SpC, and Ca^{2+} trends suggested their reductive dissolution release during Phase 1. The oxidation of As-bearing minerals (e.g., iron-sulfides) appears to have released smaller amount of As during Phases 2 and 3. In

addition, As may have been released by reductive dissolution of metal oxides formed during the core storage period. In addition to these two mechanisms, As may also have been desorbed from mineral surfaces, particularly during dramatic changes to solution chemistry, at the start of each phase, although 1-h sorption experiment did not show release of As.

Along with the abiotic reactions, there was some evidence that As release may be enhanced by biotic processes. Indigenous microbes likely played an active role in biogeochemical reactions measured in the vessels. Na-acetate fueled microbially-mediated reactions which, either directly or indirectly, mobilized As. The addition of soil NDOM did not influence the As level, probably because it sorbed to mineral surfaces and became unavailable for microbial utilization or metal chelation.

Base on the presented, it is difficult to point out a single mechanism that explains the As mobilization observed and all three mechanisms may be responsible for at least part of the As released. However, it may very well be the oscillation of redox condition, converting reduced iron-sulfides to iron oxides, and then microbial reduction of these As-bearing Fe oxides, that are the underlying cause of As release. Such oscillating conditions are exactly what might be expected to occur during an ASR operation. In regards to use of untreated surface waters for ASR or AR operations, it appears likely that modest amounts of non-labile NDOM, such as that present in most Florida freshwaters, will not strongly influence the release of As during ASR or AR operations. However, labile OM, such as the output of a sewage treatment plant or surface water with abundance algae, may result in significantly increased As release.

Desorption of indigenous OM and adsorption of soil OM and Na-acetate may be responsible for the non-conclusive DOC data. For future studies, LOI and desorption experiments are highly recommended prior to the batch incubation. The results from LOI and desorption experiment would be useful in the correction of DOC data generated from incubations. In addition, it is suggested to filter DOC sample immediately upon sample collection and run all sample consecutively. Further experiments designed to pinpoint As release mechanisms and microbial influences would include incubations with better controlled redox and ionic strength conditions, sterilized controls, and column experiments. These incubations serve as a solid starting point for future study that explores the As mobilization during ASR or AR.

Table 4-1. Summary of experimental treatments used during Phases 2 and 3

Incubation Vessel#	Experimental treatments	Note
V1–V3	300 g core + 500 mL SW	
V4–V6	300 g core (unpreserved) + 500 mL SW	
V7	500 mL SW	No core – control for V1–V6
Treatment 1 (soil NDOM)		
V8	300 g core + 500 mL SW + 500 mL NDOM	
V9	300 g core + 500 mL SW + 500 mL NDOM	duplicate of V8
V10	500 mL SW + 500 mL NDOM	No core – control for V8 & 9
Treatment 2 (soil NDOM + microbe enrichment)		
V11	300 g core + 500 mL SW + 490 mL NDOM + 10 mL microbes	
V12	300 g core + 500 mL SW + 490 mL NDOM + 10 mL microbes	duplicate of treatment 4
V13	500 mL SW + 490 mL NDOM + 10 mL microbes	No core – control for V11 & 12
Treatment 3 (labile NDOM)		
V14	300 g core + 500 mL SW + 500 mL Na-acetate	
V15	300 g core + 500 mL SW + 500 mL Na-acetate	duplicate of V13
V16	500 mL SW + 500 mL Na-acetate	No core – control for V15 & 16

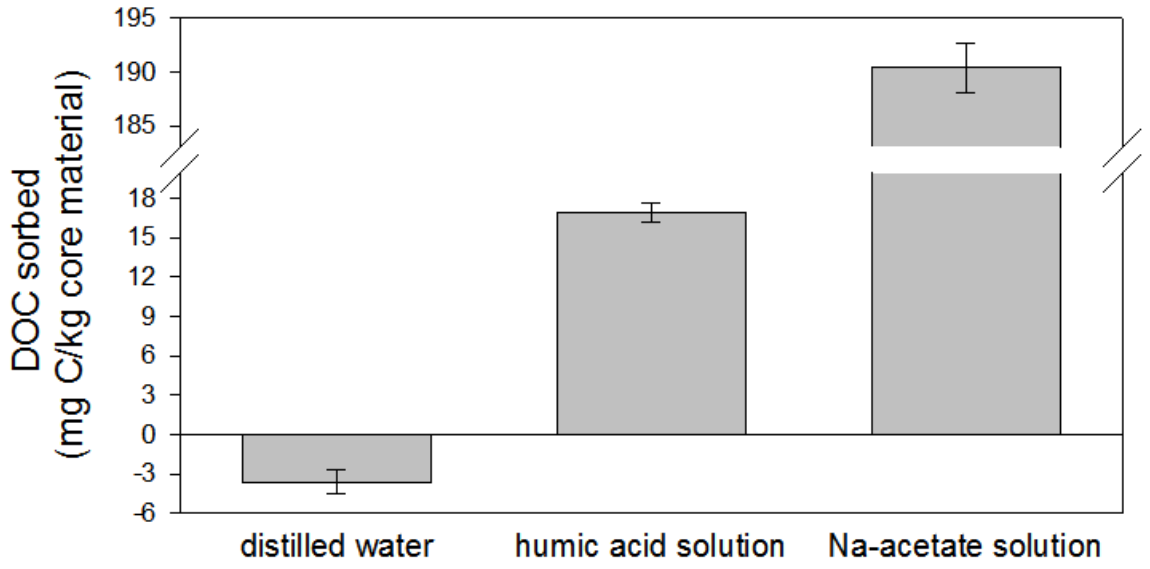

Figure 4-1. Organic C sorption/desorption onto Floridan Aquifer carbonate rock after 1 hour sorption contact time. Error bars represent the standard deviations of triplicate batches.

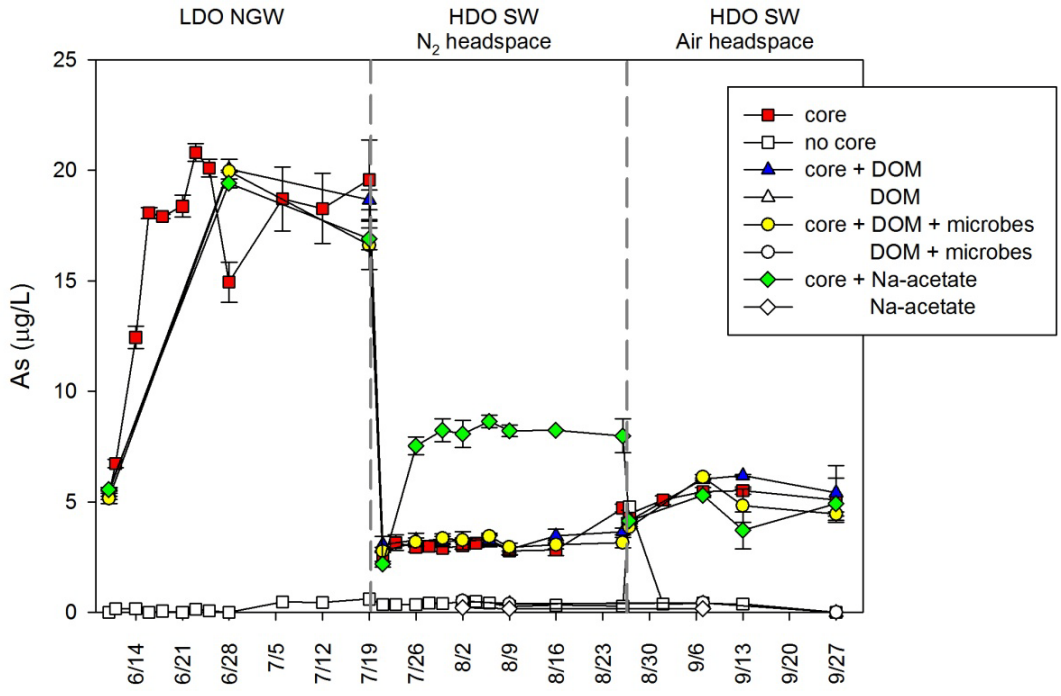

Figure 4-2. Concentration of arsenic in control (no core material) and treatment vessels (with core materials) during time-course incubations. See text for conditions during three phases of experiment.

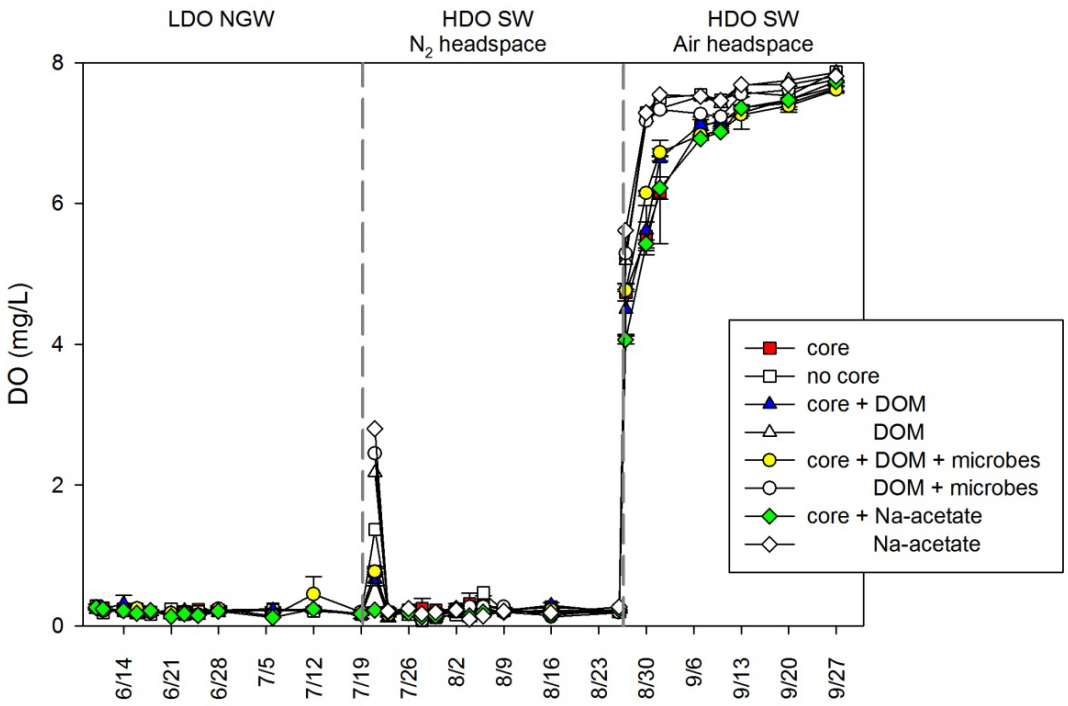

Figure 4-3. Concentration of dissolved oxygen (DO) in control (no core material) and treatment vessels (with core materials) during time-course incubations.

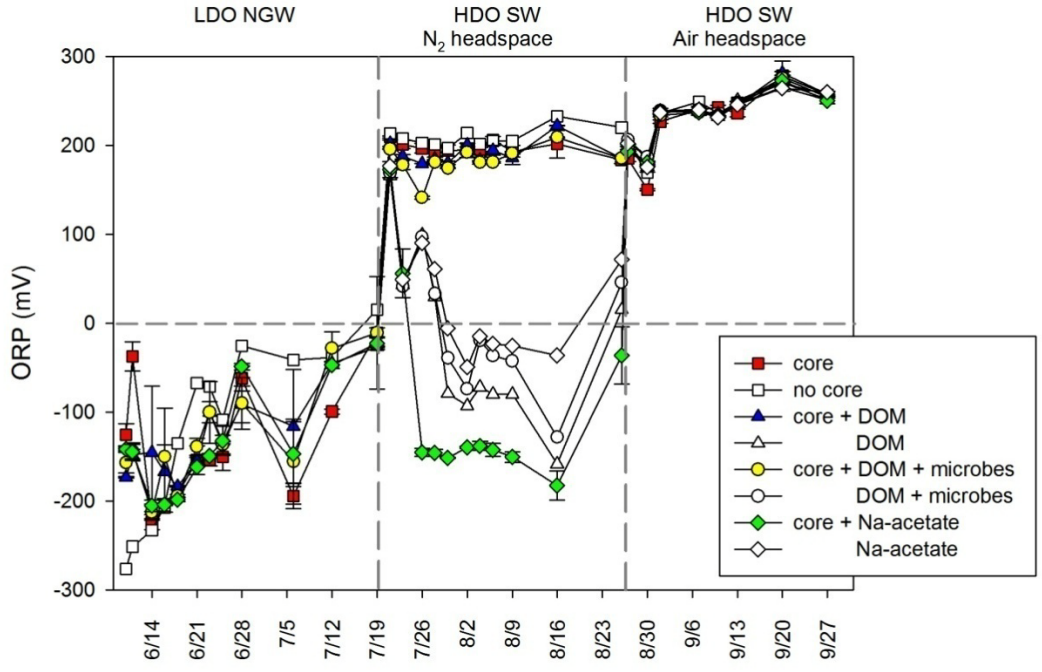

Figure 4-4. Oxidizing reduction potential (ORP) in control (no core material) and treatment vessels (with core materials) during time-course incubations.

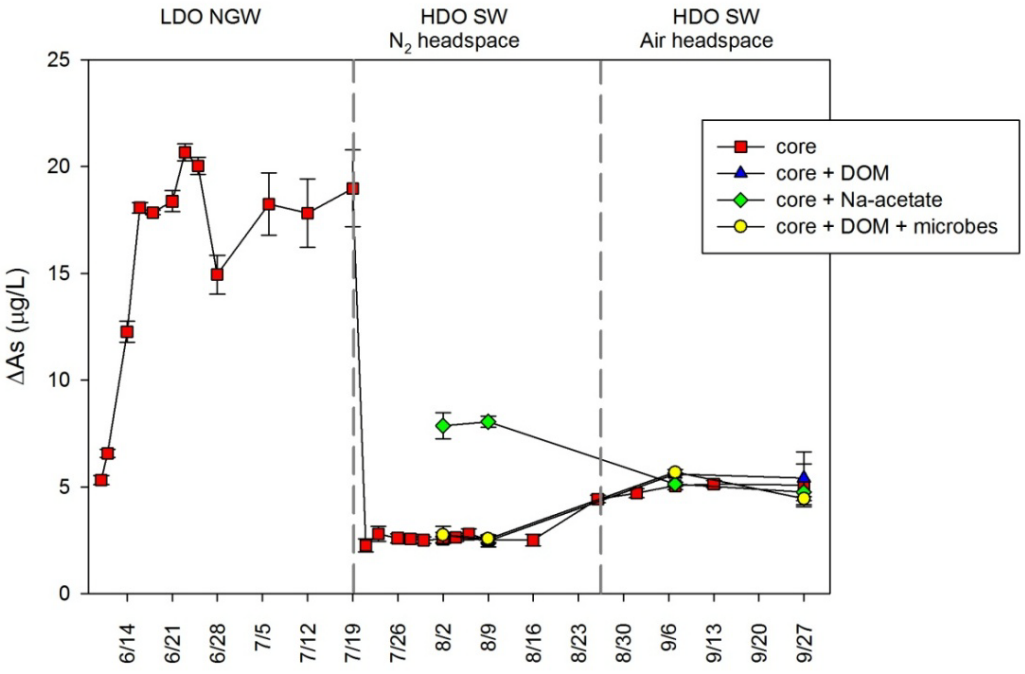

Figure 4-5. Difference between arsenic concentrations in control (no core material) and treatment vessels (with core materials) (ΔAs) during time-course incubations.

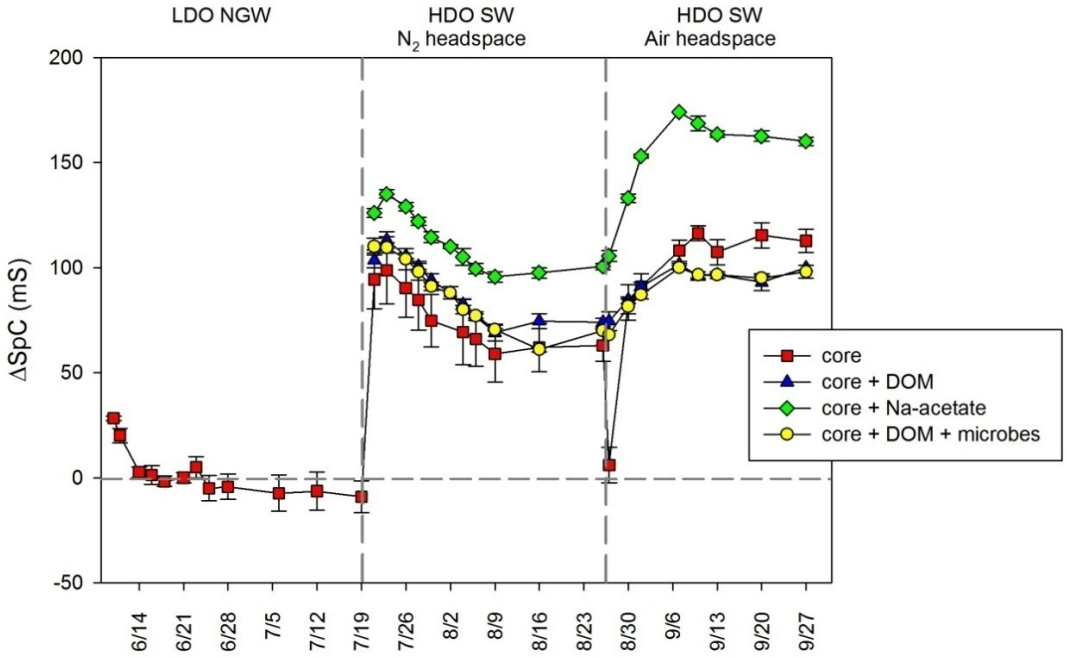

Figure 4-6. Difference between Specific conductivity (SpC) in control (no core material) and treatment vessels (with core materials) (ΔSpC) during time-course incubations.

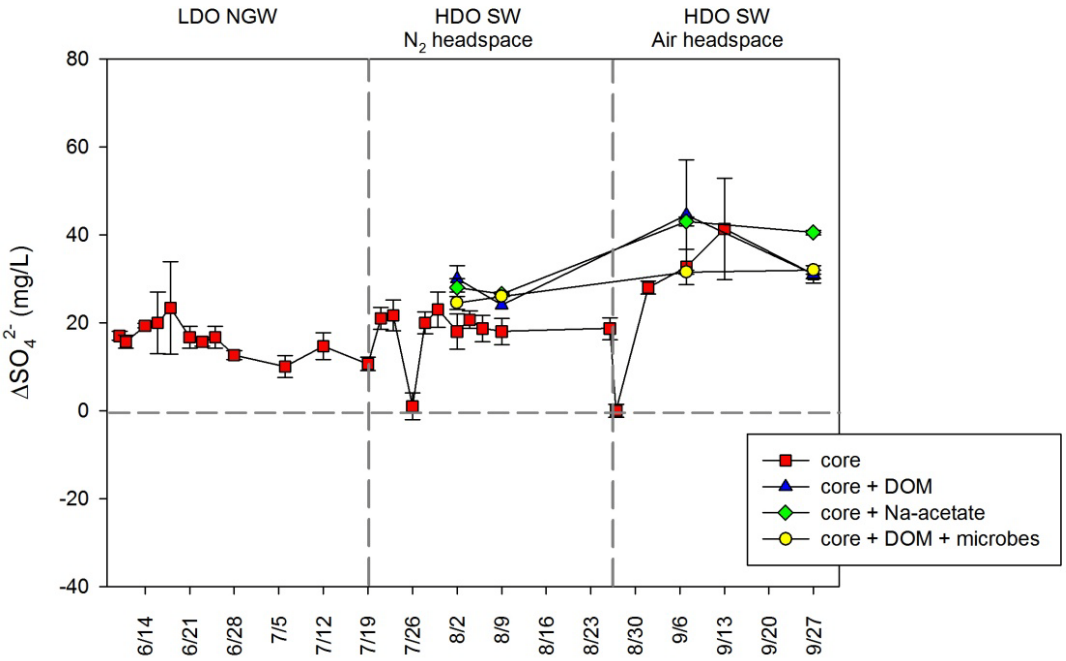

Figure 4-7. Difference between sulfate concentrations in control (no core material) and treatment vessels (with core materials) (ΔSO_4^{2-}) during time-course incubations.

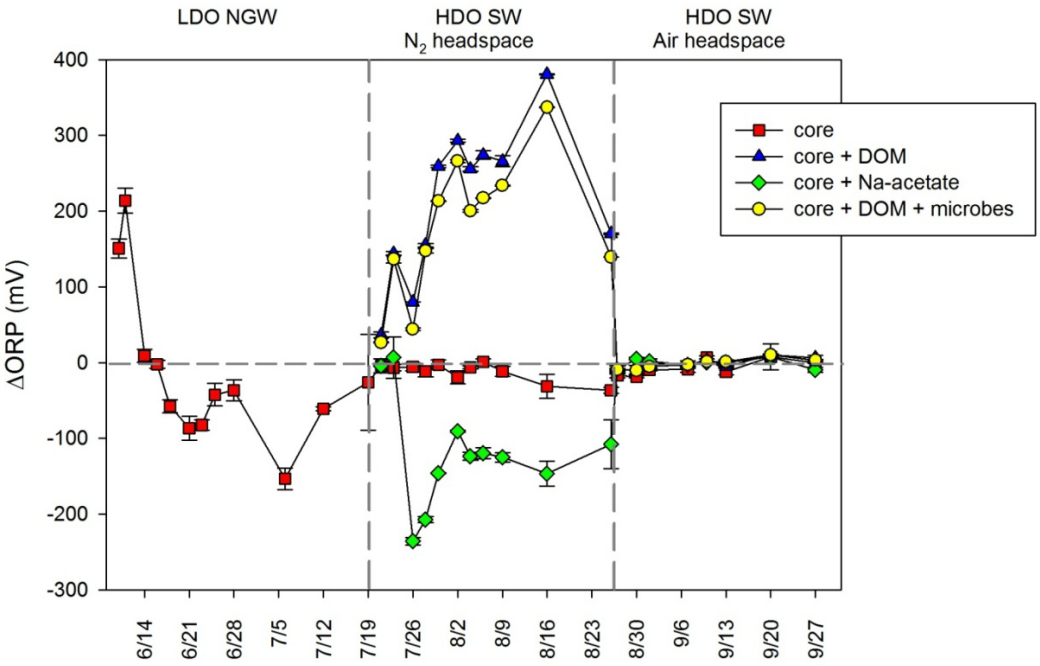

Figure 4-8. Difference between oxidation reduction potential in control (no core material) and treatment vessels (with core materials) (ΔORP) during time-course incubations.

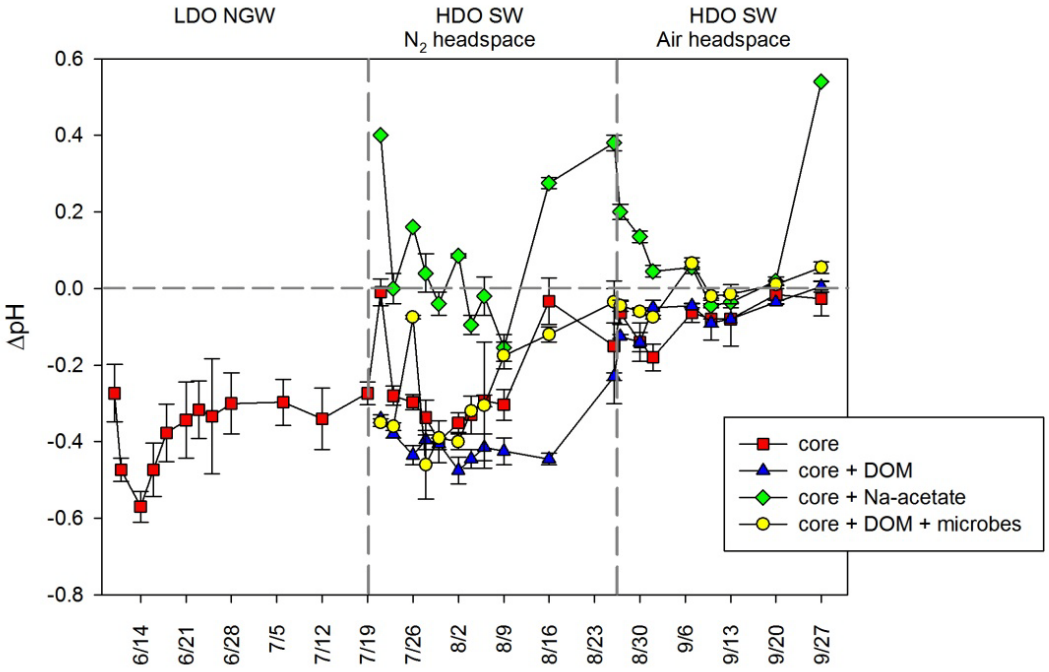

Figure 4-9. Difference between pH in control (no core material) and treatment vessels (with core materials) (ΔpH) during time-course incubations.

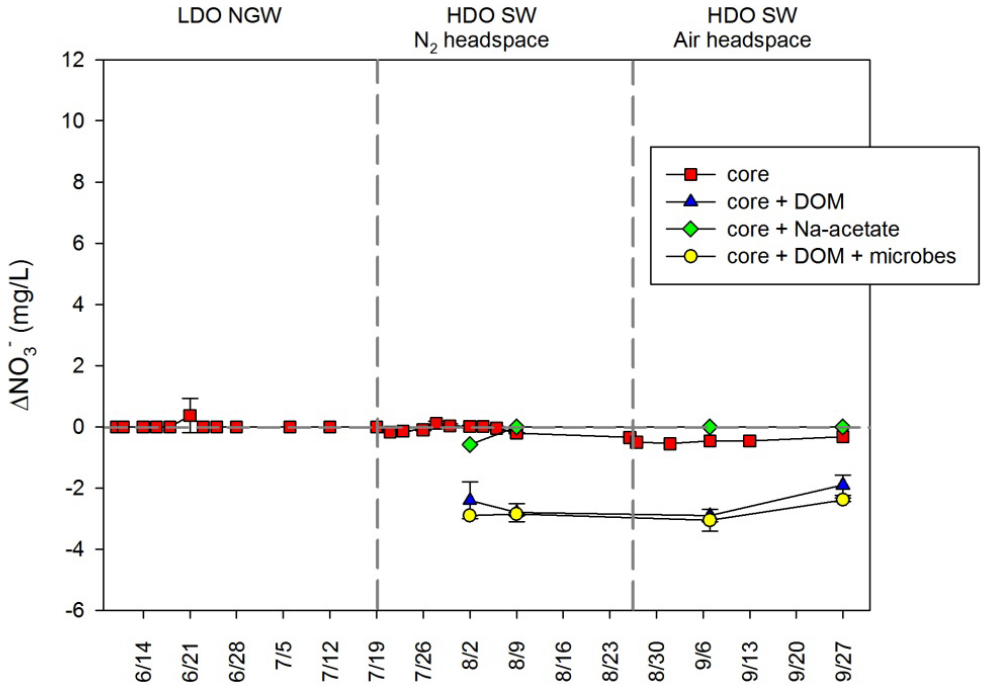

Figure 4-10. Difference between nitrate concentrations in control (no core material) and treatment vessels (with core materials) (ΔNO^{3-}) during time-course incubations.

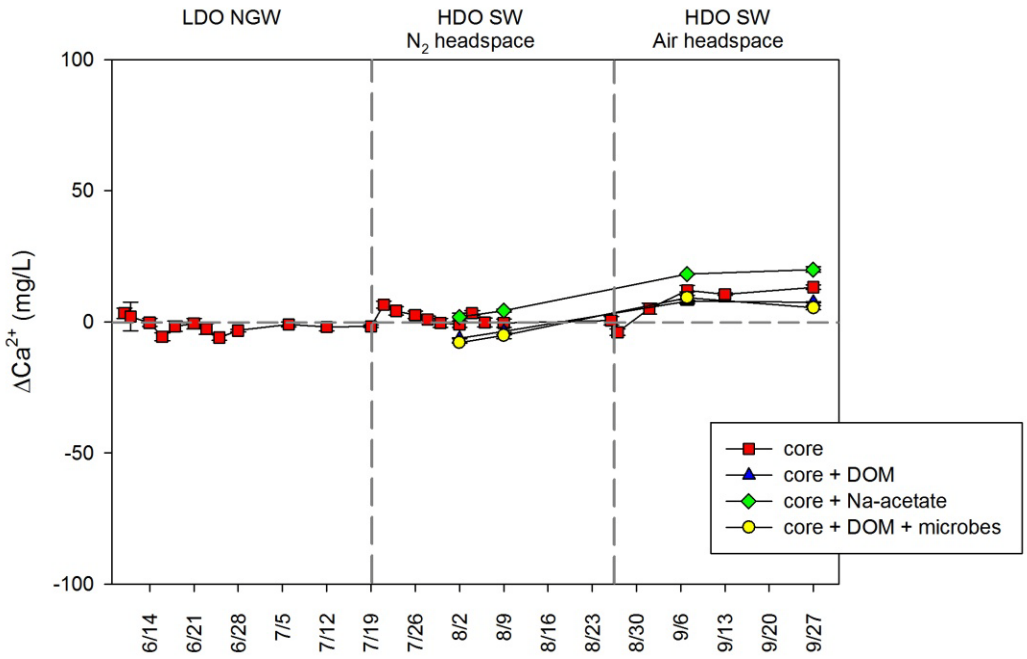

Figure 4-11. Difference between calcium concentrations in control (no core material) and treatment vessels (with core materials) (ΔCa^{2+}) during time-course incubations.

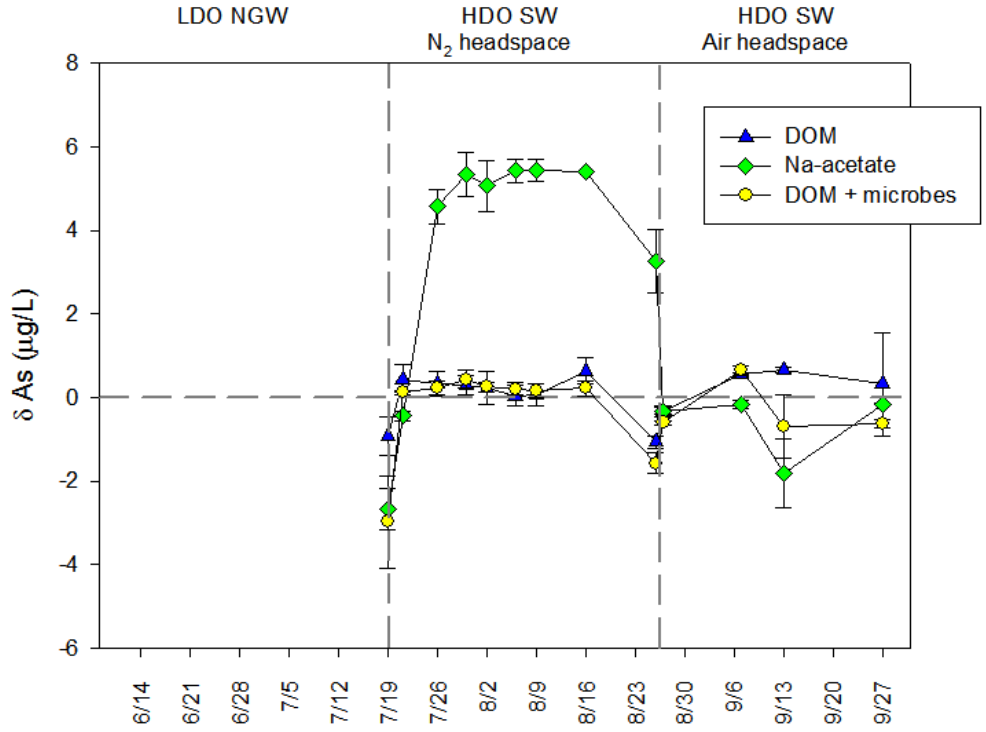

Figure 4-12. Difference between arsenic concentrations in control (no amendment) and treatment vessels (with amendment) (δAs) during time-course incubations.

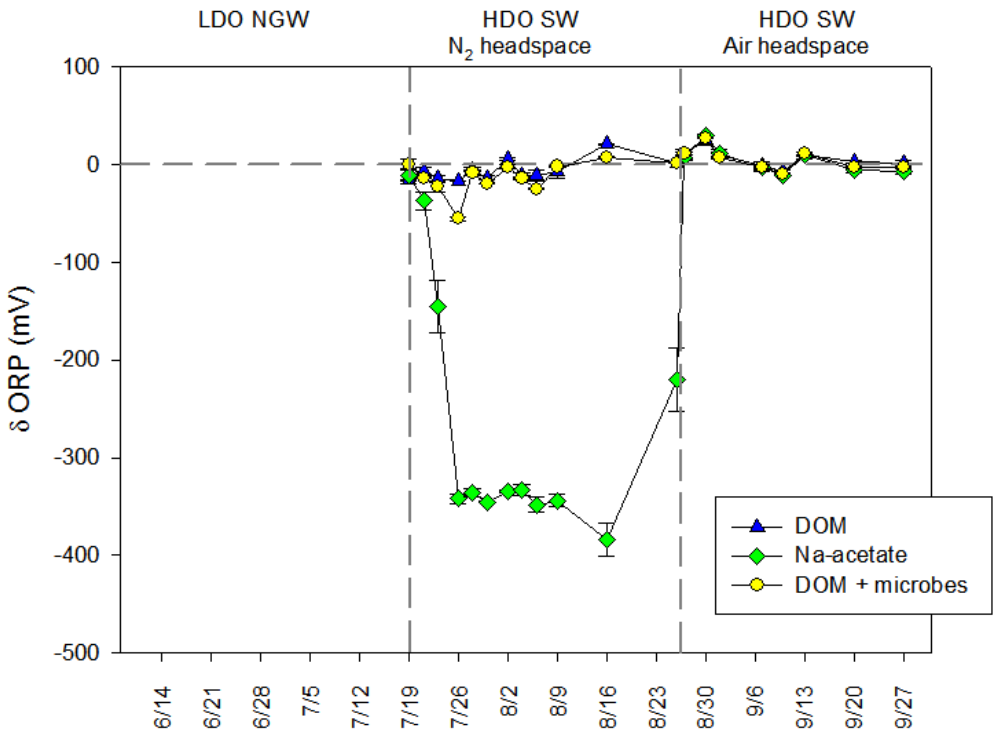

Figure 4-13. Difference between oxidation reduction potential in control (no amendment) and treatment vessels (with amendment) (δORP) during time-course incubations.

CHAPTER 5
SUMMARY AND CONCLUSIONS

The high porosity of the Floridan Aquifer allows extensive mixing of surface water and groundwater, which in turn, allows dynamic exchange of natural dissolved organic matter (NDOM) in the watershed and the aquifer beneath. However, the spatiotemporal variability of this exchange, the biogeochemical processes it fuels, and their relative magnitudes and effects has been poorly understood. This is largely because of methodological difficulties related to the heterogeneity and difficulty in sampling the karstic aquifer. This dissertation combines field, laboratory, and geochemical modeling approaches to examine the reactivity and effect of NDOM in three independent but related studies of surface-groundwater exchange systems in North Florida: the Santa Fe River watershed (SFRW), the O'Leno Sink-Rise system, and a laboratory simulation of an ASR operation.

In the surface waters of the SFRW, mineralization of NDOM was shown to occur to the greatest extent during low flow condition and in the upper watershed. Carbonate dissolution also commonly occurred in the upper watershed and during low flow conditions, while evidence for carbonate precipitation was found during high flow as well as in the lower watershed during low flow conditions. NDOM-mineral sorption and desorption were often associated with carbonate precipitation and dissolution, respectively. Thus, riparian zone biogeochemical processes in the SFRW were strongly mediated by watershed hydrology, whose spatiotemporal variations resulted in greater inorganic and organic C export from the lower watershed than the upper watershed, as well as during high flow versus low flow periods.

In the O'Leno Sink-Rise system, mineralization of NDOM occurred in both shallow and deep portions of the aquifers and to a greater extent during low flow periods. Generally, surface waters could be characterized as net autotrophic while the groundwater was net heterotrophic except for portions of the deep aquifer where chemoautotrophy was identified. Carbonate mineral dissolution was found to occur throughout the aquifer and during both high flow and low flow conditions, which contradicts the commonly held view that carbonate dissolution occurs primarily during high flow conditions.

A laboratory incubation that simulated an ASR operation showed that a relatively refractory organic matter source, soil NDOM, largely sorbed to mineral surfaces and thus, did not enhance As mobilization. By contrast, a labile organic matter source, Na-acetate, did fuel microbially-mediated reactions which, either directly or indirectly, mobilized As. Thus, during a typical ASR operation in Florida, As mobilization from the aquifer materials may display different patterns depending on the lability of NDOM carried by the storage water. Along with the biotic reactions, As release may also have been enhanced by abiotic processes such as oxidative dissolution, reductive dissolution, and As desorption. Thus, As mobilization in the Floridan Aquifer during ASR operations is likely related to the oscillation of redox conditions, converting reduced As-bearing iron-sulfides to iron oxides, which then may be microbially reduced, releasing the As.

These three studies show that, in karstic systems, NDOM found in surface water, which is mostly derived from Florida soil, may not be as reactive as previously thought, at lease on the time scales examined. One explanation is that the NDOM in north-central Florida is largely refractory, due to the subtropical climate including high

temperature, humidity and rainfall. The low reactivity of refractory NDOM may also be attributed to of its extensive sorption by aquifer materials. In fact, sorption of organic matter onto minerals that are common in soils, sediments and aquifer materials has been shown to lower the bioavailability of organic matter (Cheng et al., 2012; Luthy et al., 1997).

The results of this study also shed light on carbonate dissolution and geomorphologic evolution in a karstic aquifer. Carbonate dissolution in the Floridan Aquifer was found to be closely related to biogeochemical processes such as NDOM mineralization and autotrophic production. For example, NDOM mineralization was found to be associated with the occurrence (during low flow condition) of carbonate dissolution in surface water of the SFRW as well as in the groundwater of the Sink-Rise system. Development of secondary porosity and permeability in karstic aquifers may also have important implications for petroleum reservoir evolution and groundwater contaminant remediation. For example, injections of labile substrate may be effective course of remediation in the surficial aquifer, whereas the deep aquifer may be effectively separated from surface contamination.

The results of this study may also inform hydrogeologic operations such as ASR and AR, two important means of managing water sources in Florida. For example, the source water that is injected into the aquifer during ASR and AR may need to be more strictly regulated based on the quantity and quality of NDOM that it carries. Large amounts of labile NDOM in the source water may lead to As mobilization from the aquifer matrix and may also cause biological well-clogging whereas injection of water from blackwater systems may be relatively safe. Moreover, when selecting sites for

ASR operations, mineralogical study and laboratory incubation of aquifer materials from candidate sites are recommended. Ideal ASR sites should also avoid those that contain abundant redox sensitive minerals. To reduce the potential of As mobilization, pre-injection O_2-degassing of source water may be required to avoid significant redox oscillation and As release in the aquifer.

By combining field sampling, geochemical modeling, and laboratory experimentation, the present study provides a framework for exploring biogeochemical processes in complex systems. For instance, the traditional 'field sampling – chemical analysis' approach only measures the outcome of biogeochemical processes, whereas by coupling this traditional approach with hydrological data and a source water mixing model, one can quantitatively attribute the spatiotemporal variations in water chemistry to either hydrologic mixing or biogeochemical processes. This combined approach may be useful in investigating spatiotemporal biogeochemical variability in a variety of complex systems such as estuaries, wetlands, and hydrothermal systems.

APPENDIX A
EEMS OF WATER SAMPLE COLLECTED IN THE SFRW

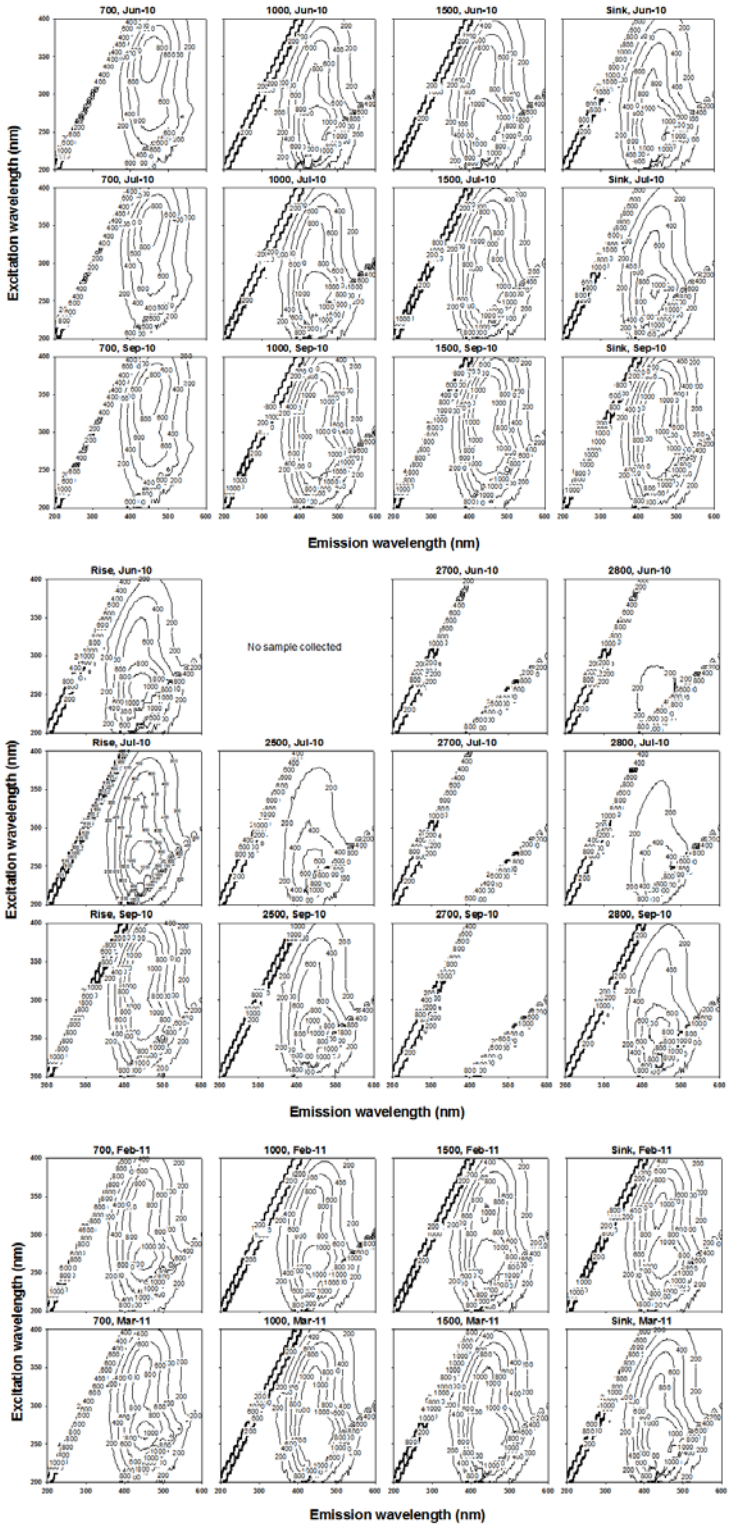

Figure A-1. EEMs of water sample collected in the SFRW

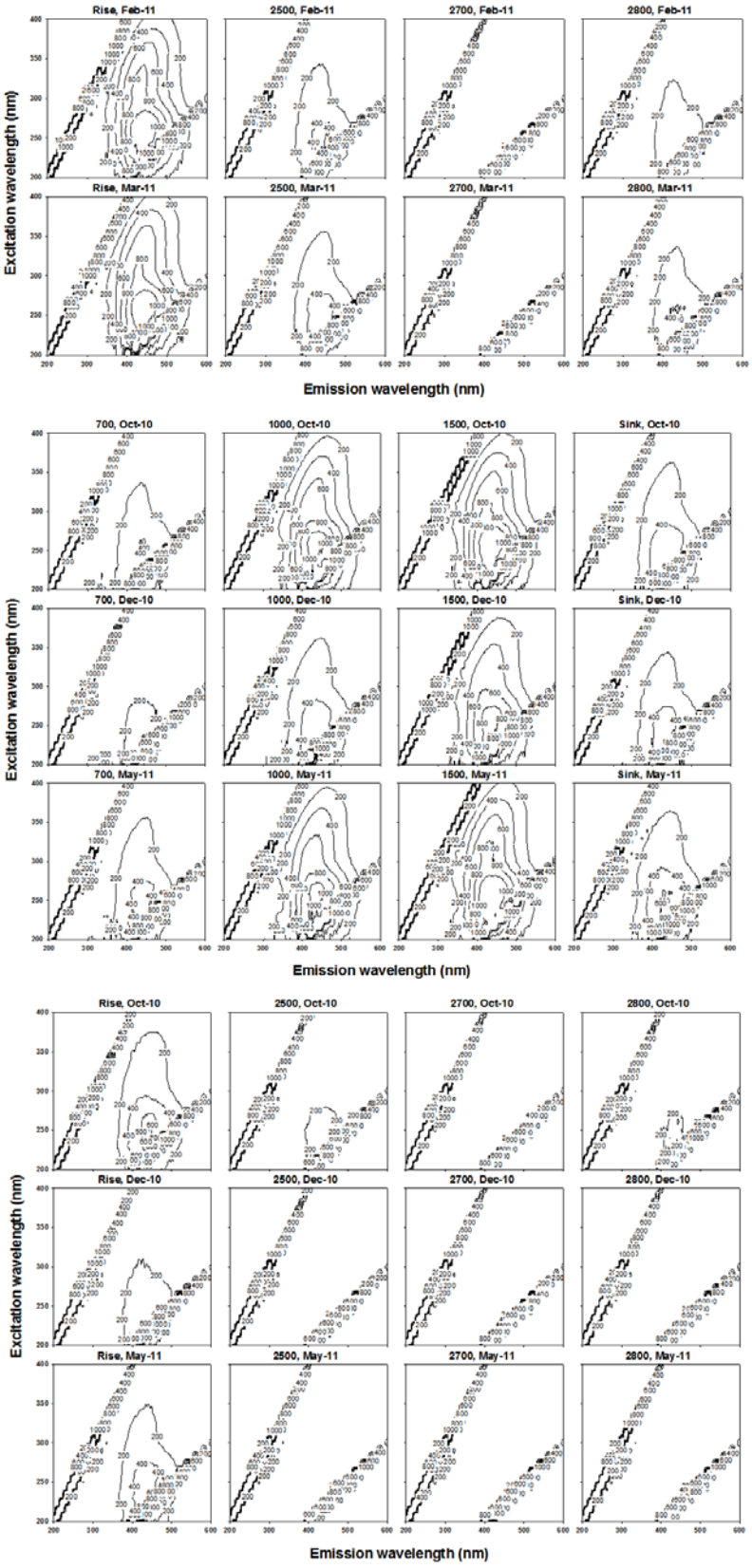

Figure A-1. Continued

APPENDIX B
CONCENTRATIONS OF NA^+ AND CL^- IN SAMPLES FROM THE SFRW

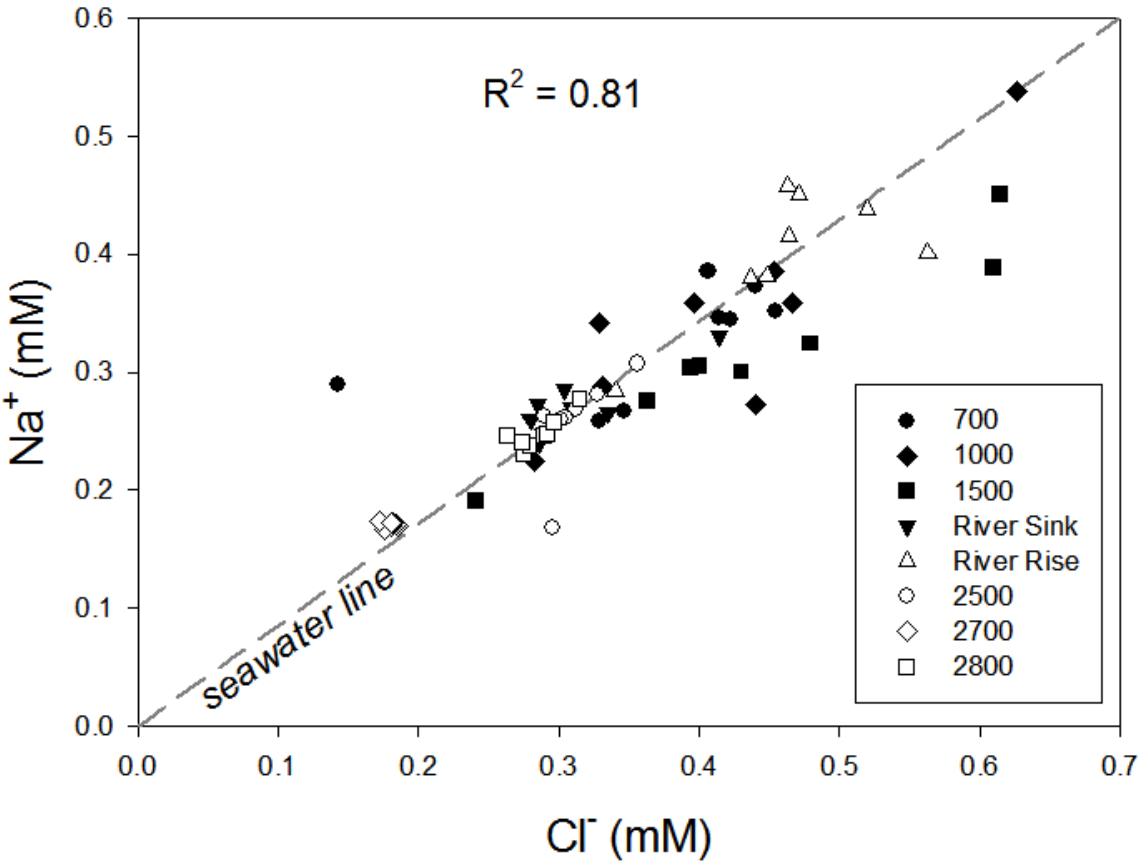

Figure B-1. The linear correlation between concentrations of Na^+ and Cl^- in all water samples collected from the eight sites within the SFRW. The dashed line indicates the mole Na/Cl ratio of seawater (0.86).

APPENDIX C
DOC AND FLUORESCENCE INTENSITY OF PROTEIN-LIKE PEAKS

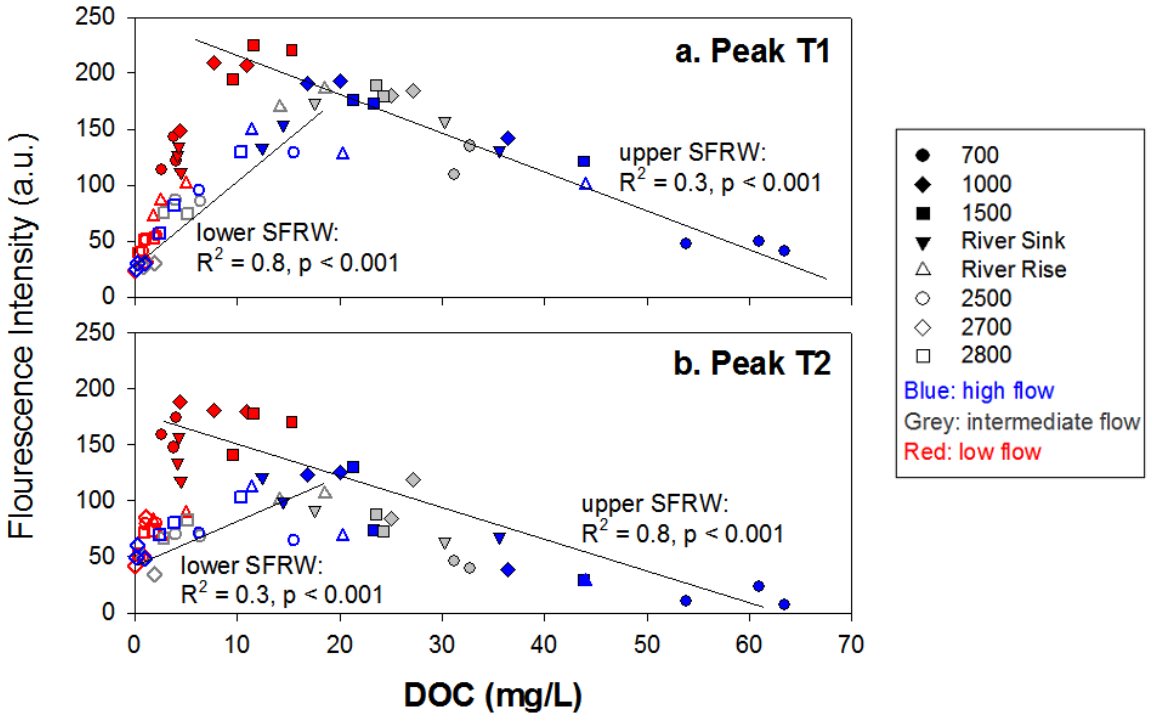

Figure C-1. Relationship between DOC concentrations and fluorescence intensity of two protein-like peaks for water samples collected from both confined (closed symbols) and unconfined (open symbols) portions of SFRW, during high (blue), intermediate (grey) and low flow (red) conditions. The solid lines represent for the regression lines for samples collected either in the upper or lower SFRW. Fluorescence intensity was represented in arbitrary unit (a.u.).

APPENDIX D
CHEMISTRY THE THREE WATER ENDMEMBERS IN THE SFRW

Table D-1. Chemical parameters of the three water endmembers defined by the chemical model

Endmember type	Samples representing endmembers	DIC (mg/L)	DOC (mg/L)	Cl^- (mM)	SO_4^{2-} (mM)	Ca^{2+} (mM)	Na^+ (mM)	Mg^{2+} (mM)	K^+ (mM)
Soil water	Site 700, 7/29/2010	1.53	63.37	0.45	0.01	0.12	0.35	0.10	0.01
Groundwater	Site 2700, 7/29/2010	31.66	0.08	0.18	0.16	1.35	0.17	0.24	0.00
Deep water [1]	Well 2, 1/17/2007	31.66	0.08	1.66	4.39	4.35	1.50	2.00	0.08

Table D-1. Continued

Endmember type	Samples representing endmembers	NO_3^- (mg/L)	pH	HIX	FI	DO (mg/L)	ORP (mV)	$\delta^{13}C$ (‰ PDB)	Alkalinity (mg/L $CaCO_3$)	SpC (µS/cm)
Soil water	Site 700, 7/29/2010	0.01	4.90	62.34	1.31	6.14	207.40	-18.46	0.20	87.00
Groundwater	Site 2700, 7/29/2010	0.03	8.18	16.13	2.10	7.26	226.00	-8.88	3.02	320.00
Deep water	Well 2, 1/17/2007	0.03	6.96	16.13	2.10	0.31	226.00	-8.88	208.00	1184.00

1. Concentrations of DOC, DIC, F^-, NO_3^-, HIX, FI, oxidation reduction potential (ORP), and $\delta^{13}C$ of deep water endmember were not measured, but they were assumed to be same as those of the groundwater endmember.

APPENDIX E
MODEL SENSITIVITY ANALYSIS

The standard deviation of Na^+, Cl^-, and SO_4^{2-} concentrations of the endmembers was selected to be the amount that was changed to the endmember chemistry. This is because they should represent the variations in water chemistry throughout our 1-year study period. The standard deviations of Na^+, Cl^-, and SO_4^{2-} in soil and groundwater endmembers were calculated from the concentrations of these ions during 8 sampling trips made for this study. As for the deep water endmember, the standard deviations were calculated based on the water chemistry of Well 2 in O'Leno State Park obtained during 16 sampling trips from February 2003 to April 2007. The standard deviation of Na^+, Cl^-, and SO_4^{2-} concentrations (in mM) of the three water endmembers are presented in as follows:

	Na^+	Cl^-	SO_4^{2-}
Soil water	0.05	0.10	0.07
Groundwater	0.00	0.01	0.01
Deep water	0.29	0.35	0.97

Table E-1. Results of model sensitivity analysis are presented as the deviations (in %) from the original model results.

	high flow			low flow			intermediate flow		
	Soil water	Ground water	Deep water	Soil water	Groun dwater	Deep water	Soil water	Groun dwater	Deep water
increase 1 stdev in Cl^-									
700	-28.0	28.0	0.0	-28.8	28.8	0.0	-19.8	20.5	-0.7
1000	-20.0	20.0	0.0	-28.0	28.5	-0.5	-6.1	6.3	-0.2
1500	-29.1	29.1	0.0	-13.6	14.0	-0.5	-4.9	5.1	-0.2
Sink	-2.9	3.0	-0.1	0.0	0.0	0.0	-3.3	3.4	-0.1
Rise	-12.4	12.8	-0.4	0.0	3.6	-3.6	-16.9	16.7	0.3
2500	-3.4	3.5	-0.1	5.2	-4.3	-0.9	-0.7	0.8	0.0
2700	0.1	-0.1	0.0	0.0	0.0	0.0	-0.3	0.3	0.0
2800	-3.9	4.0	-0.1	-5.0	5.2	-0.2	-8.5	8.8	-0.3

decrease 1 stdev in Cl^-									
700	3.9	-3.9	0.0	0.0	0.0	0.0	17.4	-18.0	0.6
1000	9.2	-9.5	0.3	-0.9	0.9	0.0	14.7	-15.2	0.5
1500	0.5	-0.5	0.0	-12.2	12.7	-0.4	0.0	0.0	0.0
Sink	17.6	-18.2	0.6	9.3	-9.6	0.3	-3.3	3.4	-0.1
Rise	0.0	0.0	0.0	0.0	-1.5	1.5	-5.1	4.4	0.7
2500	-2.4	2.4	-0.1	22.6	-22.4	-0.3	23.4	-24.2	0.8
2700	0.7	-0.7	0.1	0.0	0.0	0.0	-0.3	0.3	0.0
2800	0.0	0.0	0.0	1.7	-1.8	0.1	0.1	-0.1	0.0
increase 1 stdev in SO_4^{2-}									
700	-2.7	2.7	0.0	-21.8	21.8	0.0	7.5	-6.1	-1.4
1000	-14.0	14.0	0.0	-10.7	11.2	-0.5	3.4	-2.1	-1.4
1500	-19.6	19.6	0.0	-1.4	2.9	-1.5	5.0	-3.6	-1.4
Sink	4.9	-4.1	-0.8	8.6	-7.4	-1.2	7.9	-6.8	-1.1
Rise	14.1	-12.1	-2.0	5.8	-5.0	-0.8	12.6	-10.7	-1.9
2500	3.8	-3.1	-0.6	3.4	-2.8	-0.6	9.2	-7.8	-1.4
2700	5.6	-5.6	-0.1	6.2	-6.2	0.0	10.5	-10.5	0.0
2800	6.1	-5.3	-0.8	5.5	-4.6	-0.8	6.8	-5.6	-1.1
decrease 1 stdev in SO_4^{2-}									
700	-3.1	3.0	0.0	0.0	0.0	0.0	-4.0	3.3	0.7
1000	-3.5	3.5	0.0	-1.1	0.8	0.3	-2.2	1.4	0.8
1500	-2.8	2.7	0.0	-1.6	1.0	0.6	-2.9	2.1	0.8
Sink	-4.0	3.4	0.6	-9.5	8.2	1.3	-3.7	3.0	0.7
Rise	-16.4	14.2	2.2	0.0	-0.1	0.1	-24.8	21.5	3.4
2500	-3.4	2.8	0.6	-4.3	3.5	0.8	-8.3	6.8	1.5
2700	-1.0	0.8	0.2	-4.0	4.0	0.0	-4.1	4.1	0.0
2800	-6.7	5.8	0.9	-6.6	5.6	1.0	-9.0	7.7	1.2

increase 1 stdev in Na^+									
700	-17.1	17.1	0.0	-12.5	12.5	0.0	-3.4	3.6	-0.1
1000	-3.2	3.2	0.0	-7.7	7.9	-0.2	6.9	-7.2	0.2
1500	-1.9	1.9	0.0	-4.1	4.3	-0.1	4.0	-4.1	0.1
Sink	-1.4	1.4	-0.1	-6.2	6.4	-0.2	0.0	0.0	0.0
Rise	-14.9	15.5	-0.5	0.0	2.3	-2.3	-26.1	26.2	-0.1
2500	0.0	0.0	0.0	5.0	-4.1	-0.9	0.0	0.0	0.0
2700	0.1	-0.1	0.0	0.0	0.0	0.0	-0.3	0.3	0.0
2800	-6.6	6.8	-0.2	-4.9	5.1	-0.2	-8.6	8.9	-0.3
decrease 1 stdev in Na^-									
700	-2.7	2.7	0.0	9.0	-9.0	0.0	0.0	0.0	0.0
1000	5.7	-5.9	0.2	0.0	0.0	0.0	0.0	0.0	0.0
1500	0.5	-0.5	0.0	0.8	-0.8	0.0	4.0	-4.1	0.1
Sink	12.3	-12.7	0.4	14.9	-15.5	0.5	16.4	-17.0	0.6
Rise	2.9	-3.0	0.1	0.0	-0.3	0.3	8.5	-9.7	1.2
2500	4.6	-4.7	0.2	18.8	-18.4	-0.4	17.2	-17.9	0.6
2700	0.6	-0.6	0.0	0.0	0.0	0.0	-0.3	0.3	0.0
2800	4.0	-4.2	0.1	1.7	-1.8	0.1	0.5	-0.5	0.0

APPENDIX F
CHEMISTRY OF THE THREE WATER ENDMEMBERS IN THE SINK-RISE SYSTEM

Table F-1. Chemical parameters of the three water endmembers defined by the chemical model

Endmember type	Samples representing endmembers	DIC (mg/L)	DOC (mg/L)	pH	Cl^- (mg/L)	SO_4^{2-} (mg/L)	Ca^{2+} (mg/L)
Soil water	River Sink, 3/28/08	8.4	37.3	6.6	17.4	12.9	38.0
Groundwater	W4, 3/28/08	47.4	0.7	6.8	9.8	6.9	6.6
Deep water [1]	W2, 1/17/07	47.4	0.7	7.2	59.0	421.0	174.0

Table F-1. Continued

Endmember type	Samples representing endmembers	Na^+ (mg/L)	Mg^{2+} (mg/L)	K^+ (mg/L)	DO (mg/L)	Alkalinity (mg/L $CaCO_3$)	SpC (µS/cm)
Soil water	River Sink, 3/28/08	9.8	2.7	1.5	5.4	78.1	173.8
Groundwater	W4, 3/28/08	5.1	11.3	0.3	1.2	480.4	440.0
Deep water [1]	W2, 1/17/07	34.6	47.9	3.1	0.3	208.0	1184.0

1. Concentrations of DOC and DIC of deep water endmember were not measured, but they were assumed to be same as those of the groundwater endmember.

APPENDIX G
GROUNDWATER WELL INFORMATION

Table G-1. Summary of well locations, depths, depth to bedrock, screen intervals, estimated distance to mapped conduit, ground surface elevation of selected wells in the Sink-Rise system.

	Latitude (°N)	Latitude (°W)	Completed depth (mbgs[1])	Depth to bedrock (m)	Screened interval (mbgs)	Approximate distance to mapped conduit (m)	Ground surface elevation (masl[2])
W2	29°54'09.5"	82°35'07.9"	30	6.1	30-24	1500	15.96
W4	29°52'34.1"	82°35'32.8"	29	4.57	29-23	100	17.89
W4a	29°52'34.1"	82°35'32.8"	10	5.18	10-7	100	17.96
W5	29°52'31.9"	82°35'32.9"	30	5.48	30-24	100	16.22
W5a	29°52'31.9"	82°35'32.9"	8	3.05	8-5	100	16.2
W6	29°52'28.9"	82°35'34.0"	31	4.88	31-25	100	13.51
W6a	29°52'28.9"	82°35'34.0"	5	3.96	5-2	100	13.55
W7	29°52'07.6"	82°36'00.8"	30	5.48	30-24	1000	15.22
W7a	29°52'07.6"	82°36'00.8"	8	2.43	8-5	1000	15.19

1. meters below ground surface
2. meters above sea level

APPENDIX H
CONCENTRATIONS OF DOC AND DIC IN THE SINK-RISE SYSTEM

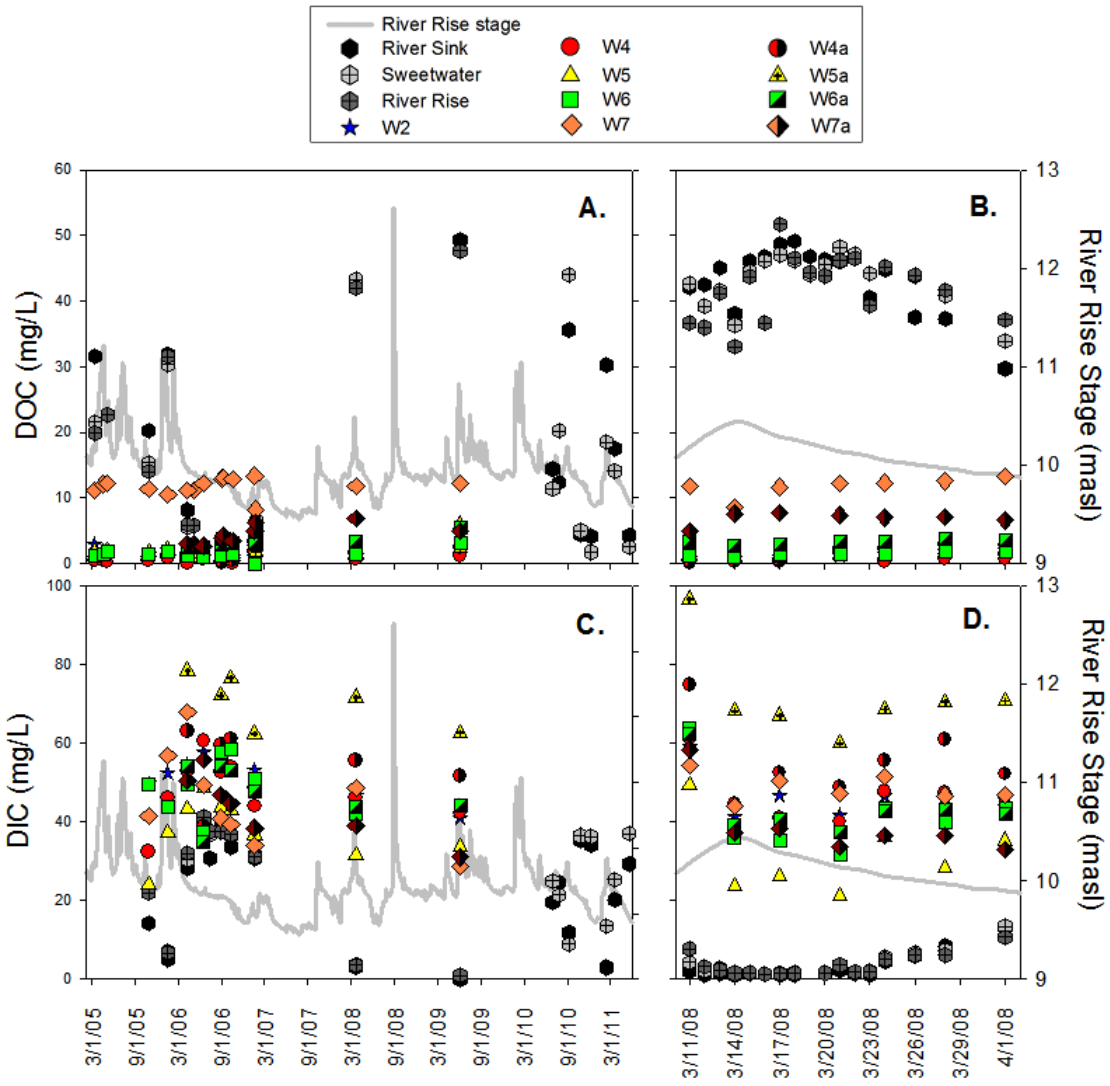

Figure H-1. Time series data of (A) DOC from March 2005 to June 2009, (B) DOC during March 2008 flood event, (C) DIC from March 2005 to June 2009, (D) DIC during March 2008 flood event at three surface water sites (River Sink, Sweetwater Lake, and River Rise, hexagon symbols), five deep wells (W2, W4-7, filled symbols), and four shallow wells (W4a-7a, half-filled symbols). Grey lines show the River Rise stage (in m above sea level).

APPENDIX I
CONCENTRATIONS OF NA^+ AND CL^- IN SAMPLES FROM THE SINK-RISE SYSTEM

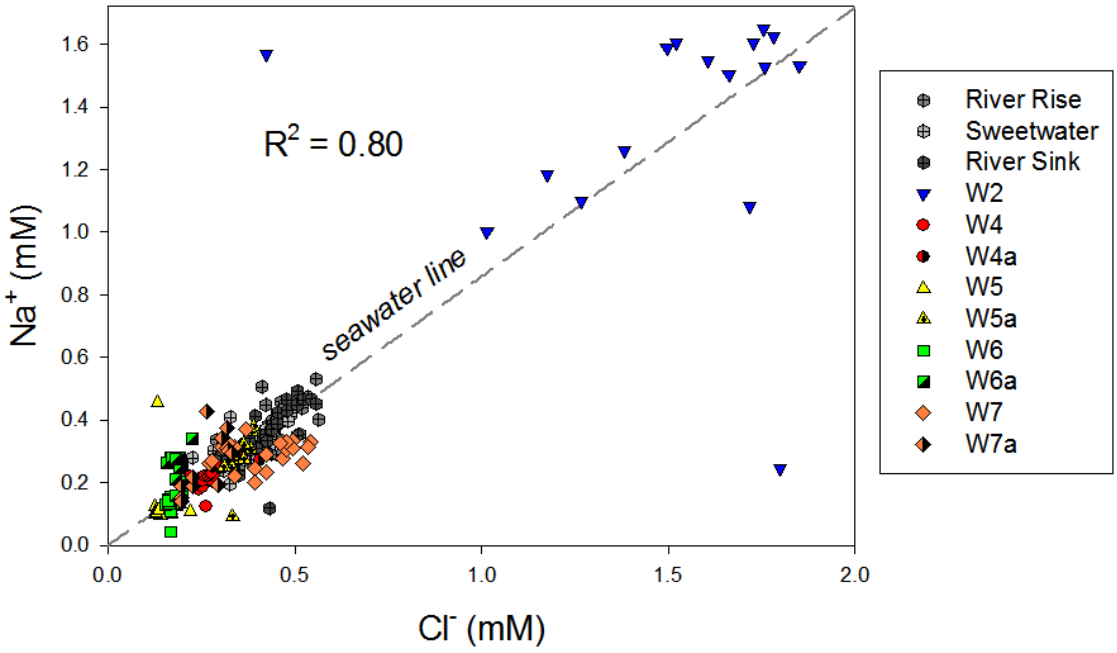

Figure I-1. The linear correlation between concentrations of Na^+ and Cl^- in all water samples collected from within the O'Leno Sink-Rise system The dashed line indicates the mole Na/Cl ratio of seawater (0.86).

APPENDIX J
CHEMISTRY OF NATIVE GROUNDWATER AND SOURCE WATER

Table J-1. Chemistry of native groundwater and source water

	Native groundwater (NGW)	Source water (SW)
pH	7.24	7.72
T (°C)	26.1	27.7
SpC (µS)	15229	835
DO (mg/L)	0.03	3.76
ORP (mV)	-79	-
Ca^{2+} (µg/L)	148000	61700
Na^{+} (µg/L)	70600	71800
K^{+} (µg/L)	2680	7320
Mg^{2+} (µg/L)	65800	17100
Total As (µg/L)	0.12	0.37
Fe^{3+} (µg/L)	< 10	20
F^{-} (mg/L)	0.54	0.76
Cl^{-} (mg/L)	226	49.1
NO_2^{-} (mg/L)	< 0.04	< 0.02
NO_3^{-} (mg/L)	< 0.04	1.22
PO_4^{3-} (mg/L)	< 0.08	0.26
SO_4^{2-} (mg/L)	380	241
Alk (mg/L CaCO3)	133	69
CO_3^{2-} (mg/L)	< 1	< 1
HCO_3^{-} (mg/L)	133	69

APPENDIX K
ORGANIC MATTER ADSORPTION AND DESORPTION EXPERIMENT

Table K-1. Summary of organic matter adsorption and desorption experiment.

Tube	Experimental treatment	Note
1	30 mL DI + 10 g core	
2	30 mL DI + 10 g core	replicate of tube 1
3	30 mL DI + 10 g core	replicate of tube 1
4	30 mL DI	No core – control for tubes 1-3
5	30 mL humic acid + 10 g core	
6	30 mL humic acid + 10 g core	replicate of tube 5
7	30 mL humic acid + 10 g core	replicate of tube 5
8	30 mL humic acid	No core – control for tubes 5-7
9	30 mL Na-acetate + 10 g core	
10	30 mL Na-acetate + 10 g core	replicate of tube 9
11	30 mL Na-acetate + 10 g core	replicate of tube 9
12	30 mL Na-acetate	No core – control for tubes 9-11

APPENDIX L
WHOLE-ROCK GEOCHEMISTRY OF THE CORE MATERIAL

Table L-1. Whole-rock geochemistry of the core material.

Analytes	As (ppm)	SiO_2 (%)	Al_2O_3 (%)	Fe_2O_3 (%)	MnO (%)	MgO (%)	CaO (%)	Na_2O (%)	K_2O (%)	P_2O_5 (%)	S (total) (%)	SO_4 (%)	C (total) (%)	C (graphite) (%)
Mean value	2.0	3.96	0.2	0.1	0.004	0.67	52.22	0.04	0.04	0.07	0.14	BDL[1]	11.6	BDL
Standard deviation (n = 3)	0.0	0.15	0.03	0.02	0.000	0.03	0.24	0.00	0.01	0.01	0.01	-	0.1	-
Detection limit	1.0	0.01	0.01	0.01	0.001	0.01	0.01	0.01	0.01	0.01	0.01	0.3	0.01	0.05

1. BDL: below detection limit

APPENDIX M
INDIGENOUS OM IN THE CORE MATERIAL

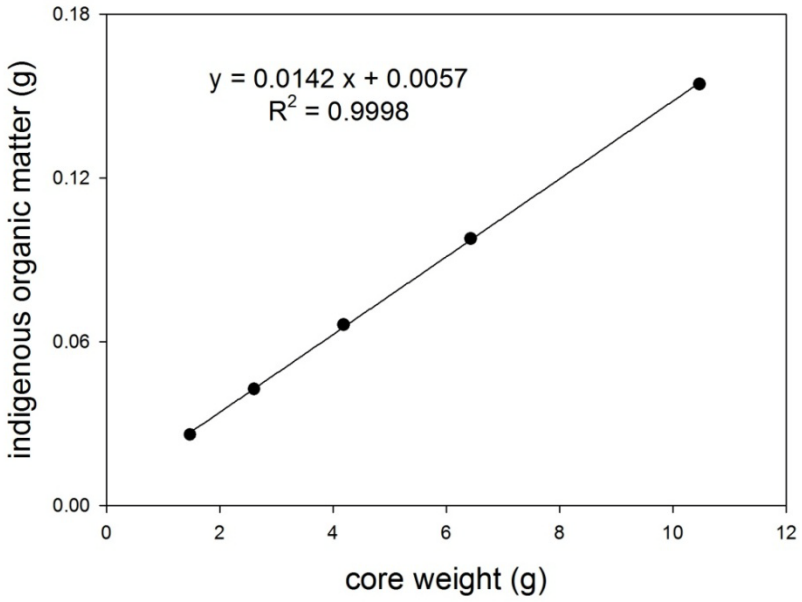

Figure M-1. The linear correlation between the amount of indigenous OM and core.

APPENDIX N
INCUBATION RESULTS

Incubation SpC Results: Compared to Phase 1, SpC in Phases 2 and 3 was much lower in all vessels due to the much lower conductivity of SW compared to NGW (Fig. 5). During both Phase 2 and Phase 3, treatment vessels always exhibited greater SpC than their corresponding 'no core' controls. The SpC of these two treatments was higher than that of Treatments 1 and 2, which had identical SpC values. Treatment 3 usually displayed lowest SpC. Treatments with and without NDOM addition did not affect SpC in solution. Treatments with and without microbes addition also did not influence the SpC.

In Phase 2, control treatments were approximately 100 mS lower in SpC than their corresponding treatments. SpC for controls were usually stable throughout Phase 2, while SpC for other treatments decreased gradually before leveling off. Abrupt drop in SpC in treatment 'no core' on 8/2 was probably due to failure in measurement or sampling. Most treatment exhibited increased SpC in Phase 3. The largest increase was found in 'core + Na-acetate', which started Phase 3 with a SpC of 593 mS and ended with 741 mS on 9/27. Treatment 'no core' had the smallest change among all treatments and an increase in SpC by 2 mS was barely noticed. Exceptional high SpC data for 'no core' on 8/27 was likely caused by failure in measurement or sampling.

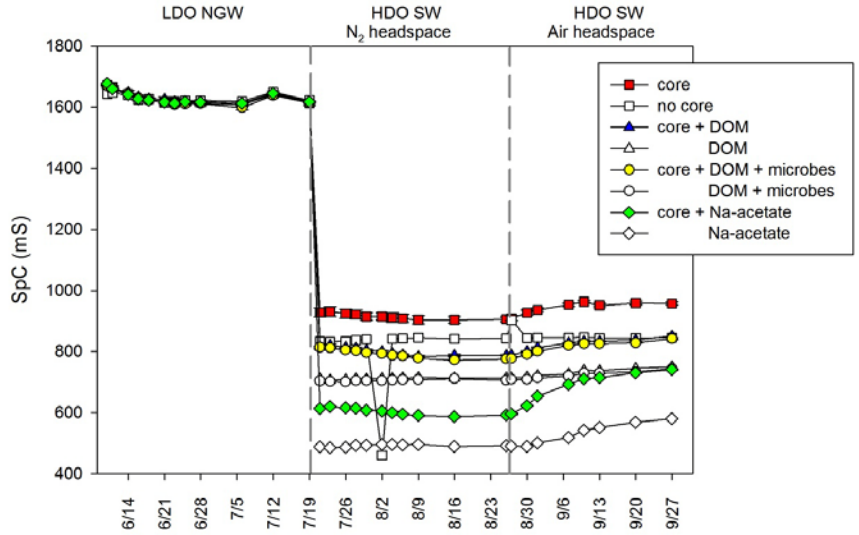

Figure N-1. Specific conductivity (SpC) in control (no core material) and treatment vessels (with core materials) during time-course incubations.

Incubation pH Results: Incubation solutions were always slightly basic, as all pH data fell in a range of 7.2 to 8.6 (Fig. 8). All treatments, including controls, displayed great variation in pH among different treatments and throughout the incubation period. Over all, pH results from both Phases 2 and 3 were higher than those from Phase 1, with the greatest pH values usually found in Phase 2. Controls unusually had greater pH than their corresponding treatments, especially during Phase 2. The greatest variation in pH

was seen in the first 20 days of Phase 2. After that, a strong decreasing trend that brought down pH for most treatments to below 7.9.

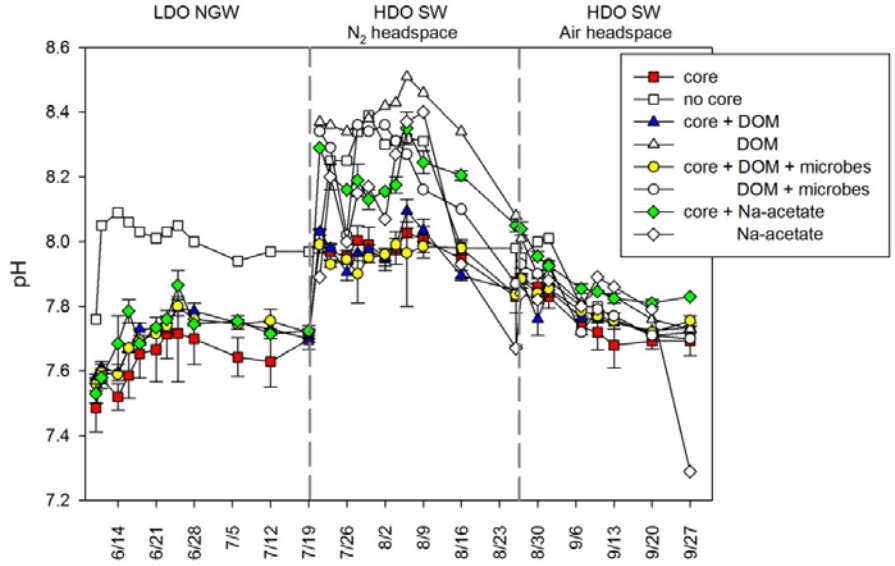

Figure N-2. pH in control (no core material) and treatment vessels (with core materials) during time-course incubations.

Incubation Nitrate Concentrations: Concentrations of nitrate (NO_3^-) over the incubation period are presented in Fig. 9. Nitrate was only present at significant levels in those vessels that had NDOM amendments. With or without the presence of core material, nitrate decreased consistently during both Phases 2 and 3, likely due to microbial utilization (about 4 mg/L consumption in all cases). This seems to indicate that none of the incubations were truly sterile, as microbial additions had no additional effect.

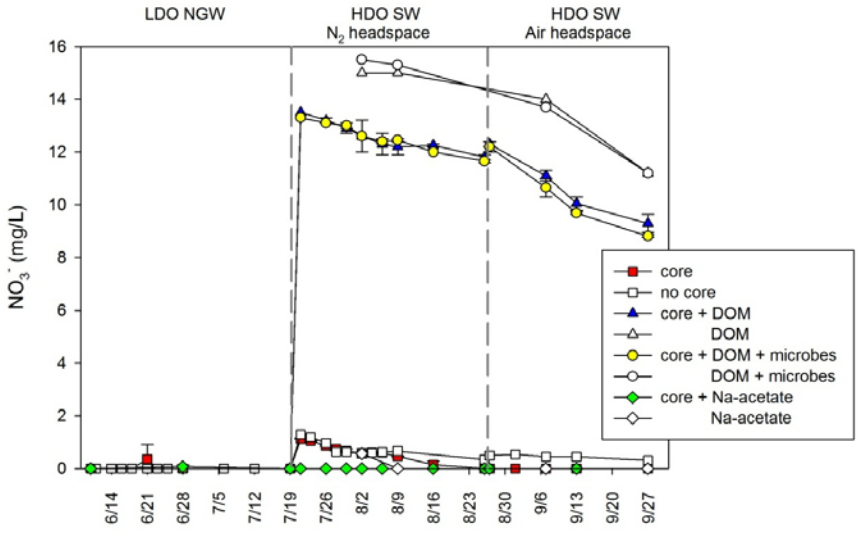

Figure N-3. Concentration of nitrate (NO_3^-) in control (no core material) and treatment vessels (with core materials) during time-course incubations.

Incubation Calcium Concentrations: The Ca^{2+} levels of all treatment in Phase 2 and 3 were about 600 mg/L lower than those in Phase 1 (Fig. 10). Concentration of Ca^{2+} remained relatively stable in Phase 2 with a value close to 600 mg/L and there was little difference between different treatments and their respective no-core controls, except in the case of the Treatment 3 (Na-acetate addition). Treatment 3 always had the lowest Ca^{2+} level (~400 mg/L) among all treatments.

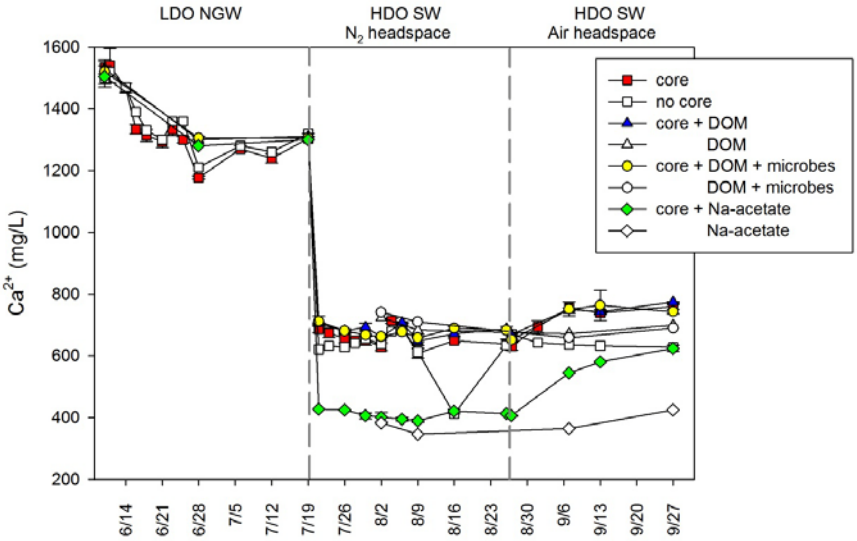

Figure N-4. Concentration of calcium (Ca^{2+}) in control (no core material) and treatment vessels (with core materials) during time-course incubations.

Incubation Sulfate Concentrations: Sulfate data (Fig. 11) and SpC data shared some common trends among treatments and over time, maintaining near constant concentrations in the order: 'core' > 'no core' > Treatment 1 ≈ Treatment 2 > Treatment 3.

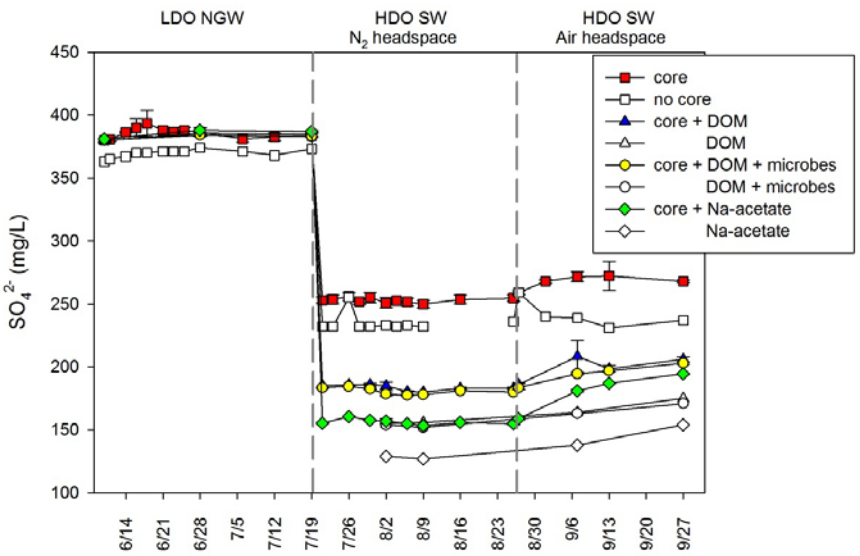

Figure N-5. Concentration of sulfate (SO_4^{2-}) in control (no core material) and treatment vessels (with core materials) during time-course incubations.

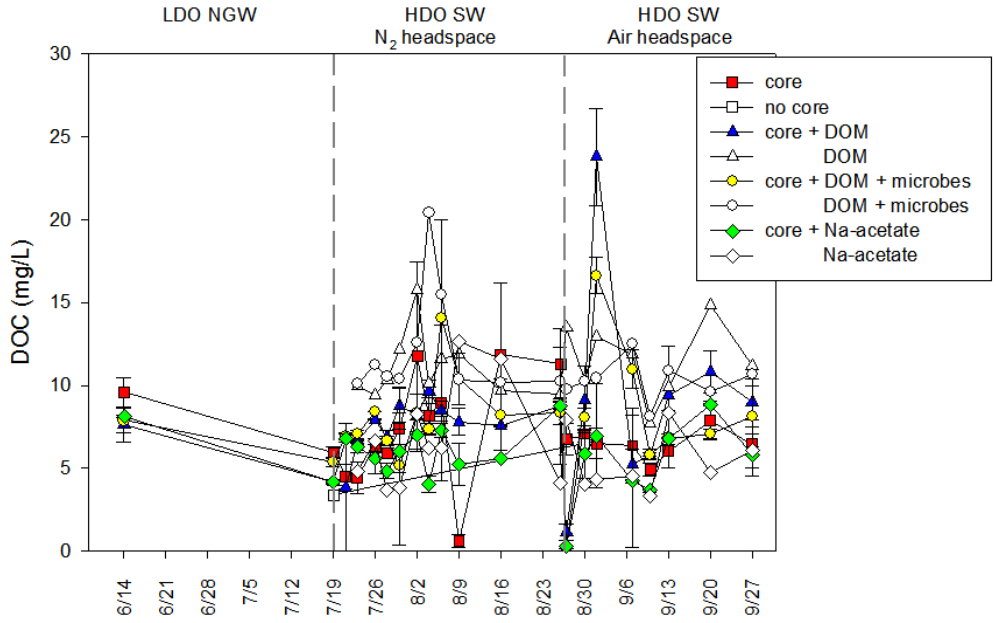

Figure N-6. Concentration of DOC in control (no core material) and treatment vessels (with core materials) during time-course incubations.

LIST OF REFERENCES

Aitkenhead, J.A. and McDowell, W.H., 2000. Soil C : N ratio as a predictor of annual riverine DOC flux at local and global scales. Global Biogeochemical Cycles, 14(1): 127-138.

Alberic, P. and Lepiller, M., 1998. Oxidation of organic matter in a karstic hydrologic unit supplied through stream sinks (Loiret, France). Water Research, 32(7): 2051-2064.

Anawar, H.M. et al., 2003. Geochemical occurrence of arsenic in groundwater of Bangladesh: sources and mobilization processes. Journal of Geochemical Exploration, 77(2-3): 109-131.

Aravena, R., Wassenaar, L.I. and Spiker, E.C., 2004. Chemical and carbon isotopic composition of dissolved organic carbon in a regional confined methanogenic aquifer. Isotopes in Environmental and Health Studies, 40(2): 103-114.

Arthur, J.D., Dabous, A. A., Cowart, J. B., 2002. Mobilization of arsenic and other trace elements during aquifer storage and recovery, southwest Florida, U.S. Geological Survey Artificial Recharge Workshop Proceedings. U.S. Geological Survey, Sacramento, California.

Baker, A. and Lamont-Black, J., 2001. Fluorescence of dissolved organic matter as a natural tracer of ground water. Ground Water, 39(5): 745-750.

Baker, A. and Spencer, R.G.M., 2004. Characterization of dissolved organic matter from source to sea using fluorescence and absorbance spectroscopy. Science of the Total Environment, 333(1-3): 217-232.

Batiot, C., Emblanch, C. and Blavoux, B., 2003. Total Organic Carbon (TOC) and magnesium (Mg2+): two complementary tracers of residence time in karstic systems. Comptes Rendus Geoscience, 335(2): 205-214.

Birdwell, J.E. and Engel, A.S., 2009. Variability in terrestrial and microbial contributions to dissolved organic matter fluorescence in the Edwards Aquifer, central Texas. Journal of Cave and Karst Studies, 71(2): 144-156.

Birdwell, J.E. and Engel, A.S., 2010. Characterization of dissolved organic matter in cave and spring waters using UV-Vis absorbance and fluorescence spectroscopy. Organic Geochemistry, 41(3): 270-280.

Boyes, S. and Elliott, M., 2006. Organic matter and nutrient inputs to the Humber Estuary, England. Marine Pollution Bulletin, 53(1-4): 136-143.

Brunet, F. et al., 2009. Terrestrial and fluvial carbon fluxes in a tropical watershed: Nyong basin, Cameroon. Chemical Geology, 265(3-4): 563-572.

Budd, D.A., 2007. Mineralogical abundances as determined by x-ray diffraction in select samples of the upper Floridan Aquifer. Appendix 15 In Geochemical and mineralogical characterization in potential aquifer storage and recovery storage zones in the Florida Aquifer system. Comprehensive Everglades Restoration Plan Report, Reference Agreement OT040175

Budd, D.A. and Vacher, H.L., 2004. Matrix permeability of the confined Floridan Aquifer, Florida, USA. Hydrogeology Journal, 12(5): 531-549.

Canfield, D.E., Jr. and Hoyer, M.V., 1988. Influence of nutrient enrichment and light availability on the abundance of aquatic macrophytes in Florida streams. Canadian Journal of Fisheries and Aquatic Sciences, 45(8): 1467-1472.

Chapelle, F.H., Bradley, P.M., Lovley, D.R., O'Neill, K. and Landmeyer, J.E., 2002. Rapid evolution of redox processes in a petroleum hydrocarbon-contaminated aquifer. Ground Water, 40(4): 353-360.

Chen, M.L., Price, R.M., Yamashita, Y. and Jaffe, R., 2010. Comparative study of dissolved organic matter from groundwater and surface water in the Florida coastal Everglades using multi-dimensional spectrofluorometry combined with multivariate statistics. Applied Geochemistry, 25(6): 872-880.

Chen, Z.R., Cai, Y., Solo-Gabriele, H., Snyder, G.H. and Cisar, J.L., 2006. Interactions of arsenic and the dissolved substances derived from turf soils. Environmental Science & Technology, 40(15): 4659-4665.

Cheng, H.F., Hu, E.D. and Hu, Y.A., 2012. Impact of mineral micropores on transport and fate of organic contaminants: A review. Journal of Contaminant Hydrology, 129: 80-90.

Clark, I.D. and Fritz, P., 1997. Environmental Isotopes in Hydrogeology. CRC Press.

Coble, P.G., 1996. Characterization of marine and terrestrial DOM in seawater using excitation emission matrix spectroscopy. Marine Chemistry, 51(4): 325-346.

Davis, J.A., 1982. Adsorption of Natural Dissolved Organic-Matter at the Oxide Water Interface. Geochimica Et Cosmochimica Acta, 46(11): 2381-2393.

de Montety, V., Martin, J.B., Cohen, M.J., Foster, C. and Kurz, M.J., 2011. Influence of diel biogeochemical cycles on carbonate equilibrium in a karst river. Chemical Geology, 283(1-2): 31-43.

Drever, J.I., 2002. The Geochemistry of Natural Waters: Surface and Groundwater Environments. Prentice Hall, Upper Saddle River, NJ, pp. 114-116.

Dreybrodt, W., 1990. The role of dissolution kinetics in the development of karst aquifers in limestone - a model simulation of karst evolution. Journal of Geology, 98(5): 639-655.

Engel, A.S., Porter, M.L., Stern, L.A., Quinlan, S. and Bennett, P.C., 2004. Bacterial diversity and ecosystem function of filamentous microbial mats from aphotic (cave) sulfidic springs dominated by chemolithoautotrophic "Epsilonproteobacteria". Fems Microbiology Ecology, 51(1): 31-53.

Essington, M.E., 2004. Soil and Water Chemistry: An Integrative Approach. CRC Press, Boca Raton, pp. 163-167.

Falkowski, P. et al., 2000. The global carbon cycle: A test of our knowledge of earth as a system. Science, 290(5490): 291-296.

Farnleitner, A.H. et al., 2005. Bacterial dynamics in spring water of alpine karst aquifers indicates the presence of stable autochthonous microbial endokarst communities. Environmental Microbiology, 7(8): 1248-1259.

Findlay, S.E.G. and Sinsabaugh, R.L., 2003. Aquatic ecosystems: interactivity of dissolved organic matter. Academic Press.

Findlay, S.E.G., Sinsabaugh, R.L., Sobczak, W.V. and Hoostal, M., 2003. Metabolic and structural response of hyporheic microbial communities to variations in supply of dissolved organic matter. Limnology and Oceanography, 48(4): 1608-1617.

Fisher, T.R., Hagy, J.D., Boynton, W.R. and Williams, M.R., 2006. Cultural eutrophication in the Choptank and Patuxent estuaries of Chesapeake Bay. Limnology and Oceanography, 51(1): 435-447.

Florea, L.J. and Vacher, H.L., 2006. Springflow hydrographs: Eogenetic vs. telogenetic karst. Ground Water, 44(3): 352-361.

Ford, D.C. and Williams, P.W., 2007. Karst Hydrogeology and Geomorphology. Wiley, Chichester, United Kingdom, 562 pp.

Frimmel, F.H., 1998. Characterization of natural organic matter as major constituents in aquatic systems. Journal of Contaminant Hydrology, 35(1-3): 201-216.

Frye, G.C. and Thomas, M.M., 1993. Adsorption of Organic-Compounds on Carbonate Minerals .2. Extraction of Carboxylic-Acids from Recent and Ancient Carbonates. Chemical Geology, 109(1-4): 215-226.

Gimenez, J., Martinez, M., de Pablo, J., Rovira, M. and Duro, L., 2007. Arsenic sorption onto natural hematite, magnetite, and goethite. Journal of Hazardous Materials, 141(3): 575-580.

Grubbs, J.W., 1998. Recharge Rates to the Upper Floridan Aquifer in the Suwannee River Water Management District, Florida. U. S. Geological Survey Water Resources Investigations Report 97-4283, 30 p.

Gulley, J., Martin, J.B., Screaton, E.J. and Moore, P.J., 2011. River reversals into karst springs: A model for cave enlargement in eogenetic karst aquifers. Geological Society of America Bulletin, 123(3-4): 457-467.

Han, N.Z. and Thompson, M.L., 2003. Impact of dissolved organic matter on copper mobility in aquifer material. Journal of Environmental Quality, 32(5): 1829-1836.

Hancock, P.J., Boulton, A.J. and Humphreys, W.F., 2005. Aquifers and hyporheic zones: Towards an ecological understanding of groundwater. Hydrogeology Journal, 13(1): 98-111.

Heffernan, J.B. et al., 2010. Hydrologic and biotic influences on nitrate removal in a subtropical spring-fed river. Limnology and Oceanography, 55(1): 249-263.

Heiri, O., Lotter, A.F. and Lemcke, G., 2001. Loss on ignition as a method for estimating organic and carbonate content in sediments: reproducibility and comparability of results. Journal of Paleolimnology, 25(1): 101-110.

Hoch, A.R., Reddy, M.M. and Aiken, G.R., 2000. Calcite crystal growth inhibition by humic substances with emphasis on hydrophobic acids from the Florida Everglades. Geochimica Et Cosmochimica Acta, 64(1): 61-72.

Hoffer-French, K.J. and Herman, J.S., 1989. Evaluation of hydrological and biological influences on CO2 fluxes from a karst stream. Journal of Hydrology, 108(1-4): 189-212.

Houghton, R.A. and Woodwell, G.M., 1989. Global climatic-change. Scientific American, 260(4): 36-44.

House, W.A., 1990. The prediction of phosphate coprecipitation with calcite in fresh-waters. Water Research, 24(8): 1017-1023.

Hudson, N., Baker, A. and Reynolds, D., 2007. Fluorescence analysis of dissolved organic matter in natural, waste and polluted waters - A review. River Research and Applications, 23(6): 631-649.

Hunn, J.D. and Slack, L.J., 1983. Water resources of the Santa Fe River Basin, Florida. U. S. Geological Survey Water Resources Investigations Report 83-4075.

Inamdar, S. et al., 2012. Dissolved organic matter (DOM) concentration and quality in a forested mid-Atlantic watershed, USA. Biogeochemistry, 108(1-3): 55-76.

Inskeep, W.P. and Bloom, P.R., 1986. Kinetics of Calcite Precipitation in the Presence of Water-Soluble Organic-Ligands. Soil Science Society of America Journal, 50(5): 1167-1172.

Inskeep, W.P., McDermott, T.R. and Fendorf, S., 2002. Arsenic (V)/(III) cycling in soils and natural waters: Chemical and microbiological processes. Environmental Chemistry of Arsenic: 183-215.

Islam, F.S. et al., 2004. Role of metal-reducing bacteria in arsenic release from Bengal delta sediments. Nature, 430(6995): 68-71.

Jiang, J. and Kappler, A., 2008. Kinetics of microbial and chemical reduction of humic substances: Implications for electron shuttling. Environmental Science & Technology, 42(10): 3563-3569.

Jin, J. and Zimmerman, A.R., 2010. Abiotic interactions of natural dissolved organic matter and carbonate aquifer rock. Applied Geochemistry, 25(3): 472-484.

Jones, G.W. and Pichler, T., 2007. Relationship between pyrite stability and arsenic mobility during aquifer storage and recovery in southwest central Florida. Environmental Science & Technology, 41(3): 723-730.

Kalbitz, K. and Wennrich, R., 1998. Mobilization of heavy metals and arsenic in polluted wetland soils and its dependence on dissolved organic matter. Science of the Total Environment, 209(1): 27-39.

Katz, B.G., 1992. Hydrochemistry of the upper Floridan aquifer, Florida. U.S. Geological Survey Water-Resources Investigations Report 91-4196, 37 p, 10.

Katz, B.G., Catches, J.S., Bullen, T.D. and Michel, R.L., 1998. Changes in the isotopic and chemical composition of ground water resulting from a recharge pulse from a sinking stream. Journal of Hydrology, 211(1-4): 178-207.

Konhauser, K., 2007. Introduction to Geomicrobiology Blackwell Publishing, Oxford, UK.

Kortelainen, N.M. and Karhu, J.A., 2006. Tracing the decomposition of dissolved organic carbon in artificial groundwater recharge using carbon isotope ratios. Applied Geochemistry, 21(4): 547-562.

Kurz, R.C. et al., 2004. Mapping and monitoring submerged aquatic vegetation in Ichetucknee springs, Suwanee River Water Management District, Live Oak, Florida.

Langston, A.L., Screaton, E.J., Martin, J.B. and Bailly-Comte, V., 2012. Interactions of diffuse and focused allogenic recharge in an eogenetic karst aquifer (Florida, USA). Hydrogeology Journal, 20(4): 767-781.

Lau, L.S. and Mink, J.F., 1987. Organic Contamination of Groundwater - a Learning-Experience. Journal American Water Works Association, 79(8): 37-42.

Laurion, I., Vincent, W.F. and Lean, D.R.S., 1997. Underwater ultraviolet radiation: Development of spectral models for northern high latitude lakes. Photochemistry and Photobiology, 65(1): 107-114.

Lee, E.S. and Krothe, N.C., 2001. A four-component mixing model for water in a karst terrain in south-central Indiana, USA. Using solute concentration and stable isotopes as tracers. Chemical Geology, 179(1-4): 129-143.

Lee, J.U., Lee, S.W., Kim, K.W. and Yoon, C.H., 2005. The effects of different carbon sources on microbial mediation of arsenic in arsenic-contaminated sediment. Environmental Geochemistry and Health, 27(2): 159-168.

Li, S.-L. et al., 2010. Geochemistry of dissolved inorganic carbon and carbonate weathering in a small typical karstic catchment of Southwest China: Isotopic and chemical constraints. Chemical Geology, 277(3-4): 301-309.

Lin, Y.P. and Singer, P.C., 2005. Inhibition of calcite crystal growth by polyphosphates. Water Research, 39(19): 4835-4843.

Lindroos, A.J., Kitunen, V., Derome, J. and Helmisaari, H.S., 2002. Changes in dissolved organic carbon during artificial recharge of groundwater in a forested esker in Southern Finland. Water Research, 36(20): 4951-4958.

Lovley, D.R. and Chapelle, F.H., 1995. Deep subsurface microbial processes. Reviews of Geophysics, 33(3): 365-381.

Lovley, D.R. and Chapelle, F.H., 1996. Hydrogen-based microbial ecosystems in the Earth. Science, 272(5263): 896-896.

Ludwig, W., AmiotteSuchet, P. and Probst, J.L., 1996. River discharges of carbon to the world's oceans: Determining local inputs of alkalinity and of dissolved and particulate organic carbon. Comptes Rendus De L Academie Des Sciences Serie Ii Fascicule a-Sciences De La Terre Et Des Planetes, 323(12): 1007-1014.

Luengo, C., Brigante, M. and Avena, M., 2007. Adsorption kinetics of phosphate and arsenate on goethite. A comparative study. Journal of Colloid and Interface Science, 311(2): 354-360.

Luthy, R.G. et al., 1997. Sequestration of hydrophobic organic contaminants by geosorbents. Environmental Science & Technology, 31(12): 3341-3347.

Martin, J.B. and Dean, R.W., 2001. Exchange of water between conduits and matrix in the Floridan aquifer. Chemical Geology, 179: 145-165.

Martin, J.B. and Moore, P.J., 2007. Hydrogeology of O'Leno State Park and Nitrate Loading from the River Rise, A First Magnitude Spring. Comprehensive Project Report. DEP Agreement S0182

McCarthy, J.F. et al., 1996. Field tracer tests on the mobility of natural organic matter in a sandy aquifer. Water Resources Research, 32(5): 1223-1238.

McKnight, D.M. et al., 2001. Spectrofluorometric characterization of dissolved organic matter for indication of precursor organic material and aromaticity. Limnology and Oceanography, 46(1): 38-48.

McMahon, P.B., 2001. Aquifer/aquitard interfaces: mixing zones that enhance biogeochemical reactions. Hydrogeology Journal, 9(1): 34-43.

Meharg, A.A. et al., 2006. Codeposition of organic carbon and arsenic in Bengal Delta aquifers. Environmental Science & Technology, 40(16): 4928-4935.

Miller, J.A., 1986. Hydrogeologic Framework of the Floridan Aquifer System in Florida and in Parts of Georgia, Alabama, and South Carolina. US Geological Survey Professional Paper 1403-B.

Mirecki, J.E., 2006. Geochemical Models of Water-Quality Changes During Aquifer Storage Recovery (ASR) Cycle Tests, Phase I: Geochemical Models Using Existing Data. , U.S. Army Engineer Research and Development Center, Vicksburg, MS.

Mladenov, N. et al., 2010. Dissolved Organic Matter Sources and Consequences for Iron and Arsenic Mobilization in Bangladesh Aquifers. Environmental Science & Technology, 44(1): 123-128.

Moore, P.J., Martin, J.B. and Screaton, E.J., 2009. Geochemical and statistical evidence of recharge, mixing, and controls on spring discharge in an eogenetic karst aquifer. Journal of Hydrology, 376(3-4): 443-455.

Moore, P.J., Martin, J.B., Screaton, E.J. and Neuhoff, P.S., 2010. Conduit enlargement in an eogenetic karst aquifer, Journal of Hydrology.

Morris, D.P. et al., 1995. The attentuation of solar UV radiation in lakes and the role of dissolved organic carbon. Limnology and Oceanography, 40(8): 1381-1391.

Mulholland, P.J. and Watts, J.A., 1982. Transport of organic carbon to the oceans by rivers of north America: a synthesis of existing data. Tellus, 34(2): 176-186.

Neal, C. et al., 2002. Phosphorus-calcium carbonate saturation relationships in a lowland chalk river impacted by sewage inputs and phosphorus remediation: an assessment of phosphorus self-cleansing mechanisms in natural waters. Science of the Total Environment, 282: 295-310.

Nimick, D.A. et al., 2003. Diel cycles in dissolved metal concentrations in streams: Occurrence and possible causes. Water Resources Research, 39(9).

Nordstrom, D.K., 2002. Public health - Worldwide occurrences of arsenic in ground water. Science, 296(5576): 2143-2145.

Norton, S.B., 2011. Ph.D. dissertation: Evaluating trace metal mobilization during managed aquifer recharge, University of Florida, Gainesville, FL, 156 pp.

Ohno, T., 2002. Fluorescence inner-filtering correction for determining the humification index of dissolved organic matter. Environmental Science & Technology, 36(4): 742-746.

Opsahl, S.P. and Chanton, J.P., 2006. Isotopic evidence for methane-based chemosynthesis in the Upper Floridan aquifer food web. Oecologia, 150(1): 89-96.

Oremland, R.S. et al., 2002. Anaerobic oxidation of arsenite in Mono Lake water and by facultative, arsenite-oxidizing chemoautotroph, strain MLHE-1. Applied and Environmental Microbiology, 68(10): 4795-4802.

Pabich, W.J., Valiela, I. and Hemond, H.F., 2001. Relationship between DOC concentration and vadose zone thickness and depth below water table in groundwater of Cape Cod, USA. Biogeochemistry, 55(3): 247-268.

Parlanti, E., Worz, K., Geoffroy, L. and Lamotte, M., 2000. Dissolved organic matter fluorescence spectroscopy as a tool to estimate biological activity in a coastal zone submitted to anthropogenic inputs. Organic Geochemistry, 31(12): 1765-1781.

Pavelic, P., Nicholson, B.C., Dillon, P.J. and Barry, K.E., 2005. Fate of disinfection by-products in groundwater during aquifer storage and recovery with reclaimed water. Journal of Contaminant Hydrology, 77(1-2): 119-141.

Pearcy, C.A. et al., 2011. Evidence of microbially mediated arsenic mobilization from sediments of the Aquia aquifer, Maryland, USA. Applied Geochemistry, 26(4): 575-586.

Pentecost, A., 1992. Carbonate chemistry of surface waters in a temperate karst region - the southern Yorkshire Dales, UK. Journal of Hydrology, 139(1-4): 211-232.

Petrovic, M., Kastelan-Macan, M. and Horvat, A.J.M., 1999. Interactive sorption of metal ions and humic acids onto mineral particles. Water Air and Soil Pollution, 111(1-4): 41-56.

Price, R.E. and Pichler, T., 2006. Abundance and mineralogical association of arsenic in the Suwannee Limestone (Florida): Implications for arsenic release during water-rock interaction. Chemical Geology, 228(1-3): 44-56.

Pronk, M., Goldscheider, N. and Zopfi, J., 2006. Dynamics and interaction of organic carbon, turbidity and bacteria in a karst aquifer system. Hydrogeology Journal, 14(4): 473-484.

Quay, P.D., Tilbrook, B. and Wong, C.S., 1992. Oceanic uptake of fossil-fuel CO2: Carbon-13 evidence. Science, 256(5053): 74-79.

Randazzo, A.F. and Jones, D.S., 1997. The Geology of Florida. University Press of Florida.

Ratasuk, N. and Nanny, M.A., 2007. Characterization and quantification of reversible redox sites in humic substances. Environmental Science & Technology, 41: 7844-7850.

Rauch, T. and Drewes, L., 2004. Assessing the removal potential of soil-aquifer treatment systems for bulk organic matter. Water Science and Technology, 50(2): 245-253.

Redman, A.D., Macalady, D.L. and Ahmann, D., 2002. Natural organic matter affects arsenic speciation and sorption onto hematite. Environmental Science & Technology, 36(13): 2889-2896.

Ritorto, M., Screaton, E.J., Martin, J.B. and Moore, P.J., 2009. Relative importance and chemical effects of diffuse and focused recharge in an eogenetic karst aquifer: an example from the unconfined upper Floridan aquifer, USA. Hydrogeology Journal, 17(7): 1687-1698.

Rowland, H.A.L., Polya, D.A., Lloyd, J.R. and Pancost, R.D., 2006. Characterisation of organic matter in a shallow, reducing, arsenic-rich aquifer, West Bengal. Organic Geochemistry, 37(9): 1101-1114.

Santisteban, J.I. et al., 2004. Loss on ignition: a qualitative or quantitative method for organic matter and carbonate mineral content in sediments? Journal of Paleolimnology, 32(3): 287-299.

Sarbu, S.M., Kane, T.C. and Kinkle, B.K., 1996. A chemoautotrophically based cave ecosystem. Science, 272(5270): 1953-1955.

Schlautman, M.A. and Morgan, J.J., 1994. Adsorption of Aquatic Humic Substances on Colloidal-Size Aluminum-Oxide Particles - Influence of Solution Chemistry. Geochimica Et Cosmochimica Acta, 58(20): 4293-4303.

Schulz, M. and Kohler, J., 2006. A simple model of phosphorus retention evoked by submerged macrophytes in lowland rivers. Hydrobiologia, 563: 521-525.

Schwarzenbach, R.P., Gschwend, P.M. and Imboden, D.M., 2003. Environmental Organic Chemistry (Second Edition). In: S. Edition (Editor). Wiley-Interscience, pp. 280-283.

Scott, D.T., McKnight, D.M., Blunt-Harris, E.L., Kolesar, S.E. and Lovley, D.R., 1998. Quinone moieties act as electron acceptors in the reduction of humic substances by humics-reducing microorganisms. Environmental Science & Technology, 32(19): 2984-2989.

Screaton, E., Martin, J.B., Ginn, B. and Smith, L., 2004. Conduit properties and karstification in the unconfined Floridan Aquifer. Ground Water, 42(3): 338-346.

Simon, K.S., Gibert, J., Petitot, P. and Laurent, R., 2001. Spatial and temporal patterns of bacterial density and metabolic activity in a karst aquifer. Archiv Fur Hydrobiologie, 151(1): 67-82.

Sprinkle, C.L., 1989. Geochemistry of the Floridan Aquifer system in Florida and in parts of Georgia, South Carolina, and Alabama, U.S. Geological Survey Professional Paper 1403-I.

Suchet, P.A., Probst, J.L. and Ludwig, W., 2003. Worldwide distribution of continental rock lithology: Implications for the atmospheric/soil CO2 uptake by continental weathering and alkalinity river transport to the oceans. Global Biogeochemical Cycles, 17(2).

Telmer, K. and Veizer, J., 1999. Carbon fluxes, pCO(2) and substrate weathering in a large northern river basin, Canada: carbon isotope perspectives. Chemical Geology, 159(1-4): 61-86.

Thomas, M.M., Clouse, J.A. and Longo, J.M., 1993. Adsorption of organic-compounds on carbonate minerals. 3. influence on dissolution rates. Chemical Geology, 109(1-4): 227-237.

Tipping, E. et al., 1997. Organic carbon in the Humber rivers. Science of the Total Environment, 194: 345-355.

Upchurch, S.B. and Lawrence, F.W., 1984. Impact of ground water chemistry on sinkhole development along a retreating scarp. In: B.F. Beck (Editor), Sinkholes: Their Geology, Engineering, and Environmental Impact. Rotterdam: A.A. Balkema, pp. 189-195.

USEPA, 1983. Methods for the Chemical Analysis of Water and Wastes. Office of Research and Development, US Environmental Protection Agency, Cincinnati, Ohio, 552p.

USEPA, 2012. Inventory of U.S. Greenhouse Gas Emissions and Sinks: 1990-2010, U.S. Environmental Protection Agency Washington, DC

Van Geen, A. et al., 2004. Decoupling of As and Fe release to Bangladesh groundwater under reducing conditions. Part II: Evidence from sediment incubations. Geochimica Et Cosmochimica Acta, 68(17): 3475-3486.

Vanderzalm, J.L., La Salle, C.L.G. and Dillon, P.J., 2006. Fate of organic matter during aquifer storage and recovery (ASR) of reclaimed water in a carbonate aquifer. Applied Geochemistry, 21(7): 1204-1215.

Vlasceanu, L., Sarbu, S.M., Engel, A.S. and Kinkle, B.K., 2000. Acidic cave-wall biofilms located in the Frasassi Gorge, Italy. Geomicrobiology Journal, 17(2): 125-139.

Wang, S.L. and Mulligan, C.N., 2006. Natural attenuation processes for remediation of arsenic contaminated soils and groundwater. Journal of Hazardous Materials, 138(3): 459-470.

Wetzel, R.G., 2001. Limnology: lake and river ecosystems. Academic Press, San Diego, California.

Wolthers, M., Charlet, L., Van der Weijden, C.H., Van der Linde, P.R. and Rickard, D., 2005. Arsenic mobility in the ambient sulfidic environment: Sorption of arsenic(V) and arsenic(III) onto disordered mackinawite. Geochimica Et Cosmochimica Acta, 69(14): 3483-3492.

Worthington, S.R.H., 1994. Flow velocities in unconfined carbonate aquifers. Cave and Karst Science 21, 21-22.

Wu, Y., 2003. Mechanism analysis of hazards caused by the interaction between groundwater and geo-environment. Environmental Geology, 44(7): 811-819.

Wu, Y.T. and Grant, C., 2002. Effect of chelation chemistry of sodium polyaspartate on the dissolution of calcite. Langmuir, 18(18): 6813-6820.

Young, K.C., Docherty, K.M., Maurice, P.A. and Bridgham, S.D., 2005. Degradation of surface-water dissolved organic matter: influences of DOM chemical characteristics and microbial populations. Hydrobiologia, 539: 1-11.

Young, K.C., Maurice, P.A., Docherty, K.M. and Bridgham, S.D., 2004. Bacterial degradation of dissolved organic matter from two northern Michigan streams. Geomicrobiology Journal, 21(8): 521-528.

Zachara, J.M., Cowan, C.E. and Resch, C.T., 1991. Sorption of divalent metals on calcite. Geochimica Et Cosmochimica Acta, 55(6): 1549-1562.

Zsolnay, A., Baigar, E., Jimenez, M., Steinweg, B. and Saccomandi, F., 1999. Differentiating with fluorescence spectroscopy the sources of dissolved organic matter in soils subjected to drying. Chemosphere, 38(1): 45-50.

BIOGRAPHICAL SKETCH

Jin Jin was born in Shanghai, China. He attended University of Science and Technology of China (USTC) from 2002 through 2006. Upon earning B.S. in environmental sciences from USTC, he was admitted to University of Florida and began his graduate study in the Department of Geological Sciences under the guidance of Dr. Andrew Zimmerman. Jin served as both teaching and research assistant during his graduate study and received Ph.D. in geology in 2012.